CHAPTER 3

Cloudwater and Aerosol Composition at Elevated Sites During the South Coast Air Quality Study

by

Jeff Collett, Jr., J. William Munger,
Bruce Daube, Jr., and Michael R. Hoffmann

Environmental Engineering Science
W. M. Keck Laboratories, 138–78
California Institute of Technology
Pasadena, CA 91125

March 1988

Introduction

The Suggested Program Plan for SCAQS (Blumenthal et al., 1986) identifies the need to measure cloud and fog in the SoCAB in order to properly understand gas and aerosol processes. There is considerable evidence that the presence of fog or low cloud in the basin is associated with high SO_4^{2-} aerosol loadings and poor visibility in the SoCAB (Blumenthal et al., 1986, and references therein). Previous research sponsored by the CARB at Caltech has identified pre–existing aerosol as a major contributor to the acidity level in fog and cloud. Conversely, evaporated fog and cloud droplets are a major source of aerosol. The primary objectives of Caltech's participation in SCAQS are to assess the role that fog and cloud play in the formation of aerosol in the SoCAB (Objective 3, issue 1 of SCAQS) and to quantify the scavenging of precursor aerosol and gases during droplet formation. The extensive data available from SCAQS on meteorology, emissions, gas and aerosol concentrations will be used to evaluate cloud and fog droplet chemistry models. In this chapter we present the results of cloudwater and aerosol sampling at elevated sites in the SoCAB during SCAQS.

Methods

During the summer of 1987 cloudwater, aerosol and selected gases were sampled in conjunction with the South Coast Air Quality Study (SCAQS). During the period June 13 to July 17 sites were in operation at San Pedro Hill, Henninger Flats, and Kellogg Hill. A fourth site on Flint Peak, near Pasadena, was set up but could not be used because interference from FM transmitters located near the site disrupted the sampling equipment.

Site Descriptions

The San Pedro Hill site was located at a radar and communications facility operated by the U. S. Air Force and the Federal Aviation Administration. The elevation of the site is 450 m. The distance from the site to the ocean is 2.5 km. Los Angeles Harbor is 6 km east. The sampling equipment was placed at the edge of a flat grassy area. A steep hillside sloped away from the site, giving it unobstructed exposure from 70–270°. A SCAQS meteorological station was located a few hundred meters away from the sampling site.

Henninger Flats is at an elevation of 780 m, 7 km NE of Pasadena, and 45 km NE of the coastline. This site has been used in previous sampling programs (Waldman et al., 1985) and in a fog sampler intercomparison (Hering et al., 1987). A SCAQS meteorological station was also located at Henninger Flats.

Kellogg Hill is 38 km E of downtown Los Angeles at an elevation of 370 m. It lies 50 km NE of the coastline. The sampling equipment was located in a fenced enclosure adjacent to a small building that housed radio transmission equipment. The building partially obstructed the sampler when winds were from the south to west, which is the prevailing daytime wind. The site was unobstructed in the direction of the prevailing night–time winds. Construction activity near the site increased aerosol concentrations of soil dust during the daytime, and may have affected samples collected here.

Sampling Procedure

Each site was equipped with a Caltech Active Strand Collector with an automated fractionating sampler and a cloudwater sensor (see Chapter 1). The CASC collects droplets by inertial impaction on 510 μm Teflon strands. The 50% collection efficiency

cutoff, predicted from impaction theory and based on droplet diameter, is 3.5 μm. Also located at each site was an automated filter pack aerosol sampler. Teflon filters (Gelman Zefluor, 1μm pore size) were used to collect aerosol for inorganic analysis. $HNO_{3(g)}$ was collected on a nylon filter (Gelman Nylasorb) placed behind one Teflon filter. $NH_{3(g)}$ was collected on two oxalic acid impregnated glass fiber filters behind a second Teflon filter. The species that were measured in aerosol, gas and droplet phases are listed in Tables 1 and 2.

During the late afternoon or evening prior to expected cloud impaction, the samplers were cleaned by rinsing the collection strands, sample tubing, and reservoir with distilled, deionized water (DDH_2O). After rinsing, the strands were sprayed again with DDH_2O, which was collected in the fraction collector as a system blank. Rinsing and blank collection was repeated the following morning whether cloud was collected or not. Three sets of filters were loaded on the aerosol collector. A timer on the collector controlled the times that each filter set was run.

Some samples of cloudwater, fractionated by droplet size, were also collected and analyzed to determine whether any significant difference exists between the chemical composition of small vs. large cloudwater droplets. One of the CASC's was adapted for this purpose by adding an inlet containing four rows of eight 12.7 mm Teflon rods. These rods provide a 50% lower size cut of 16 μm at the sampling velocity of 9 m/s. Each row covers 46% of the cross–sectional area. The four rows together sample 91.5% of the air passing through the collector. The sample collected by impaction on these rods is fed into a sample bottle. Droplets smaller than 15 μm are collected inefficiently on the rods and pass through to be collected on the CASC strands in the main body of the collector.

Analytical Procedures

Samples were retrieved in the morning following a cloud event and transported to the lab at Caltech. The samples were weighed to determine their volume and the sample pH was measured with a Radiometer PHM82 pH meter using a combination electrode calibrated against pH 4 and 7 buffers. For selected samples small aliquots of the sample were removed and treated to stabilize reactive species. S(IV) was stabilized as the hydroxymethanesulfonate by adding buffered CH_2O (Dasgupta et al., 1981). CH_2O was stabilized with a solution of SO_3^{2-} (Dong and Dasgupta, 1987). A buffered solution of p–OH phenylacetic acid (POPA) and peroxidase was used to preserve peroxide (Lazrus et al., 1985). Carboxylic acids were preserved by addition of chloroform (Keene and Galloway, 1984). Carbonyls were derivatized with 2,4–dinitrophenylhydrazine in acidic solution (Grosjean and Wright, 1983).

The samples and preserved aliquots were stored in a refrigerator at 4°C until analysis. Major anions were determined by ion chromatography with a Dionex AS4 or AS4A separator column and a micromembrane suppressor. The eluent was 2.8 mM HCO_3^-/ 2.2 mM CO_3^{2-}. The metallic cations were determined by atomic absorption spectrophotometry. An air/acetylene flame was used for Na^+ and K^+; N_2O/acetylene was used for Ca^{2+} and Mg^{2+} to minimize interferences. NH_4^+ was determined by flow injection analysis employing the indophenol blue method.

The stabilized CH_2O was determined by a modification of the Nash method for use with an autoanalyzer (Dong and Dasgupta, 1987) Hydrogen peroxide was added to eliminate S(IV), which interferes by forming an adduct with CH_2O. The absorbance of the colored product was measured at 412 nm. S(IV) was analyzed by the pararosaniline method (Dasgupta et al., 1980) adapted for flow injection analysis. Peroxide was determined from the flourescence of the POPA enzyme solution (Lazrus et al., 1985). The method is sensitive to H_2O_2 and some organic peroxides, however, the significantly lower

Henry's law coefficients of CH_3OOH and peroxoacetic acid suggest that they will not be important in fog and cloud water (Lazrus et al.,1985). Carboxylic acids were determined by ion exclusion chromatography (Dionex ICE–AS1) with dilute HCl as eluent.

The Teflon and oxalic acid impregnated glass fiber filters were extracted in distilled deionized water (DDH_2O) on a shaker table. A small volume of ethanol was added to the filter prior to extraction to more effectively wet the filter surface. The nylon filters were extracted in HCO_3^-/CO_3^{2-} IC eluent. Composition of the extracts was determined by the same procedures used for the fogwater samples, with the exception of additional buffer in the complexing reagent and oxalic acid in the rinse solution of the ammonia analysis to account for the effect of the oxalic acid.

The precision and accuracy of the measurements was determined from the mean and standard deviation of repeated analyses of the same standard (Standard Methods). Detection limits were estimated from analyses of blanks (or the lowest standard). The stated detection limit is defined as the concentration giving a signal 3 times the blank (or low standard) standard deviation. The expected precision, accuracy and detection limits for the major species measured are listed in Table 3. For gas–phase species the variance of the flow measurements is included in the estimates of precision and detection limit.

Results and Discussion

Cloudwater and Aerosol Composition

During the summer portion of SCAQS, stratus clouds frequently impacted the coastal slopes near San Pedro. This is reflected in the fact that over 240 samples were collected at San Pedro Hill during the study. Clouds were present at this site primarily during the night, although some events lasted until mid–day. On several occasions, the stratus extended as far inland as the slopes of the San Gabriel Mountains and was at the right elevation to be collected at Henninger Flats, where 76 samples were obtained. Stratus were rarely observed at the Kellogg Hill site during this study, where only a couple

of samples were obtained. The compositional data for the San Pedro Hill and Henninger Flats samples are presented in Tables 4 and 5.

Samples at both San Pedro Hill and Henninger Flats were consistently acidic. Sample pH values at San Pedro Hill varied from 2.4 to 5.0, while those at Henninger Flats ranged from 2.6 to 4.8. The arithmetic average of the pH at each site was 3.25. Frequency distributions of the sample pH for each site are presented in Figures 2 and 3.

The composition of the cloudwater sampled at both sites was usually dominated by NO_3^-, SO_4^{2-}, NH_4^+, and H^+. In some samples Na^+ and Cl^- were also found to be important contributors. Concentrations of Na^+ and Cl^- were generally both observed at higher levels in the San Pedro Hill cloudwater, consistent with its proximity to the ocean. NH_4^+ concentrations averaged higher at Henninger Flats, while NO_3^- concentrations averaged approximately 1200 μeq/l at both sites. SO_4^{2-} concentrations averaged one–third higher at San Pedro Hill (917 μeq/l) than at Henninger Flats (689 μeq/l).

Most of the samples obtained at the two sites were collected during non–overlapping time periods. Often the stratus clouds would impact one site on a given day and not the other. At other times, the clouds were observed to impact the hillside at San Pedro during the period shortly after midnight, while impaction at Henninger Flats did not begin until a few hours later. By this time, clouds were no longer intercepting the slopes of San Pedro Hill. The only event with simultaneous collection at both sites was on July 16. This event, which was associated with drizzle and rainfall in the L.A. Basin, was one of the most extended observed during the study. The sampling capacity of the autosampler carousel was exceeded at both sites at approximately 2300 on the 16th. The event was also one of the least acidic observed at San Pedro Hill. The cloudwater pH there climbed as high as 4.98 during the event, while all of the samples collected at Henninger Flats had a pH less than 4. Like H^+ concentrations, concentrations of NO_3^-, SO_4^{2-},and NH_4^+ were also much higher at Henninger Flats during this event than they were at San Pedro Hill.

The combination of the high sampling rate of the CASC (the CASC has sampled at rates of up to 8.5 ml min^{-1} in past field studies) and the use of the autosampler enabled us to collect samples with a very fine time resolution. During some events, 60 ml samples were collected at San Pedro Hill as quickly as one every 10 minutes. This time resolution enables an examination of rapid fluctuations in the cloudwater composition as a function of changes in wind direction or liquid water content. An example of this resolution is depicted in Figure 4. The diagrams in this figure illustrate the changes in the sample pH, the concentrations of the measured ions, and the estimated liquid water content (based on the collection rate and the theoretical sampling efficiency of the CASC), as a function of time, observed at San Pedro Hill for the period from 0100 to 0315 on June 25, 1987. In just over two hours, the observed levels of all these parameters were seen to change dramatically. Concentrations of all measured species were observed to drop by at least a factor of two between 0130 and 0230. These drops coincided with a doubling of the liquid water content, suggesting that the concentration changes were largely due to dilution. When the liquid water content began to fall after 0230, however, not all of the species' concentrations increased. Levels of SO_4^{2-}, NO_3^-, and H^+ did rise, but Na^+, Cl^-, Ca^{2+}, and Mg^{2+} concentrations remained steady or declined. Analysis of meteorological data from San Pedro Hill, which is part of the SCAQS data set, will enable us to correlate changes in chemical composition with meteorological variables.

The aerosol and gas–phase data for San Pedro Hill, Henninger Flats, and Kellogg Hill are presented in Tables 6 through 8. The major species present are NH_4^+, NO_3^-, and SO_4^{2-}. Na^+ and Cl^- are also major components in some samples, particularly at the San Pedro Hill site in the daytime samples, which were collected during onshore flow conditions. The concentration of NH_4^+ is greater at the inland sites, Henninger Flats and Kellogg Hill, than at San Pedro Hill. During the daytime concentrations of $HNO_{3(g)}$ are quite high; they often equal or exceed the aerosol NO_3^- concentration. The gas–phase NH_3

concentrations are fairly low at Hennigner Flats and San Pedro Hill. Kellogg Hill, which is the closest site to the dairy feedlots in Chino, has the highest $NH_{3(g)}$ concentrations.

Blank Concentrations

In order to determine the efficacy of our collector cleaning procedure the collection strands in the CASC were sprayed with distilled water to generate blanks. The concentrations of major ions in the collector blanks are presented in Table 9. In general the blank concentrations are an order of magnitude less than the measured concentrations of the samples, although there were a few cases of fairly high concentrations in the blanks. Rinsing the strands effectively removed material from the collector; analysis of successive blanks indicates decreased concentrations in the second rinse compared to the first.

Size–fractionated Samples

Clouds began impacting the San Pedro Hill site at approximately 1900 on July 14 and remained there until approximately 1300 on July 15. The event was sampled by the CASC and the autosampler from 1900 until approximately midnight, when the last bottle in the carousel was used. Manual operation of the CASC, with the size–fractionating inlet installed, began at 0400. Samples were collected at half–hour intervals until noon on the 15th. A final one–hour unfractionated sample was collected from 1200 to 1300. The size–fractionating inlet, as discussed earlier, is used to collect the larger droplets in the cloud (those with diameters greater than about 16 μm), leaving the smaller droplets to be collected on the CASC strands. Figure 5 depicts the fraction of the droplet–size spectrum collected by each portion of the sampler for three different liquid water contents. The droplet–size spectra are typical representations based on the work of Best (1951a). The fraction of the liquid water sampled by each part of the collector is calculated based on

impaction theory for droplets on a cylinder. At low liquid water contents, where a higher proportion of the water is typically contained in smaller droplets, most of the droplets will pass through the fractionating inlet and collect on the CASC strands. At higher liquid water contents, however, the preponderance of large droplets will shift the bulk of the collected sample volume to the fractionating inlet. As shown in the figure, considerable overlap in the portions of the droplet spectrum sampled by each part of the collector are expected. Any differences seen in the composition of the two sample fractions, therefore, should be considered as a lower bound on the differences present between more sharply divided portions of the spectrum.

The chemical compositions of the samples collected using the size–fractionating inlet are displayed in Table 10. The samples have been labeled "f" for those fractions collected on the large rods in the front of the collector, and "b" for those collected on the CASC strands in the back. The volume weighted average concentration of each species, obtained by mathematically combining the two fractions for each sampling period, is also presented. The two fraction volumes collected during each sampling interval are compared in Figure 6. The ratio of volumes collected in each fraction was on the order of two or three to one, in favor of the fraction collected on the large rods, for all sampling intervals. During several periods the cloud grew dense enough to produce a light drizzle. Consistent with the predictions in Figure 5, the ratio of volumes collected by each fraction was higher during the periods when the liquid water content was higher.

Comparisons of the ion concentrations in the two fractions collected during each interval suggest that there is a large difference between the average composition of the smaller droplets and that of the larger droplets. Figures 6 through 8 illustrate the case for each of the species measured. For every interval sampled, the concentration of Na^+ and Mg^{2+} in the small droplet fraction was observed to be higher than in the large droplet fraction. With the exception of one very low concentration sample, the same was true for Ca^{2+}. Concentrations of SO_4^{2-}, NO_3^-, NH_4^+, and H^+ were almost always higher in the

small droplet fraction (the fact that they were lower in this fraction for the first couple of samples may be due to dilution by residual rinsewater on the CASC strands). Concentrations of Cl^- showed no consistent preference for one fraction over the other, and were generally at similar levels in both fractions. The composition of the fractionated sample collected between 0600 and 0630 is depicted in a pie diagram (Figure 9). In addition to the differences discussed above, this figure illustrates that the total of the ionic species concentrations is much higher in the smaller droplets, on average, than in the larger ones.

Similar results were observed when comparing samples collected by the Caltech Rotating Arm Collector and the CASC at a coastal site in the Santa Barbara Channel. The RAC (Jacob et al., 1984) which has a 50% lower size cut, based on droplet diameter, of about 20 μm, collected samples with higher concentrations of Na^+, Ca^{2+}, and Mg^{2+} than were observed in samples collected by the CASC (Collett et al., 1988). The difference in the concentrations was attributed to differences in the portions of the droplet–size spectrum sampled by the two collectors. The CASC, with its theoretical lower size cut of 3.5 μm, collects almost all of the liquid water contained in cloud droplets, while the higher size cut of the RAC allows it to only collect the larger droplets efficiently. Typically, larger condensation nuclei lead to the formation of larger cloud droplets in the lower portions of a cloud not subjected to significant horizontal entrainment of dry air (Best, 1951b; Mason and Chien, 1962; Hudson, 1984). Since sea salt and soil dust are found to reside in the larger end of the aerosol size spectrum (Seinfeld, 1986), the elements found predominantly in these types of particles (e.g. Cl, Na, Mg, and Ca) will reside there as well. Therefore, as cloud droplets form on the available aerosol nuclei and grow by condensation, it is expected that these elements will be found predominantly in the upper end of the droplet size spectrum.

During the same study, no preference was shown by either collector for higher concentrations of NO_3^-, SO_4^{2-}, NH_4^+, or Cl^-. NO_3^-, SO_4^{2-}, and NH_4^+, which make their

way into the aerosol phase largely by gas–to–particle conversion processes, are found to reside largely in smaller aerosol particles (Seinfeld, 1986). One might expect then that smaller cloud droplets would be enriched in these ions relative to their larger counterparts. The differences might not be so readily apparent in the droplet phase, however, since all three species may also be introduced by absorption of gas phase precursors, coupled with oxidation of S(IV) to S(VI) in the case of SO_4^{2-}. Absorption of $NH_{3(g)}$, and particularly of $HNO_{3(g)}$, was seen to play an important role in determining the composition of cloudwater at the study site (Collett et al., 1988). Since gas phase absorption can make important contributions to the composition of all droplet sizes, it may tend to mask the initial chemical signature given to the droplets by their condensation nuclei.

Observing differences in the chemical composition of small vs. large droplets in the present study is facilitated by the way the droplet size spectrum has been split. While there is still considerable overlap in the portions of the size spectrum collected by the large rods and the small CASC strands, there is more difference than in the Santa Barbara Channel comparison, where the average composition of the large droplets was being compared to the average composition of the whole spectrum. This may at least partially explain why differences in the concentrations of NO_3^-, SO_4^{2-}, H^+, and NH_4^+ are evident this time.

The distribution of Cl^- between large and small droplets is somewhat different from the other ions discussed, being found at roughly equivalent concentrations in each fraction. Cl^- is initially associated with Na^+ in sea–salt aerosol. If it remained there until nucleation of the aerosol within the cloud, we would expect to see Cl^- concentrations higher in the large droplets, as was observed for Na^+. This clearly is not the case, suggesting the possibility that Cl^- was introduced into the droplets in another form. Aerosol samples collected on the afternoon of July 14 at San Pedro Hill show substantial concentrations of Na^+, but essentially no Cl^- (see Table 6). High $HNO_{3(g)}$ concentrations also observed during this period could have resulted in acid exchange of $HCl_{(g)}$ for $HNO_{3(g)}$ in the sea

salt aerosol. Introduction of Cl^- to the cloudwater droplets that evening as HCl(g) would have produced the type of uniform distribution among all droplet sizes that was observed.

References

Best, A. C. (1951a) Drop–size distribution in cloud and fog. *Q. Jl. R. met. Soc.* 77,

Best, A. C. (1951b) The size of cloud droplets in layer–type cloud. *Q. Jl. R. met. S* 241.

Blumenthal, D., Watson, J., and Lawson, D. (1986) Southern California Air Qualit (SCAQS) Suggested Program Plan, Sonoma Technology Incorporated Report, Refe No. 10 95050–605.

Collett, J. L., Jr., Munger, J. W., Daube, B. D., Jr., and Hoffmann, M. R. (1988) comparison of two cloudwater/fogwater collectors: the rotating arm active strand collector. submitted to *Atmos. Environ.*

Dasgupta, P. K., DeCesare, K. and Ullrey, J. C. (1980) Determination of atmosph sulfur dioxide without tetrachloromercurate (II) and the mechanism of the Schiff r *Anal. Chem.* **52**, 1912–1922.

Dasgupta, P. K. (1981) Determination of atmospheric sulfur dioxide without tetrachloromercurate(II): Further refinements of a pararosaniline method and a fie application, *J. Air Pollut. Cont. Assoc.* **31**, 779–782.

Dong, S. and Dasgupta, P. K (1987) Fast flourimetric flow injection analysis of formaldehye in atmospheric water, *Environ. Sci. Technol.* **21**. 581.

Grosjean, D. and Wright, B. (1983) Carbonyls in urban fog, ice fog, cloudwater an rainwater, *Atmos. Environ.* **17**, 2093–2096.

Hering, S. V., Blumenthal, D. L., Brewer, R. L., Gertler, A., Hoffmann, M., Kadle A., and Pettus, K. (1987) Field intercomparison of five types of fogwater collectors *Environ. Sci. Technol.* **21**, 654–663.

Hudson, J. G. (1984) Ambient CCN and FCN measurements, in *Hygroscopic Aero* H. Ruhnke and A. Deepak, Eds., A. Deepak Publishing, Hampton, VA.

Jacob, D. J., Wang, R. F. T., and Flagan, R. C. (1984) Fogwater collector design a characterization, *Environ. Sci. Technol.* **18**, 827–833.

Keene, W. C. and Galloway, J. N. (1984) Organic acidity in precipitation of North America, *Atmos. Environ.* **18**, 2491–2497.

Lazrus, A., Kok, G. L., Gitlin, S. N., Lind, J. A., and McLaren, S. E. (1985) Auto flourometric method for hydrogen peroxide in atmospheric precipitation, Anal. *Che* 917–922.

Mason, B. J. and Chien, C. W. (1962) Cloud–droplet growth by condensation in c *Q. Jl. R. met. Soc.* 88, 133–138.

Seinfeld, J. H. (1986) *Atmospheric Chemistry and Physics of Air Pollution*, Wiley–Interscience, New York.

Waldman, J. M., Munger, J. W., Jacob, D. J., and Hoffmann, M. R. (1985) Chemi characterization of stratus cloudwater and its role as a vector for pollutant depositi Los Angeles pine forest. *Tellus* **37**, 91–108.

Table 1. Analysis of liquid samples.

Species	Method
pH	Combination Electrode
Cl^-	Ion chromatography - HCO_3^-/CO_3^{2-} eluent
NO_3^-	"
SO_4^{2-}	"
NH_4^+	Indophenol blue - Flow Injection Analysis
Na^+	Flame Atomic Absorption Spectrometry
K^+	"
Ca^{2+}	"
Mg^{2+}	"
	"
S(IV)	Pararosaniline - FIA
CH_2O	Nash Method
C_1 - C_6 Carbonyls	DNPH Derivative - HPLC
Carboxylic Acids	Ion Chromatography - $B_4O_7^{2-}$ eluent
	Ion Exclusion Chromatography - HCl eluent
H_2O_2	POPA - flourescent dimer

Table 2. Analysis of gas and aerosol samples.

Species	Filter	Method
	— (aerosol) —	
SO_4^{2-}	Teflon	H_2O extract - IC
NO_3^-	Teflon	"
Cl^-	Teflon	"
Na^+	Teflon	H_2O extract - Flame AAS
Ca^{2+}	Teflon	"
Mg^{2+}	Teflon	"
NH_4^+	Teflon	H_2O extract - indophenol FIA
	—— (gas) ——	
NH_3	Oxalic acid - imp. Glass	H_2O extract - indophenol FIA
HNO_3	Nylon	HCO_3^-/CO_3^{2-} extract - IC
O_2	Base - imp. Quartz	"

Table 3.

PRECISION, ACCURACY, AND MINIMUM DETECTION LIMIT

Aqueous Phase

Species	nominal conc.	Acc.	Prec.	RSD	MDL
	μN	μN	μN	%	μN
NH_4^+	20	0.28	0.58	2.92	1.75
Na^+	10.9	0.13	0.45	4.15	1.36
Ca^{2+}	12.5	-0.42	0.87	6.97	2.61
Mg^{2+}	10.25	0.30	0.48	4.66	1.43
Cl^-	20	0.26	2.04	10.20	6.12
NO_3^-	20	0.11	0.92	4.60	2.76
SO_4^{2-}	20	0.20	0.86	4.29	2.57
Cl^-	2	0.87	2.22	111.07	6.66
NO_3^-	2	0.31	0.35	17.71	1.06
SO_4^{2-}	2	0.26	0.38	19.13	1.15

Gas Phase (4 hour run)

Species	nominal conc.	Acc.	Prec.	RSD	MDL
	neq m^{-3}	neq m^{-3}	neq m^{-3}	%	neq/m^{-3}
NH_4^+	69.42	0.96	2.90	4.18	8.70
Na^+	37.84	0.44	1.95	5.16	5.86
Ca^{2+}	43.39	-1.46	3.28	7.56	9.84
Mg^{2+}	35.58	1.04	1.99	5.61	5.98
Cl^-	69.42	0.90	7.40	10.65	22.19
NO_3^-	69.42	0.38	3.83	5.52	11.49
SO_4^{2-}	69.42	0.69	3.66	5.27	10.97
NH_3	69.42	0.96	2.90	4.18	8.70
HNO_3	69.42	0.38	3.83	5.52	3.69
Cl^-	6.94	3.02	7.71	111.07	23.13
NO_3^-	6.94	1.09	1.23	17.71	3.69
SO_4^{2-}	6.94	0.91	1.33	19.13	3.98

Table 4 San Pedro Hill Cloudwater Data

San Pedro Hill Cloudwater Data

Date	Sec	Date	Seq	Start	Stop	Vol (ml)	pH	Na+ (uN)	K+ (uN)	NH4+ (uN)	Ca2+ (uN)	Mg2+ (uN)	"Fo" (uN)	Cl- (uN)	NO3- (uN)	SO42- (uN)	CH2O (uM)	H2O2 (uM)	MFo (uM)	HAc (uM)	LWC ml/m3
06/13	1	06/13	1	20:43	21:22	49	3.28	516	21	471	88	119	161	474	855	678					0.070
06/13	2	06/13	2	21:22	21:52	53	3.19	369	14	377	52	166	144	407	743	661					0.099
06/13	3	06/13	3	21:52	23:19	68	3.18	592	21	496	74	178	176	558	904	781					0.044
06/13	4	06/13	4	23:19	00:20	62	3.08	587	22	588	70	184	171	605	957	824					0.057
06/14	5	06/14	5	00:20	00:56	48	2.89	688	24	562	80	214	147	681	1321	1215					0.075
06/14	6	06/14	6	00:56	01:41	56	2.80	647	22	555	71	190	139	587	1608	1329					0.070
06/14	7	06/14	7	01:41	02:45	57	2.85	706	24	625	78	202	172	762	1554	1296					0.050
06/14	8	06/14	8	02:45	03:13	47	3.07	731	23	495	75	214	133	771	962	895					0.094
06/14	9	06/14	9	03:13	03:46	51	3.09	440	15	376	43	119	118	465	796	722					0.087
06/14	10	06/14	10	03:46	04:09	42	3.00	361	13	402	38	95	116	400	893	872					0.102
06/14	11	06/14	11	04:09	04:31	44	3.06	265	10	375	27	64	113	327	819	736					0.111
06/14	12	06/14	12	04:31	04:59	53	3.12	149	6	323	15	47	119	247	702	574					0.106
06/14	13	06/14	13	04:59	05:40	34	2.98	263	11	477	27	82	141	400	993	870					0.047
06/14	14	06/14	14	05:40	06:16	34	2.91	536	20	648	55	155	169	599	1249	1125					0.052
06/14	15	06/14	15	06:16	07:13	18	2.82	734	28	744	77	208	181	787	1569	1407					0.017
06/19	4	06/19	4	04:48	05:22	36	3	3796		1237	460	731	163	1701	2137	1125	25				0.055
06/19	5	06/19	5	05:22	06:02	36	3	3405		827	318	634	158	1672	1803	1131	31				0.051
06/19	6	06/19	6	06:02	07:04	26	3	3258		665	281	593	130	1654	1281	978	27				0.023
06/20	1	06/20	1	00:29	01:44	59	3.11	2574		555	268	488	150	1430	1402	1094	31				0.044
06/20	2	06/20	2	01:44	02:28	62	3.14	1768		605	187	410	126	1384	1888	1046	24				0.075
06/20	3	06/20	3	02:28	03:25	65	3.26	2318		485	173	444	117	1379	716	783	21				0.064
06/20	4	06/20	4	03:25	04:02	65	3.35	1722		356		388	96	1421	518	749	21				0.098
06/20	5	06/20	5	04:02	04:42	30	3.35	1740		347		411	140	1435	498	1232					0.042
06/20	6	06/20	6	04:46	05:05	9	3.20			517	272	715	176	1756	877	1290					0.028
06/21	8	06/21	8	00:14	00:55	65	3.48	995		295	142	253	90	735	915	447	14				0.089
06/21	9	06/21	9	00:55	01:17	66	3.52	822		219	103	199	72	807	477	359	12				0.167
06/21	10	06/21	10	01:17	01:42	12	3.55	706		169	79	192	81	837	377	312					0.026
06/22	1	06/22	1	00:24	01:13	61	3.43	1257		353	243	311	186	978	1014	507	11				0.070
06/22	2	06/22	2	01:13	01:41	62	3.37	414		311	66	116	105	440	547	428	12				0.124
06/22	3	06/22	3	01:41	02:17	62	3.31	297		327	41	75	109	353	476	381	15				0.095
06/22	4	06/22	4	02:17	02:50	61	3.34	243		355	31	61	97	289	436	354	14				0.103
06/22	5	06/22	5	02:50	03:27	62	3.36	206		376	27	53	100	267	458	368	15				0.094
06/22	6	06/22	6	03:27	04:13	62	3.26	214		461	29	54	127	303	571	465					0.075
06/22	7	06/22	7	04:13	05:17	60	3.09	342		640	51	84	146	436	862	665	20				0.052
06/22	8	06/22	8	05:17	05:34	13	2.89	602		1025	109	168	510	689	1447	1121					0.042
06/22	9	06/22	9	06:00	07:16	60	2.84	578		1126	113	161	202	611	1632	1478	27				0.044
06/22	1	06/22	1	23:18	23:58	66	3.32	285		371	85	82	97	334	644	480					0.09
06/22	2	06/22	2	23:58	00:26	62	3.44	242		349	81	70	102	266	479	370					0.12
06/23	3	06/23	3	00:26	01:05	62	3.31	212		354	57	60	92	263	537	459					0.09
06/23	4	06/23	4	01:05	01:39	62	3.36	250		348	53	68	76	307	473	391					0.10
06/23	5	06/23	5	01:39	02:15	62	3.49	247		309	44	66	76	322	334	284					0.10
06/23	6	06/23	6	02:15	02:44	61	3.51	255		270	39	67	57	317	362	333					0.12
06/23	7	06/23	7	02:44	03:07	62	3.54	200		231	30	54	55	262	298	285					0.15
06/23	8	06/23	8	03:07	03:31	62	3.48	196		229	30	54	56	259	322	318					0.15
06/23	9	06/23	9	03:31	03:55	62	3.54	174		234	24	47	58	231	296	269					0.15
06/23	10	06/23	10	03:55	04:18	62	3.50	181		264	27	48	60	226	349	320					0.15
06/23	11	06/23	11	04:18	04:49	62	3.50	162		295	24	42	71	290	424	352					0.11
06/23	12	06/23	12	04:49	05:16	62	3.62	141		280	18	38	25	196	277	224					0.13

Table 4 San Pedro Hill Cloudwater Data (continued)

San Pedro Hill Cloudwater Data

Date	Seq	Date	Seq	Start	Stop	Vol (ml)	pH	Na+ (uN)	K+ (uN)	NH4+ (uN)	Ca2+ (uN)	Mg2+ (uN)	*Fe* (uN)	Cl- (uN)	NO3- (uN)	SO42- (uN)	CH2O (uM)	H2O2 (uM)	HFo (uM)	HAc (uM)	LWC g^3/m3
06/23	13	06/23	13	05:16	05:41	61	3.55	136		239	19	37	24	189	320	283					0.14
06/23	14	06/23	14	05:41	06:07	62	3.56	123		223	17	33	21	173	301	288					0.13
06/23	15	06/23	15	06:07	06:29	62	3.58	131		233	20	35	25	177	307	277					0.16
06/23	16	06/23	16	06:29	06:54	62	3.58	130		226	21	36	27	184	297	269					0.14
06/23	17	06/23	17	06:54	07:20	62	3.52	148		272	23	40	36	203	323	293					0.13
06/23	18	06/23	18	07:20	07:43	62	3.47	169		308	28	45	43	218	388	371					0.15
06/23	19	06/23	19	07:43	08:06	62	3.43	171		293	30	47	44	226	392	358					0.15
06/23	20	06/23	20	08:06	10:27	62	3.15	452		528	95	131	104	505	1024	606					0.02
06/23	1	06/23	1	19:55	20:47	30	2.53	2941		1659	527	561	586	1574	5623	3246	35				0.03
06/23	8	06/23	8	22:30	23:18	61	2.64	3148		1510	560	601	497	1548	5240	2846	26				0.07
06/23	9	06/23	9	23:18	00:21	53	2.57	2953		1725	505	577	470	1613	5267	2934	22				0.05
06/24	10	06/24	10	00:36	01:09	61	2.62	1289		1520	240	313	259	924	3617	2291	26				0.10
06/24	11	06/24	11	01:09	01:33	61	2.82	446		789	78	134	147	492	1770	1341	18				0.14
06/24	12	06/24	12	01:33	02:04	61	2.79	276		726	45	82	116	393	1586	1329	19				0.11
06/24	13	06/24	13	02:04	02:31	61	2.81	236		843	38	68	133	339	1667	1254	23				0.13
06/24	14	06/24	14	02:31	03:03	61	2.77	225		1443	48	68	133	386	2171	1493	30				0.11
06/24	15	06/24	15	03:03	03:38	61	2.71	295		2147	55	84	152	466	2715	2053	31				0.10
06/24	16	06/24	16	03:38	04:12	61	2.75	298		2859	60	86	160	505	2757	2501	49				0.10
06/24	17	06/24	17	04:12	04:42	61	2.75	284		2441	48	79	157	476	2618	2205	46				0.11
06/24	18	06/24	18	04:42	05:03	61	2.86	350		1485	50	96	115	441	1849	1561	31				0.16
06/24	19	06/24	19	05:03	05:17	62	2.94	248		966	30	65	84	360	1291	1119	29				0.25
06/24	20	06/24	20	reservoir		66	2.84	189		1748	33	57	113	309	2073	1538					
06/24	208	06/24	208	reservoir		64	2.83	194		1916	34	58	118	318	2108	1587	47				
06/24	21	06/24	21	06:41	07:08	60	2.81	189		2088	36	56	130	400	2095	1853	43				0.12
06/24	22	06/24	22	07:08	07:56	60	2.76	230		2150	45	68	162	397	2340	1951	45				0.07
06/24	23	06/24	23	07:56	08:21	60	2.78	257		1448	46	71	157	390	2000	1540	46				0.13
06/24	24	06/24	24	08:21	08:32	20	2.78	294		1310	88	104	148	409	2100	1521	51				0.10
06/24	25	06/24	25	08:32	08:56	61	2.77	454		1272	107	136	141	539	2074	1588	36				0.14
06/24	26	06/24	26	08:56	09:14	61	2.88	273	16	462		67	98	478	1526	1224	29				0.19
06/24	27	06/24	27	09:14	09:33	61	2.92	385	15	595		91	90	477	1434	1125	30				0.18
06/24	28	06/24	28	09:33	10:42	60	2.65	1790	55	1457		377	229	1365	3521	2358	34				0.05
06/24	29	06/24	29	10:42	11:19	17	2.60	1803	59	1341		406	240	1396	3602	2452					0.02
06/24	1	06/24	1	19:39	23:02	11	2.66	1618	307	9383	1143	1151	393	2096	8191	5796					0.00
06/25	3	06/25	3	00:37	01:04	66	2.63	594	27	1855	200	135	211	480	3658	2438	35				0.14
06/25	4	06/25	4	01:04	01:33	66	2.67	810	30	1915	239	173	210	488	3481	2422	37				0.13
06/25	5	06/25	5	01:33	01:53	67	2.73	708	25	1242	193	159	151	440	2646	1815	31				0.19
06/25	6	06/25	6	01:53	02:07	67	2.72	395	14	724	77	81	82	270	1471	1105	24				0.27
06/25	7	06/25	7	02:07	02:20	67	3.09	244	11	470	43	53	46	176	832	662	16				0.29
06/25	8	06/25	8	02:20	02:31	67	3.11	205	8	410	38	50	33	157	845	711	16				0.34
06/25	9	06/25	9	02:31	02:42	67	3.11	270	10	429	55	61	44	184	870	761	17				0.34
06/25	10	06/25	10	02:42	02:56	67	3.04	177	7	509	30	40	34	132	891	660	30				0.27
06/25	11	06/25	11	02:56	03:12	67	2.87	158	7	1078	32	37	101	174	1805	1120	30				0.23
06/25	12	06/25	12	03:12	03:14	10	2.88	142	7	1031	33	37	82	162	1837	1095					0.29
06/25	13	06/25	13	03:16	03:41	68	2.74	171	10	1270	36	44	132	230	2583	1528	34				0.15
06/25	14	06/25	14	03:45	03:53	18	2.66	273	15	1753	57	66	146	276	3270	1896					0.13
06/25	15	06/25	15	03:57	04:06	26	2.67	289	13	1708	52	66	132	265	3020	1828	28				0.16
06/25	16	06/25	16	04:09	04:17	20	2.65	315	14	1631	60	72	152	281	4000	1954					0.14
06/25	17	06/25	17	04:20	04:27	23	2.70	224	13	1064	55	65	140	272	2823	1688	22				0.18
06/25	18	06/25	18	04:30	04:37	21	2.73	289	13	1423	54	69	135	295	2490	1702	23				0.17
06/25	19	06/25	19	04:35	04:45	13	2.71	434	18	1735	88	86	148	364	2888	2106					0.12
06/25	20	06/25	20	04:48	04:52	10	2.67	541	20	1779	113	105	132	386	3089	2185					0.14

Table 4 San Pedro Hill Cloudwater Data (continued)

San Pedro Hill Cloudwater Data

Date	Sec	Date	Seq	Start	Stop	Vol (ml)	pH	Na+ (uN)	K+ (uN)	NH4+ (uN)	Ca2+ (uN)	Mg2+ (uN)	"Fo" (uN)	Cl- (uN)	NO3- (uN)	SO42- (uN)	CH2O (uM)	H2O2 (uM)	HFo (uM)	HAc (uM)	LWC g/m3
06/25	21	06/25	21	04:55	05:04	19	2.65	611	22	1684	115	110	152	407	3233	2222					0.12
06/25	22A	06/25	22A	reservoir		67	2.74	512	18	1955	90	91	135	476	2575	2234	25				
06/25	22B	06/25	22B	reservoir		44	2.76	520	16	1736	88	96	127	468	2362	2058	24				
06/25	23	06/25	23	05:17	07:33	17	2.64	1266	44	2373	270	256	216	838	3435	3229					0.01
06/26	1	06/26	1	01:48	02:08	33	2.99	315	19	1979	164	86	129	213	2462	1528					0.09
06/26	2	06/26	2	02:08	02:19	39	3.26	113	7	1704	41	30	68	89	1445	1045					0.20
06/26	3	06/26	3	02:19	02:30	40	3.33	87	4	906	19	18	26	77	822	713					0.20
06/26	4	06/26	4	02:30	02:57	37	3.30	168	8	1035	43	39	33	84	1054	762					0.08
06/26	5	06/26	5	02:57	03:06	33	3.27	83	5	1363	22	24	23	43	912	645					0.20
06/26	6	06/26	6	03:06	03:15	36	3.36	49	4	1124	13	16	26	51	1015	747					0.23
06/26	7	06/26	7	03:15	03:24	32	3.39	67	5	1119	23	23	49	88	1096	810					0.20
06/26	8	06/26	8	03:24	03:39	64	3.42	103	7	1415	22	26	58	87	1113	823					0.24
06/26	9	06/26	9	03:39	03:53	68	3.48	41	4	879	17	16	39	55	814	590					0.27
06/26	10	06/26	10	03:53	04:04	39	3.48	98	5	593	19	24	26	106	572	534					0.20
06/26	11	06/26	11	04:04	04:24	66	3.51	114	7	479	27	30	22	94	489	461					0.19
06/26	12	06/26	12	04:24	04:43	65	3.47	59	4	423	12	17	23	58	454	387					0.19
06/26	13	06/26	13	04:43	05:00	69	3.43	41	3	478	11	13	29	51	560	393					0.23
06/26	14	06/26	14	05:00	05:14	64	3.40	28	3	585	9	11	39	49	718	482					0.26
06/26	15	06/26	15	05:14	05:27	63	3.38	33	3	709	8	10	46	47	750	496					0.27
06/26	16	06/26	16	05:27	05:45	69	3.24	46	3	943	10	13	64	64	1051	680					0.21
06/26	17	06/26	17	05:45	05:58	68	3.28	36	3	886	9	10	58	78	955	643					0.29
06/26	18	06/26	18	05:58	06:12	69	3.28	31	3	787	8	11	65	65	966	663					0.27
06/26	19	06/26	19	06:12	06:26	63	3.26	36	3	1026	13	12	70	66	1055	748					0.25
06/26	20A	06/26	20A	reservoir		65	3.06	169	8	1977	38	43	123	196	1626	1553					
06/26	20B	06/26	20B	reservoir		69	3.00	160	10	1818	46	49	146	223	1998	1971					
07/01	1	07/01	1	20:34	21:57	29	3.18	912		638	215	248	88	745	1138	836					0.02
07/01	4	07/01	4	22:07	22:10	8	3.15	618		613	159	176	79	544	936	775					0.15
07/01	8	07/01	8	22:33	22:39	13	3.15	386		522	97	108	67	366	722	658					0.12
07/01	10	07/01	10	22:51	22:56	10	3.18	336		496	79	90	52	339	682	585					0.11
07/01	11	07/01	11	22:59	23:08	17	3.19	372		566	88	99	66	378	704	666					0.11
07/01	13	07/01	13	23:19	23:24	11	3.23	348		545	80	90	54	351	605	609					0.12
07/01	20	07/01	20	reservoir				385		242	57	90	46	453	401	435					
07/02	1	07/02	1	20:00	21:10	60	3.19	528		494	95	133	109	510	713	836					0.05
07/02	2	07/02	2	21:10	22:46	34	3.30	379		394	78	93	98	400	535	492					0.02
07/03	3	07/03	3	00:06	00:55	62	2.91	683		2132	286	202	221	438	3206	1546					0.07
07/03	4	07/03	4	00:55	01:32	61	2.99	345		2309	125	96	210	327	2325	1464					0.09
07/03	5	07/03	5	01:32	02:48	52	2.60	515		2770	209	158	236	532	4131	2562					0.04
07/03	6	07/03	6	02:51	03:50	61	2.47	487		2568	167	149	271	562	4656	3028					0.06
07/03	7	07/03	7	03:50	04:35	62	2.61	392		2156	118	110	219	488	3278	2305					0.08
07/03	8	07/03	8	04:35	05:12	60	2.67	377		1725	98	105	179	454	2768	1903					0.09
07/03	9	07/03	9	05:12	05:46	61	2.64	405		1557	100	115	176	479	2994	1959					0.10
07/03	10	07/03	10	05:46	06:22	60	2.63	308		1682	72	83	180	440	2924	2030					0.09
07/03	11	07/03	11	06:22	06:53	59	2.61	315		1195	71	83	159	365	2874	1691					0.11
07/03	12	07/03	12	06:53	07:25	58	2.58	355		1037	82	95	180	381	2973	1687					0.10
07/03	13	07/03	13	07:25	08:16	58	2.48	446		1426	110	124	256	491	3823	2340					0.06
07/03	14	07/03	14	08:16	09:08	20	2.42	672		1693	186	192	298	656	4631	2957					0.02
07/07	1	07/07	1	00:54	01:29	66	3.33	647		1108	127	145	135	582	1301	810	20	4			0.11
07/07	2	07/07	2	01:29	01:47	57	3.31	388		544	61	88	84	406	812	588	15	9			0.18
07/07	3	07/07	3	01:47	02:02	58	3.34	235		320	28	53	72	284	554	455	14	18			0.21

Table 4 San Pedro Hill Cloudwater Data (continued)

San Pedro Hill Cloudwater Data

Date	Sec	Date	Sec	Start	Stop	Vol (ml)	pH	Na+ (uN)	K+ (uN)	NH4+ (uN)	Ca2+ (uN)	Mg2+ (uN)	"Fe" (uN)	Cl- (uN)	NO3- (uN)	SO42- (uN)	CH2O (uM)	H2O2 (uM)	HFo (uM)	HAc (uM)	LWC ml/m3
07/07	4	07/07	4	02:02	02:24	61	3.25	280		347	32	65	80	341	669	523	18	13			0.16
07/07	5	07/07	5	02:24	03:06	62	3.14	647		433	56	135	109	734	790	722	22	54			0.08
07/07	6	07/07	6	03:06	03:40	61	3.51	503		266	36	106	72	591	332	384	13	61			0.10
07/07	7	07/07	7	03:40	04:21	23	3.44	719		296	57	156	80	821	488	454	12	72			0.03
07/08	1	07/08	1	00:48	01:59	65	2.81	1365		2458	508	335	185	1055	3419	2647					0.05
07/08	2	07/08	2	01:59	02:26	57	2.87	798		1875	213	208	174	623	2446	1878					0.12
07/08	3	07/08	3	02:26	02:48	60	2.93	498		926	126	123	86	363	1557	1123					0.15
07/08	4	07/08	4	02:48	03:10	61	3.02	467		683	100	111	115	355	1211	932					0.15
07/08	5	07/08	5	03:10	03:31	59	3.08	287		431	54	65	89	290	915	686					0.16
07/08	6	07/08	6	03:31	03:54	56	3.12	314		424	56	70	40	353	901	606					0.14
07/08	7	07/08	7	03:54	04:18	60	3.04	274		428	45	61	51	294	1088	687					0.14
07/08	8	07/08	8	04:18	04:19	4	3.91	59		88	20	15		71	172	143					0.25
07/08	9	07/08	9	04:19	04:52	1	3.91														0.00
07/08	10	07/08	10	04:52	04:52	59	3.00	303		481	51	68	59	331	1208	697					
07/08	17	07/08	17	unknown		58	2.86	888		808	166	208	116	760	2142	1190					
07/13	1	07/13	1	02:48	03:25	36	3.79	223		210	52	57	39	264	217	230	10	47	15	6	0.05
07/13	2	07/13	2	03:25	04:07	9	3.83	204		240	45	57	42	242	174	230			17	6	0.01
07/14	1	07/14	1	01:56	02:14	39	3.65	82		220	32	28	40	120	180	292	9		16	8	0.12
07/14	2	07/14	2	02:14	02:24	37	3.75	68		167	17	19	19	95	136	217					0.21
07/14	3	07/14	3	02:24	02:33	35	3.68	97		198	23	28	39	163	154	243	8		14	8	0.22
07/14	4	07/14	4	02:33	02:41	38	3.78	149		161	21	35	1	174	135	218					0.27
07/14	5	07/14	5	02:41	02:53	59	3.83	134		140	16	30	48	171	146	231	5		13	6	0.28
07/14	6	07/14	6	02:53	03:02	38	3.86	147		129	17	34	28	170	113	194					0.23
07/14	7	07/14	7	03:02	03:12	38	3.83	133		153	15	31	28	153	120	219	6		13	6	0.21
07/14	8	07/14	8	03:12	03:22	37	3.80	87		191	13	24	29	123	128	236					0.21
07/14	9	07/14	9	03:22	03:30	36	3.81	77		186	13	22	30	113	130	227	9		12	6	0.25
07/14	10	07/14	10	03:30	03:38	44	3.91	98		148	16	26	26	132	112	182					0.31
07/14	11	07/14	11	03:38	03:47	36	3.82	97		154	13	25	32	135	127	204	7		14	6	0.22
07/14	12	07/14	12	03:47	03:56	39	3.81	85		150	13	24	29	123	129	202					0.24
07/14	13	07/14	13	03:56	04:07	46	3.79	65		159	13	19	30	100	132	196	18		15	7	0.24
07/14	14	07/14	14	04:07	04:19	38	3.61	64		224	19	19	35	100	209	291					0.18
07/14	15	07/14	15	04:19	04:33	40	3.34	84		568	34	27	52	124	547	572	27		18	11	0.16
07/14	16	07/14	16	04:33	04:45	38	3.32	89		659	39	28	62	135	592	622					0.18
07/14	17	07/14	17	04:45	04:55	38	3.32	79		683	40	25	64	134	549	618	38		22	14	0.21
07/14	18	07/14	18	04:55	05:06	39	3.33	78		748	42	25	71	147	559	670					0.20
07/14	19	07/14	19	05:06	05:17	38	3.32	86		977	50	29	79	180	597	757	8		34	18	0.19
07/14	20	07/14	20	reservoir		65	3.14	204		694	55	57	79	240	600	820	28		27	31	
07/14	21	07/14	21	reservoir		29	3.13	207		669	53	59	80	239	592	814					
07/14	1	07/14	1	19:06	19:54	40	3.26	164		391	77	47	72	154	589	473	15	31	43	22	0.05
07/14	2	07/14	2	19:54	20:21	38	3.23	162		391	44	41	120	206	541	521					0.08
07/14	3	07/14	3	20:21	20:39	37	3.41	147		313	33	36	64	161	364	413	10	53	35	13	0.11
07/14	4	07/14	4	20:39	20:54	39	3.47	132		254	29	32	49	137	305	355					0.15
07/14	5	07/14	5	20:54	21:11	40	3.48	121		215	22	29	41	125	251	306					0.13
07/14	6	07/14	6	21:11	21:26	41	3.50	122		184	18	28	39	152	243	293	6	62	20	9	0.15
07/14	7	07/14	7	21:26	21:39	39	3.53	96		182	15	25	41	123	221	272					0.17
07/14	8	07/14	8	21:39	21:51	39	3.54	140		197	22	32	37	138	245	295					0.18
07/14	9	07/14	9	21:51	22:03	37	3.58	177		194	27	38	36	173	238	272	6	62	20	9	0.17
07/14	10	07/14	10	22:03	22:14	38	3.67	180		173	22	38	29	174	199	244					0.20
07/14	11	07/14	11	22:14	22:26	41	3.62	193		169	24	42	29	186	209	268					0.19

Table 4 San Pedro Hill Cloudwater Data (continued)

San Pedro Hill Cloudwater Data

Date	Seq	Date	Seq	Start	Stop	Vol (ml)	pH	Na+ (uN)	K+ (uN)	NH4+ (uN)	Ca2+ (uN)	Mg2+ (uN)	'Fe' (uN)	Cl- (uN)	NO3- (uN)	SO42- (uN)	CH2O (uM)	H2O2 (uM)	HFo (uM)	HAc (uM)	LWC ml/m3
07/14	12	07/14	12	22:26	22:36	38	3.58	185		176	28	41	37	192	235	302	9	53	17	7	0.21
07/14	13	07/14	13	22:36	22:46	40	3.63	177		145	23	39	28	165	192	259					0.23
07/14	14	07/14	14	22:46	22:56	40	3.69	174		138	22	38	26	168	172	230					0.22
07/14	15	07/14	15	22:56	23:06	41	3.73	193		131	25	42	39	186	167	212	10	62	16	7	0.23
07/14	16	07/14	16	23:06	23:17	38	3.68	191		152	28	43	30	173	197	240					0.20
07/14	17	07/14	17	23:17	23:37	38	3.41	216		264	42	51	53	190	383	390					0.11
07/14	18	07/14	18	23:37	23:49	38	3.25	267		377	66	65	73	272	602	550	14	49	29	11	0.18
07/14	19	07/14	19	23:49	00:01	42	3.38	225		299	44	53	53	187	449	401					0.20
07/14	20A	07/14	20A	reservoir			3.44	52		205	17	18	25	57	325	284					
07/14	20B	07/14	20B	reservoir			3.43	40		201	10	13	30	87	316	285	13	19	21	9	
07/15	2	07/15	2	13:18	13:38	18	2.98	242		764	199	79	147	315	857	1417					0.05
07/15	3	07/15	3	19:45	20:50	54	3.28	224		754	197	76	130	181	565	1074					0.05
07/15	4	07/15	4	20:50	21:18	12	3.23	172		746	158	61	222	245	621	995					0.02
07/15	5	07/15	5	22:00	22:43	55	3.05	271		1141	236	100	248	357	1013	1583					0.07
07/15	6	07/15	6	22:43	23:09	55	3.00	145		828	134	51	99	139	927	1214					0.12
07/15	7	07/15	7	23:09	23:33	56	3.07	89		538	81	34	81	117	674	876					0.13
07/15	8	07/15	8	23:33	23:56	55	3.08	79		482	68	30	93	120	685	805					0.13
07/15	9	07/15	9	23:56	00:55	55	2.64	198		2161	235	71	213	217	2797	2438					0.05
07/16	10	07/16	10	00:55	01:11	55	2.86	157		1225	165	58	154	218	1528	1438					0.19
07/16	11	07/16	11	01:11	01:25	56	3.04	101		606	90	36	108	158	880	872					0.22
07/16	12	07/16	12	01:25	01:38	56	3.14	65		427	55	24	78	112	640	643					0.24
07/16	13	07/16	13	01:38	01:53	59	3.12	55		507	52	22	82	110	699	684					0.22
07/16	14	07/16	14	01:53	02:10	55	3.14	29		404	29	13	70	61	591	630					0.18
07/16	15	07/16	15	02:10	02:28	56	3.16	22		391	21	10	57	40	547	548					0.17
07/16	16	07/16	16	02:28	02:44	56	3.27	28		330	31	12	48	47	448	438					0.19
07/16	17	07/16	17	Reservoir		68	3.93	24		328	14	8	22	47	190	219					
07/16	2	07/16	2	15:35	16:07	55	3.56	84		284			36	84	249	259					0.10
07/16	3	07/16	3	16:07	16:19	55	3.74	33		160			29	50	147	215					0.26
07/16	4	07/16	4	16:19	16:45	25	3.67	33		142			29	44	167	203					0.05
07/16	5	07/16	5	17:40	18:30	55	3.50	92		207			51	98	280	277					0.06
07/16	6	07/16	6	18:30	19:02	27	3.64	63		187	27	22	43	70	231	248					0.05
07/16	7	07/16	7	19:14	19:37	56	3.51	75		242	47	28	47	88	295	329					0.14
07/16	8	07/16	8	19:37	19:49	56	3.55	52		126			18	55	145	295					0.26
07/16	9	07/16	9	19:49	20:03	26	3.86	35		98	13	11	15	39	116	170					0.10
07/16	10	07/16	10	20:03	20:18	56	4.06	24		80	9	7	13	30	96	114					0.21
07/16	11	07/16	11	20:18	20:33	55	4.14	20		70	8	7	10	28	84	93					0.21
07/16	12	07/16	12	20:33	20:50	56	4.15	20		66	9	7	10	27	77	104					0.18
07/16	13	07/16	13	20:50	21:04	56	4.30	19		56	8	6	8	25	53	74					0.23
07/16	14	07/16	14	21:04	21:25	56	4.48	16		66			11	23	43	58					0.15
07/16	15	07/16	15	21:25	21:43	55	4.58	10		80				21	37	69					0.17
07/16	16	07/16	16	21:43	22:04	56	4.32	8		71				14	35	77					0.15
07/16	17	07/16	17	22:04	22:23	56	4.46	9		53				11	34	60					0.16
07/16	18	07/16	18	22:23	22:40	55	4.98	6		47	3	1		13	28	39					0.18
07/16	19	07/16	19	22:40	22:53	56	4.75	11		44	5	3		14	30	55					0.24
07/17	20	07/17	20	reservoir		33	3.80	49		504			33	79	300	376					
07/17	21	07/17	21	reservoir		34	4.65	45		134			?	56	60	98					
				Number		240	242	241	63	242	225	231	236	242	242	242	80	16	21	21	227
				Minimum			2.42	6	3	44	3	1	1	11	28	39	5	4	12	6	0.00
				Maximum			4.98	3796	307	9383	1143	1151	586	2096	8191	5796	51	72	43	31	0.34
				Aritm. Avg			3.25	404	19	775	82	107	103	369	1185	917	23	42	21	10	0.14

Table 5 Henninger Flats Cloudwater Data

Henninger Flats Cloudwater Data

Date	Seq	Start	Stop	Vol (ml)	pH	Na+ (uN)	NH4+ (uN)	Ca2+ (uN)	Mg2+ (uN)	Cl- (uN)	NO3- (uN)	SO42- (uN)	CH2O (uM)	H2O2 (uM)	HFo (uM)	HAc (uM)	LWC ml/m3
06/20	1	05:00	06:19	65	3.59	272	1009	73	71	181	974	455	75				0.05
06/20	2	06:19	06:56	45	3.35	180	805	39	48	169	877	447	75				0.07
06/20	3	06:56	07:36	24	3.19	192	921	46	52	177	1220	537	80				0.03
06/20	5	08:08	08:47	64	3.04	387	1461	90	103	308	1841	845	91				0.09
06/20	6	08:47	09:30	45	2.92	571	1742	117	155	452	2329	996	66				0.06
06/20	7	09:30	11:03	43	2.75	1652	3505	454	435	975	4034	2028	68				0.03
06/21	1	01:28	02:30	7	3.75	314	603	118	86	161	787	36					0.01
06/21	5	02:49	05:06	44	3.15	901	2411	269	257	496	2796	1371	76				0.02
06/21	6	05:06	05:53	43	3.04	454	1743	75	129	314	1982	1061	67				0.05
06/21	7	05:53	06:20	44	2.97	330	1467	93	86	258	1802	934	65				0.09
06/21	8	06:20	06:34	45	3.04	243	1161	63	63	215	1420	773	54				0.18
06/21	9	06:34	06:50	44	3.06	193	945	46	54	202	1270	705	53				0.15
06/21	10	06:50	07:08	44	3.04	183	954	42	49	195	1252	704	58				0.14
06/21	11	07:08	07:41	44	2.91	254	1229	60	67	223	1254	842	62				0.08
06/21	12	07:41	08:12	44	2.87	339	1487	85	91	266	1986	1094	64				0.08
06/21	13	08:12	08:39	44	2.84	434	1708	111	113	295	2233	1243	66				0.09
06/21	14	08:39	09:19	44	2.77	624	2122	188	157	400	3143	1642	75				0.06
06/21	15	09:19	10:03	18	2.62	1553	3172	520	400	666	5472	2606	105				0.02
07/09	1	23:47	01:38	36	3.88	127	1502	129	51	198	802	582					0.02
07/10	2	01:38	03:09	35	3.58	157	1760	167	63	214	1181	937					0.02
07/10	3	03:09	05:07	29	3.28	125	1530	127	52	197	1377	810					0.01
07/10	4	05:22	05:58	35	3.12	195	1295	159	99	200	1665	802					0.06
07/10	5	05:58	07:07	35	3.07	92	996	96	46	124	1327	438					0.03
07/10	6	07:07	07:31	35	3.21	50	796	47	20	101	923	368					0.08
07/10	7	07:31	08:08	34	3.16	55	843	49	20	111	993	412					0.05
07/10	8	08:08	08:31	36	3.15	65	954	61	24	112	1144	608					0.09
07/10	9	08:31	09:05	35	3.15	77	1103	71	30	117	1053	544					0.06
07/10	10	09:05	09:19	36	3.24	66	912	70	31	108	984	642					0.14
07/10	11	09:19	09:33	36	3.26	48	671	55	21	91	747	429					0.14
07/10	12	09:33	09:46	36	3.31	58	700	62	23	92	735	408					0.16
07/10	13	09:46	10:00	36	3.28	58	743	64	24	93	854	545					0.14
07/10	14	10:00	10:14	36	3.25	56	761	65	26	104	786	431					0.14
07/10	15	10:14	10:26	36	3.26	56	704	66	24	100	786	431					0.17
07/10	16	10:26	10:44	36	3.20	70	880	87	29	109	941	524					0.11
07/10	17	10:44	10:59	36	3.20	59	845	80	25	104	917	497					0.14
07/10	18	10:59	11:15	35	3.15	75	970	102	31	127	1096	591					0.12
07/10	19	11:15	11:30	35	3.17	67	937	96	31	112	1152	691					0.13
07/10	20	reservoir		63	2.88	92	1545	159	47	140	2065	1094					
07/16	1	00:17	01:42	50	2.95	83	2597	146	46	66	1153	916					0.03
07/16	2	01:43	02:17	9	2.73	149	4085	234	75	68	1908	1474					0.01
07/16	4	02:48	03:50	62	2.83	77	3301	126	41	55	1307	1103					0.06
07/16	5	03:50	04:59	62	2.84	58	3108	90	29	59	1211	908					0.05
07/16	6	04:59	05:24	62	2.95	40	2219	61	19	43	879	772					0.14
07/16	7	05:24	05:43	63	3.05	33	1395	42	14	44	635	426					0.19
07/16	8	05:43	06:08	62	3.12	25	1397	32	11	40	641	464					0.14
07/16	9	06:08	06:24	63	3.14	28	1172	31	11	44	1164	842					0.22
07/16	10	06:24	06:36	64	3.46	50	724	43	17	41	683	480					0.30
07/16	11	06:36	06:45	64	3.65	50	597	40	17	38	478	310					0.40
07/16	12	06:45	06:55	64	3.65	41	571	31	14	54	464	294					0.36
07/16	13	06:55	07:05	64	3.69	31	562	23	11	59	482	315					0.36
07/16	14	07:05	07:14	64	4.78	23	502	19	9	25	452	281					0.40
07/16	15	07:14	07:24	65	3.84	15	492	12	6	22	413	259					0.36
07/16	16	07:24	07:35	64	3.70	13	447	11	5	26	397	238					0.33
07/16	17	07:35	07:45	65	3.77	10	393	9	3	19	332	177					0.37

Table 5 Henninger Flats Cloudwater Data (continued)

Henninger Flats Cloudwater Data

Date	Seq	Start	Stop	Vol (ml)	pH	Na+ (uN)	NH4+ (uN)	Ca2+ (uN)	Mg2+ (uN)	Cl- (uN)	NO3- (uN)	SO42- (uN)	CH2O (uM)	H2O2 (uM)	HFo (uM)	HAc (uM)	LWC ml/m3
07/16	18	07:45	07:54	64	3.80	6	324	7	3	18	284	139					0.40
07/16	19	07:54	08:06	65	3.81	5	329	8	2	18	288	137					0.30
07/16	20A	reservoir		63	2.68	80	2118	397	77	115	1643	787					
07/16	20B	reservoir		31	2.83	52	1515	242	50	103	1164	648					
07/16	2	16:56	17:49	61	3.03	273	2435	985	171	301	3319	2028					0.07
07/16	3	17:49	18:16	61	3.30	139	1235	518	86	155	1416	993					0.13
07/16	4	18:16	18:40	62	3.29	85	1149	265	65	98	1167	796					0.15
07/16	5	18:40	19:03	62	3.29	77	1016	234	59	90	1055	758					0.15
07/16	6	19:03	19:28	63	3.20	64	1092	189	50	81	1030	824					0.14
07/16	7	19:28	19:51	63	3.25	50	1020	136	41	80	1011	906					0.15
07/16	8	19:51	20:14	63	3.26	51	999	128	38	80	979	874					0.15
07/16	9	20:14	20:35	63	3.26	50	848	125	36	76	929	741					0.17
07/16	10	20:35	20:53	63	3.24	35	786	101	31	54	940	565					0.20
07/16	11	20:53	21:11	64	3.22	31	741	87	28	48	1029	660					0.20
07/16	12	21:11	21:28	64	3.27	23	639	56	20	39	827	447					0.21
07/16	13	21:28	21:44	64	3.32	27	516	66	22	40	751	366					0.22
07/16	14	21:44	22:00	65	3.41	18	398	43	16	22	604	274					0.23
07/16	15	22:00	22:16	65	3.52	12	356	33	12	29	496	221					0.23
07/16	16	22:16	22:34	65	3.48	20	404	38	13	32	560	241					0.20
07/16	17	22:34	22:55	64	3.49	17	387	32	12	32	513	212					0.17
07/16	18	22:55	23:27	64	3.48	13	411	32	12	38	549	235					0.11
07/17	19	reservoir		40	3.94	3	273	15	7	27	231	155					
		N		76	76	76	76	76	76	76	76	76	17				72
		Arith. Avg.		3765	3.25	166	1203	118	57	142	1206	689	71				0.14
		Min			2.62	3	273	7	2	18	231	36	53				0.01
		Max			4.78	1652	4085	985	435	975	5472	2606	109				0.40

Table 6 San Pedro Hill Aerosol Data

Date	Seq	START	STOP	Na+	NH4+	Ca2+	Mg2+	Cl-	NO3-	SO42-	NH3	HNO3
				neq / m3							—	—
06/19	A	01:00	05:00	170	119	25.1	44.3	90.2	142	113	-0.9	15.5
06/19	B	06:00	09:00	188	74	15.9	42.4	105.4	81	124	-1.2	26.6
06/19	C	09:00	12:00	181	93	22.1	46.3	88.9	103	133	-1.2	27.1
06/19	D	20:00	00:00	115	94	24.8	33.5	51.5	102	104	14.5	28.4
06/20	A	02:00	06:00	60	73	17.2	29.5	60.2	94	93	2.9	10.7
06/20	B	08:00	12:00	168	89	17.8	45.2	72.3	99	127	-0.9	23.6
06/23	A	20:00	00:00	110	NA	19.9	26.2	34.1	187	294	-0.9	123.7
06/24	A	00:00	03:00	24	NA	14.4	2.5	7.9	51	37	-1.2	-0.5
06/24	B	03:00	06:00	67	NA	27.2	18.6	86.9	435	475	-1.2	12.9
06/24	C	07:30	08:00	13	318	16.1	6.7	0.0	43	340	-7.5	106.8
06/24	D	10:00	14:00	171	194	18.4	19.1	8.8	108	267	-0.9	140.5
06/24	E	14:00	18:00	173	162	34.9	48.8	39.5	147	188	38.4	131.8
06/24	F	20:00	00:00	59	447	17.5	26.0	7.6	211	317	-0.9	46.7
06/25	A	01:15	05:00	32	297	17.0	6.3	NA	32	338	0.6	17.3
06/25	B	05:00	09:00	5	17	15.3	0.0	NA	7	22	19.1	-0.1
06/25	C	07:57	10:30	90	261	47.3	15.4	0.0	68	314	-1.5	162.7
06/25	D	11:00	15:00	99	197	30.4	26.3	0.0	81	255	6.8	133.0
06/25	E	16:00	20:00	NA	NA	NA	NA	NA	NA	NA	0.0	92.3
06/25	F	22:00	02:00	53	624	34.9	17.2	7.5	385	291	10.6	41.3
07/06	A	20:00	00:00	122	NA	23.8	26.4	64.4	189	131	-0.9	NA
07/07	A	00:00	04:00	70	NA	18.0	14.5	67.2	136	125	-0.9	21.1
07/07	C	09:00	12:00								0.0	35.9
07/07	E	09:00	12:00	NA	NA	NA	NA	NA	NA	NA	49.2	38.5
07/07	D	14:00	18:00	NA	NA	NA	NA	NA	NA	NA	0.0	26.7
07/12	A	20:00	00:00	15	55	19.9	3.6	0.0	20	55	16.0	49.1
07/13	A	00:00	03:00	0	1	18.7	1.8	0.0	6	4	-1.2	-2.3
07/13	B	03:00	06:00	17	94	55.9	8.6	20.7	38	70	21.4	79.0
07/13	C	08:00	12:00	69	375	32.9	18.8	0.7	90	182	104.8	158.2
07/13	D	12:00	15:00	76	132	25.6	17.3	2.9	89	135	61.5	80.3
07/13	E	15:00	18:00	44	79	17.7	10.9	0.0	34	79	36.8	38.5
07/13	F	20:10	00:00	21	68	27.4	11.5	0.0	20	94	28.8	22.0
07/14	A	02:00	06:00	14	161	6.8	1.7	0.0	6	180	-0.9	6.3
07/14	B	08:00	12:00	61	430	25.4	17.7	0.0	41	448	2.9	166.0
07/14	C	14:00	18:00	73	NA	28.9	16.6	10.8	57	179	45.4	79.9
07/14	D	20:00	00:00	11	0	15.8	3.7	12.7	NA	42	-0.9	3.4
07/15	A	02:00	04:00	7	0	5.6	0.0	NA	23	32	-1.9	5.9
07/15	B	04:00	06:00	0	NA	0.0	0.0	NA	86	96	-1.9	0.9
07/15	C	06:00	08:00	20	NA	7.1	0.9	19.9	124	166	-1.9	NA
07/15	D	08:00	10:00	7	NA	19.0	0.0	35.0	46	82	-1.9	NA
07/15	E	10:00	11:30	0	NA	0.0	0.0	NA	16	75	-2.5	NA
07/15	F	14:00	18:00	24	NA	17.8	7.3	16.3	36	101	19.9	NA
07/15	G	20:00	00:00	14	NA	38.8	8.3	26.8	137	200	-0.9	NA

NA indicates sample not analyzed

Table 7 Henninger Flats Aerosol Data

Date	Seq	START	STOP	Na+	NH4+	Ca2+	Mg2+	Cl-	NO3-	SO42-	NH3	HNO3
				neq / m3								
06/19	A	01:00	05:00	5	3	0.1	0.0	0.0	9	5	-0.9	12.8
06/19	B	06:00	09:00	0	5	0.0	0.0	0.0	8	5	-1.2	10.9
06/19	C	09:00	12:00	1	4	1.4	1.4	0.0	7	7	-1.2	17.5
06/24	A	02:00	06:00	33	77	24.3	11.8	2.3	51	74	2.9	65.4
06/24	B	06:00	10:00	36	117	12.5	13.9	0.0	63	102	-0.9	161.5
06/24	C	10:00	14:00	134	838	71.3	53.6	28.7	442	533	78.5	812.2
06/24	A	17:00	20:00	107	551	63.9	23.2	0.0	193	446	24.5	479.1
06/24	B	20:00	00:00	59	239	28.3	13.8	NA	114	189	30.7	47.4
06/25	B	14:00	18:00	106	645	92.9	27.3	22.5	287	479	98.6	897.0
06/25	C	20:00	00:00	38	284	32.8	9.4	0.0	83	234	18.4	78.4
06/25	A	02:00	06:00	54	250	34.7	14.8	NA	77	217	10.6	69.4
06/26	A	02:00	06:00	44	188	34.6	12.9	21.2	65	174	20.7	112.7
07/06	A	20:00	00:00	56	193	30.9	13.7	0.0	123	141	-0.9	63.1
07/07	A	02:00	06:00	29	75	16.4	7.6	0.0	46	66	-0.9	28.4
07/07	B	08:00	12:00	75	421	46.3	22.4	0.0	202	311	6.8	277.8
07/12	A	20:00	00:00	21	93	33.5	9.3	7.8	28	81	26.8	72.9
07/13	A	02:00	06:00	4	27	2.9	4.0	0.0	12	33	9.1	17.4
07/13	B	08:00	12:00	21	183	27.9	13.7	0.0	99	96	91.7	251.2
07/14	A	20:00	00:00	35	151	27.7	13.2	NA	76	116	23.8	
07/15	A	02:00	06:00	15	111	10.7	4.0	0.0	30	95	1.4	
07/15	B	08:00	12:00	54	543	38.8	14.8	NA	254	313	58.5	

NA indicates sample not analyzed

Table 8 Kellogg Hill Aerosol Data

Date	Seq	START	STOP	Na+	NH4+	Ca2+	Mg2+	Cl-	NO3-	SO42-	NH3	HNO3
				neq / m3							--	
06/19	A	01:00	05:00	183	178	73.4	60.3	72.1	190	136	283.0	9.5
06/19	B	06:00	09:00	168	273	95.8	60.8	62.7	226	191	192.2	16.0
06/19	C	09:00	12:00	8	9	62.3	12.0	0.0	10	7	-1.2	6.1
06/24	A	02:00	06:00	140	581	64.6	41.9	15.6	452	291	-0.9	59.8
06/24	B	06:00	10:00	145	767	153.6	59.8	15.8	582	359	26.8	152.2
06/24	C	10:00	13:50	149	875	192.8	61.6	0.0	567	451	131.9	624.0
06/24	D	20:00	00:00	124	250	78.3	35.8	0.0	234	203	34.6	52.7
06/24	E	02:00	06:00	125	594	109.3	25.6	0.0	392	372	26.8	63.1
06/25	B	20:00	00:00	84	279	51.3	28.2	10.9	191	167	58.5	52.3
06/25	C	02:00	06:00	62	549	40.1	11.1	12.0	372	271	34.6	43.4
06/25	D	08:00	12:00	66	838	116.3	32.2	0.2	496	441	154.9	385.8
06/25	A	08:00	12:00	115	784	179.0	48.8	NA	629	415	279.2	360.8
07/06		20:00	00:00	95	258	88.4	20.6	6.8	232	155	65.4	48.2
07/07		08:00	12:00	108	383	160.6	39.4	10.8	300	249	46.9	210.7
07/07		02:00	06:00	140	494	103.3	41.8	25.6	423	220	35.3	37.8
07/12	A	20:10	00:00	44	139	60.1	16.9	1.3	91	94	146.4	44.0
07/13	A	01:00	05:00	70	177	58.4	21.7	12.4	124	108	102.5	8.8
07/13	B	07:00	11:00	54	368	269.7	53.1	4.9	309	149	339.3	197.4

NA indicates sample not analyzed

Table 9 Collector Blank Analyses

Date	Site	Description	Na+ (uN)	NH4+ (uN)	Ca2+ (uN)	Mg2+ (uN)	Cl- (uN)	NO3- (uN)	SO42- (uN)
06/13	SPH	reservoir only after rinse	0	0	0	0	0	0	0
06/13	SPH	first after rinse	2	4	3	1	7	0	0
06/13	SPH	second after rinse	1	3	1	0	6	0	0
06/18	SPH	reservoir only after rinse	7	2		2	13	9	9
06/18	SPH	blank #1 after rinsing	50	16		10	49	22	21
06/16	SPH	blank #2 after rinsing	27	10		6	32	17	18
06/20	SPH	clean bottle left in fridge	0	0	0	0	6	0	9
06/21	SPH	blank after rinsing	78	16	14	20	68	48	26
06/22	SPH	blank after rinsing	40	54	13	12	33	77	71
06/23	SPH	reservoir only after rinse	5	7	1	2	8	15	11
06/24	SPH			64	4		6	44	52
06/25	SPH	blank after cleaning			5		23	80	74
07/02	SPH	blank after rinsing	211	83	39	54	134	228	144
07/06	SPH	blank after rinsing		30	4	5	20	47	46
07/07	SPH	unused bottle		0	0	0	0	0	0
07/07	SPH	blank after rinsing		11	3	5	25	20	16
07/12	SPH	blank after rinsing	2	3	4	2	5	7	6
07/13	SPH	blank after rinsing	3	7	1	2	8	12	8
07/13	SPH	blank at 2000	24	17	10	9	16	33	20
07/14	SPH	blank after rinsing	15	27	8	6	3	22	42
07/14	SPH	blank after rinsing	5	11	4	2	1	11	15
07/15	SPH	blank on large rods	0	0	0	0	0	0	0
06/09	HF	blank after rinsing	1	2	0	0	0	0	0
06/05	HF	blank after rinsing	1	3	0	0	0	0	0
06/14	HF	blank after rinsing	7	27	7	3	7	0	32
06/15	HF	blank after rinsing	2	6	2	1	0	0	0
06/18	HF	rinse blank	3	15	2	1	11	20	11
06/15	HF	sitting overnight w/o rinse	67	80	30	19	18	133	72
06/19	HF	after 100 ml rinse	18	27	10	5	10	44	24
06/20	HF	reservoir only after rinse	13	25	1	3	8	36	20
06/20	HF	system after rinse	33	50	9	8	14	75	36
06/22	HF	post cleaning strands, left in fridge	5	19	2	2	3	23	19
06/23	HF	blank after rinsing	8	29	0	5	27	48	23
06/24	HF	blank after rinsing	0	0	0	0	7	0	0
06/25	HF	reservoir only after rinse	1	2	0	0	0	0	0
06/30	HF	blank #1 after rinsing	9	17	8	4	7	47	14
06/30	HF	blank #2 after rinsing	5	10	4	1	8	23	8
07/02	HF	blank after rinsing	3	13	5	1	23	19	12
07/04	HF	blank after rinsing	1	9	2	0	6	15	7
07/07	HF	blank after rinsing	27	28	13	8	8	73	21
07/08	HF	blank after rinsing	147	314			74	419	206
07/05	HF	reservoir only after rinse	1	0	0	0	6	6	0
07/09	HF	system after rinse	10	3	1	0	8	12	0
07/05	HF	system after rinse	6	3	1	0	7	10	6
07/10	HF	blank after rinsing	0	3	1	0	6	8	0
07/11	HF	rinse of bottle sitting in fridge	0	0	0	0	24	0	0
07/12	HF	before rinsing, sat 2 days w/o sampling	19	117	39	15	10	102	98
07/12	HF	after rinsing	1	4	2	0	4	6	6
07/13	HF	collector only, left in fridge overnight	1	7	3	1	6	14	6
07/14	HF	blank after rinsing	3	11	6	1	5	18	8
07/14	HF	blank after rinsing	3	11	6	2	4	17	10
07/15	HF	blank after rinsing	2	104	2	1	6	17	0
07/15	HF	blank after rinsing	1	60	2	0	8	21	0
07/17	HF	blank after rinsing	1	10	1	0	4	11	0

Table 10 Size-fractionated sample concentrations

Date	f/b	Seq	Start	Stop	Vol (ml)	pH	Na+ (uN)	NH4+ (uN)	Ca2+ (uN)	Mg2+ (uN)	Cl- (uN)	NO3- (uN)	SO42- (uN)	S(IV) (uM)	CH2O (uM)	H2O2 (uM)	HFo (uM)	HAc (uM)	-/+	Rate ml/min
07/15	f	21	04:00	04:30	70	3.40	18	190	7	5	38	356	251						1.04	2.3
07/15	f	22	04:33	05:00	68	3.34	30	251	12	8	66	396	355		10	10	19	11	1.08	2.5
07/15	f	23	05:00	05:30	71	3.27	48	323	22	13	75	465	461		16	0	21	13	1.06	2.4
07/15	f	24	05:30	06:00	71	3.26	53	615	55	16	70	618	595		27	0	40	19	1.00	2.4
07/15	f	25	06:00	06:30	74	3.29	64	899	40	19	65	706	732		29	0	37	18	0.98	2.5
07/15	f	26	06:30	07:00	112	3.42	87	391	22	21	81	399	436		16	0	26	11	1.02	3.7
07/15	f	27	07:00	07:30	121	3.42	55	202	12	14	72	276	343		13	0	17	9	1.04	4.0
07/15	f	28	07:30	08:00	136	3.44	36	191	8	10	58	219	328		13	4	18	9	0.99	4.5
07/15	f	29	08:00	08:30	122	3.49	25	192	6	7	42	223	298		13	10	18	10	1.02	4.0
07/15	f	30	08:30	09:00	116	3.52	23	166	8	7	40	204	271		13	16	20	9	1.02	3.9
07/15	f	31	09:00	09:30	114	3.56	45	164	17	13	48	188	242						0.93	3.8
07/15	f	32	09:30	10:00	110	3.64	39	138	13	11	122	178	214						1.19	3.7
07/15	f	33	10:00	10:30	56	3.42	27	234	20	10	35	182	228						0.68	1.9
07/15	f	34	10:30	11:00	64	3.40	48	275	54	19	84	337	418		18	49	33	13	1.06	2.1
07/15	f	35	11:30	12:00	40	3.54	161	274	217	57	116	341	564						1.02	1.3
07/15	f	36	12:00	13:00	30	3.38	478	432	515	175	326	730	1087						1.06	0.5
			Samples from rear strands: Small droplets																	
07/15	b	21	04:00	04:30	43	3.56	7	171	4	2	25	233	182						0.98	1.4
07/15	b	22	04:33	05:00	29	3.42	11	267	5	3	57	326	301		11	9	16	10	1.03	1.1
07/15	b	23	05:00	05:30	28	3.28	12	376	6	4	57	478	433		13	0	18	11	1.05	0.9
07/15	b	24	05:30	06:00	31	3.10	13	804	8	3	100	823	684		26	8	34	17	0.99	1.0
07/15	b	25	06:00	06:30	28	3.08	14	1479	7	4	118	1152	1016		55	8	38	22	0.98	0.9
07/15	b	26	06:30	07:00	38	3.24	11	945	4	2	88	728	692		25	8	32	20	0.98	1.3
07/15	b	27	07:00	07:30	39	3.35	13	424	4	4	76	401	432		17	0	18	9	1.02	1.3
07/15	b	28	07:30	08:00	38	3.38	12	341	3	3	52	303	383		16	3	19	9	0.96	1.3
07/15	b	29	08:00	08:30	30	3.42	16	317	7	5	51	281	397		17	6	19	10	1.01	1.0
07/15	b	30	08:30	09:00	32	3.47	18	260	9	7	52	242	352		14	11	23	10	1.02	1.1
07/15	b	31	09:00	09:30	22	3.49	10	242	5	3	34	187	280						0.86	0.7
07/15	b	32	09:30	10:00	35	3.59	14	205	7	5	105	184	250						1.11	1.2
07/15	b	33	10:00	10:30	16	3.46	21	282	15	8	50	256	350						0.97	0.5
07/15	b	34	10:30	11:00	30	3.25	35	488	22	14	123	462	606		21	39	40	17	1.06	1.0
07/15	b	35	11:30	12:00	16	3.24	29	478	30	12	96	408	654						1.03	0.5
07/15	b	36	12:00	13:00	14	2.96	76	685	73	30	172	705	1143						1.03	0.2
			Combined Values																	"LWC" (ml/m3
07/15		21	04:00	04:30	112	3.45	14	182	6	4	33	309	229						1.02	0.21
07/15		22	04:33	05:00	97	3.36	24	256	10	6	63	376	339		10				1.06	0.20
07/15		23	05:00	05:30	99	3.27	38	338	18	10	70	469	453		15				1.06	0.18
07/15		24	05:30	06:00	102	3.20	41	672	41	12	79	680	622		27				0.99	0.19
07/15		25	06:00	06:30	101	3.22	50	1057	31	15	79	827	809		36				0.98	0.19
07/15		26	06:30	07:00	150	3.37	67	532	18	16	83	483	501		18				1.00	0.28
07/15		27	07:00	07:30	160	3.40	45	256	10	12	73	307	365		14				1.04	0.30
07/15		28	07:30	08:00	174	3.43	31	224	7	8	57	238	342		14				0.99	0.32
07/15		29	08:00	08:30	151	3.48	23	216	6	7	44	234	318		13				1.01	0.28
07/15		30	08:30	09:00	147	3.51	22	186	8	7	42	212	288		13				1.02	0.28
07/15		31	09:00	09:30	136	3.55	39	177	15	11	46	188	248						0.92	0.25
07/15		32	09:30	10:00	145	3.63	33	154	12	10	118	180	223						1.17	0.27
07/15		33	10:00	10:30	71	3.43	26	244	19	10	38	206	255						0.74	0.13
07/15		34	10:30	11:00	94	3.35	44	344	44	17	97	377	478		19				1.06	0.18
07/15		35	11:30	12:00	57	3.43	123	332	164	44	110	360	590						1.03	0.11
07/15		36	12:00	13:00	44	3.20	351	512	374	129	277	722	1105						1.05	0.04

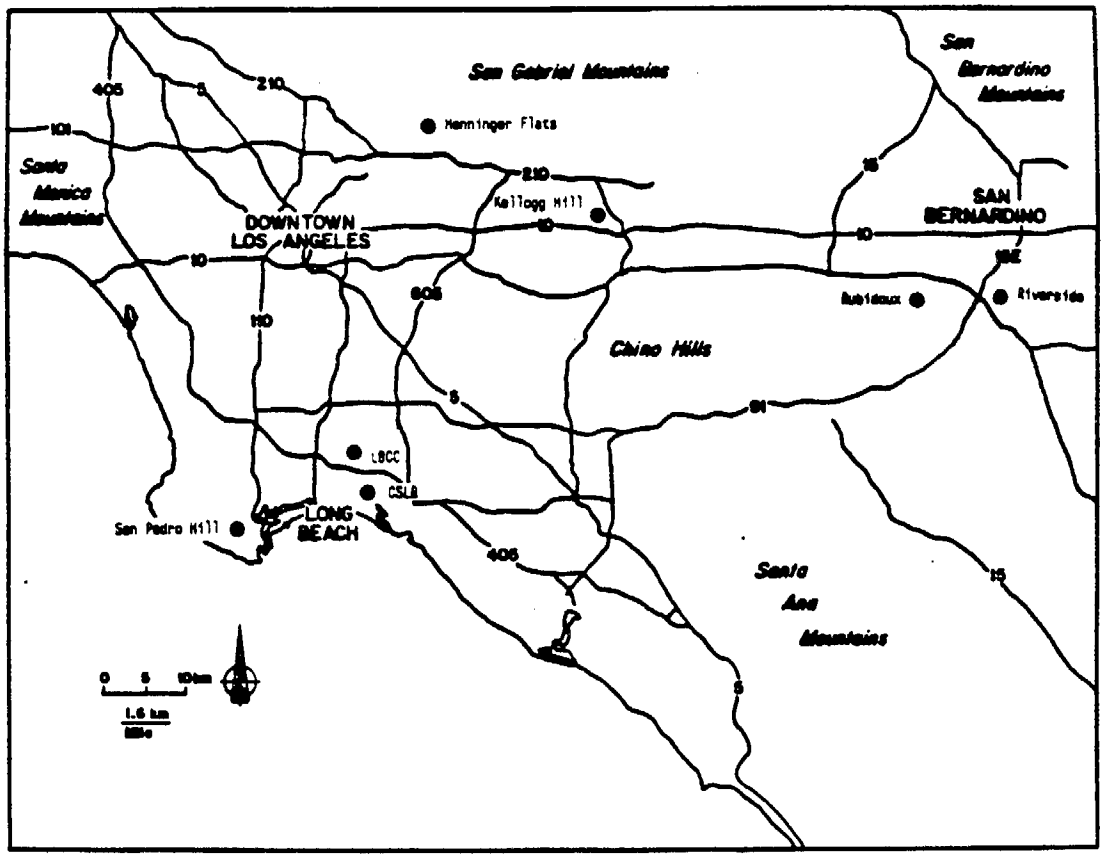

Figure 1. Map of the Los Angeles area showing the seven sites used for sampling cloud and fogwater, aerosol, and selected gases during the summer and winter portions of the South Coast Air Quality Study (SCAQS). Sites are depicted by a bold dot. Also shown on the map are major freeways and mountains.

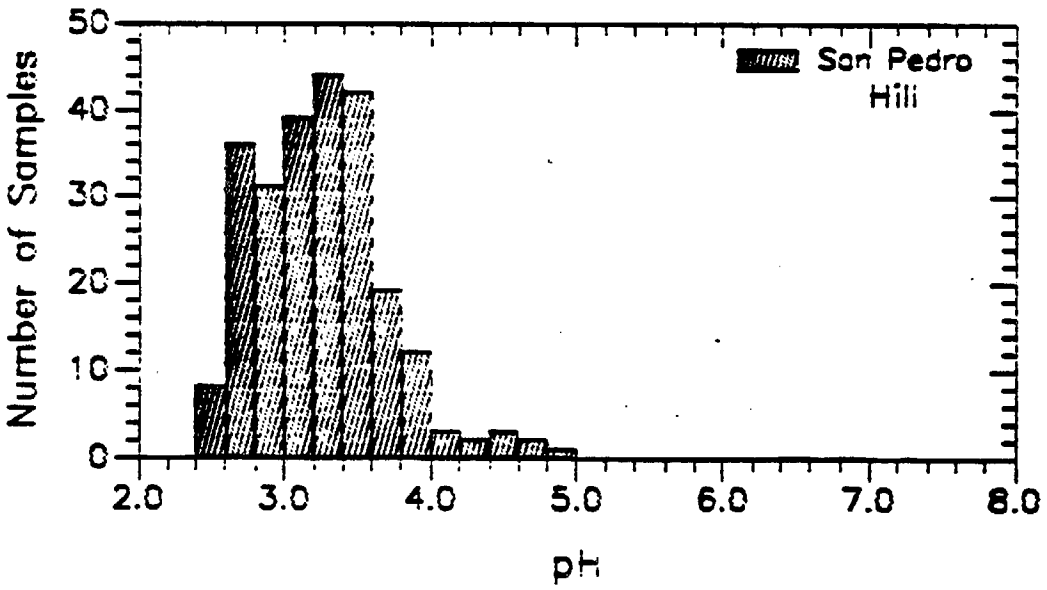

Figure 2. pH distribution of intercepted stratus cloudwater samples collected at San Pedro Hill during the summer of 1987.

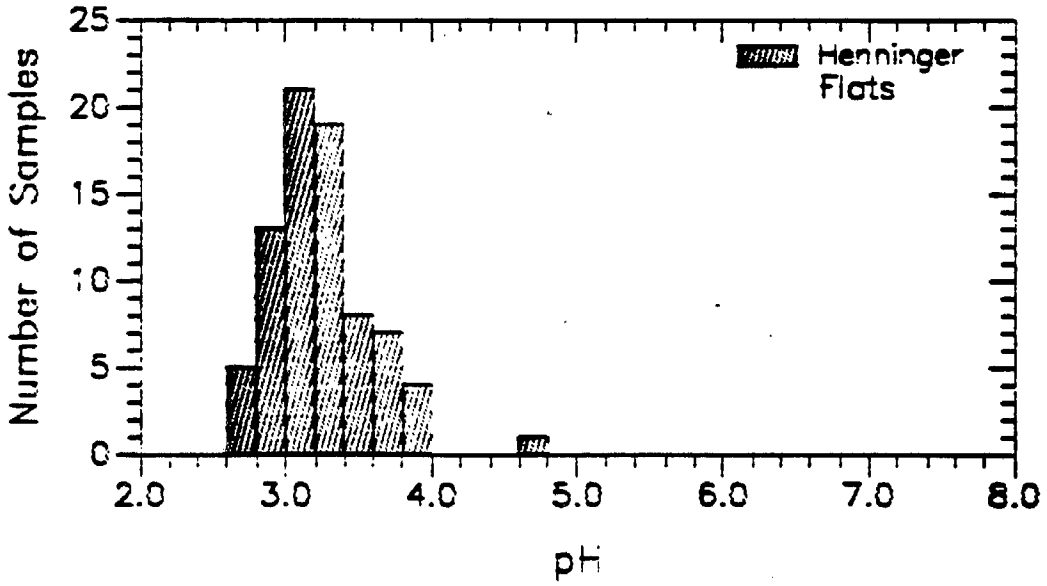

Figure 3. pH distribution of intercepted stratus cloudwater samples collected at Henninger Flats during the summer of 1987.

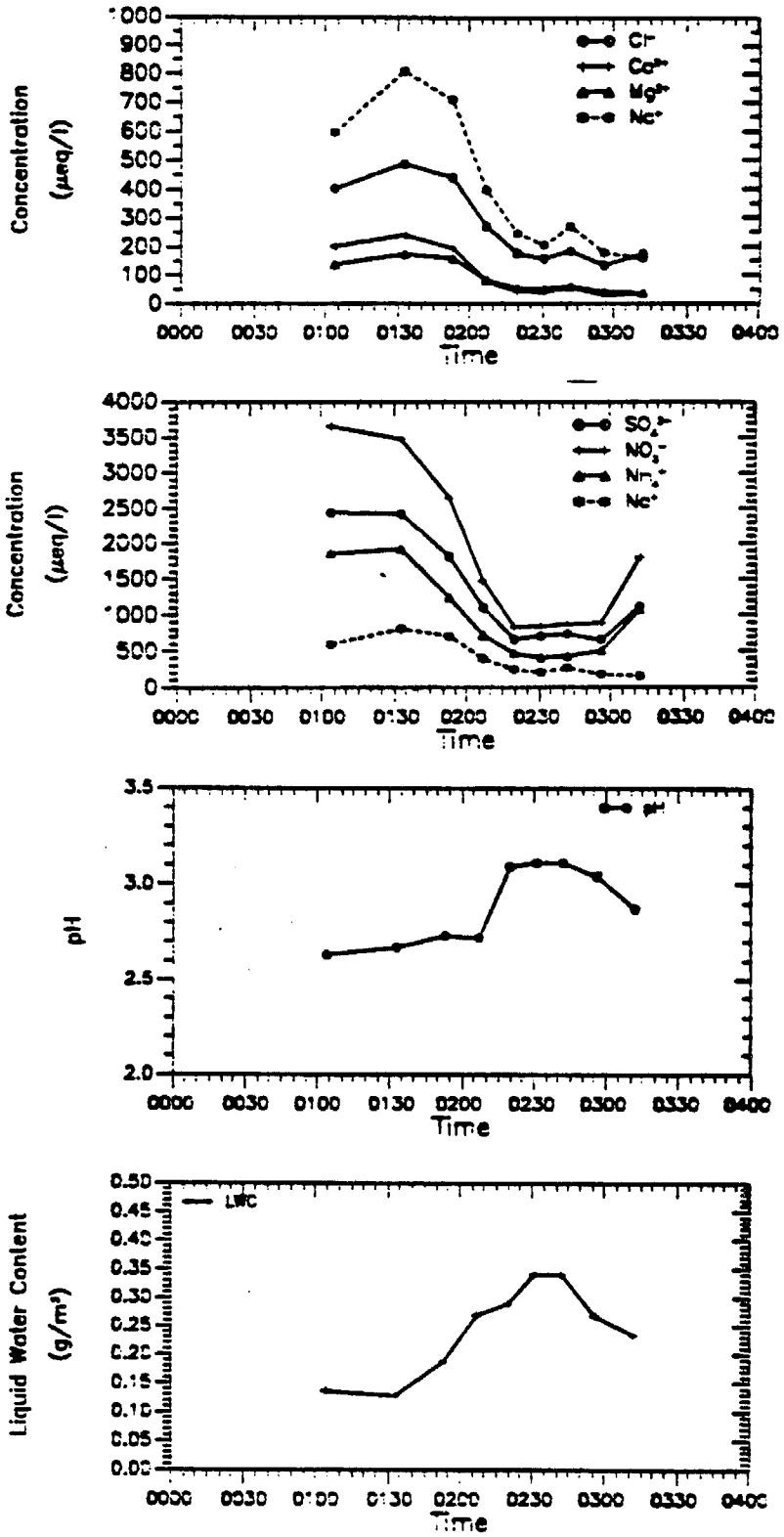

Figure 4. Time trace indicating rapid changes of observed species concentrations, pH, and liquid water content during the morning of June 25, 1987, at San Pedro Hill. Samples were collected as rapidly as one every ten minutes by the CASC and the autosampler during this period.

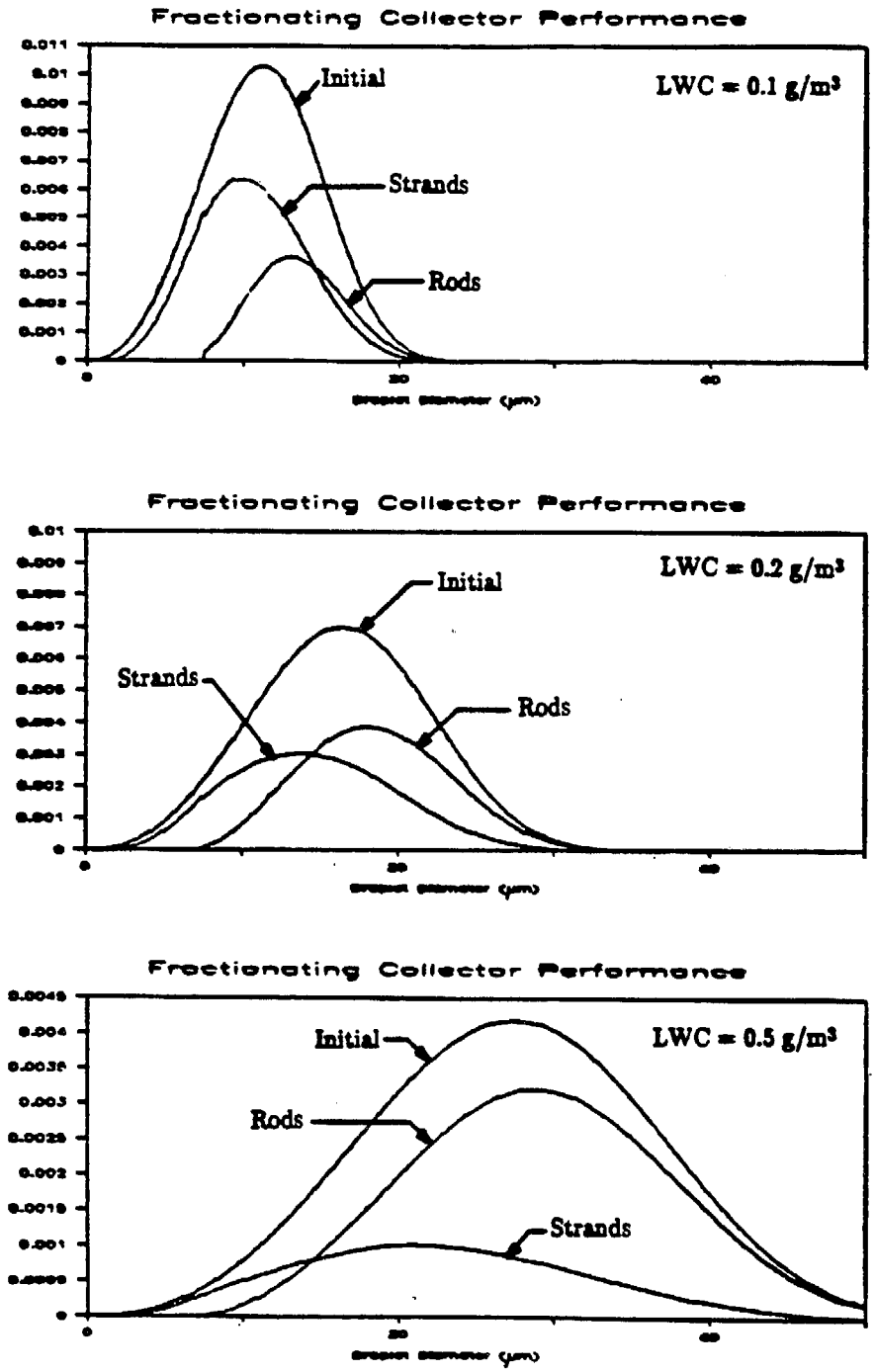

Figure 5. Performance of the fractionating collector is illustrated for three different liquid water contents. Shown for each liquid water content are the initial droplet distribution (based on Best's formula; Best, 1951), the portion of the droplet spectrum collected on the large rods in the fractionating inlet, and the portion collected by the CASC strands in the main body of the collector. The collection efficiencies are based on impaction theory and the percentage of airflow through the collector sampled by each collection surface.

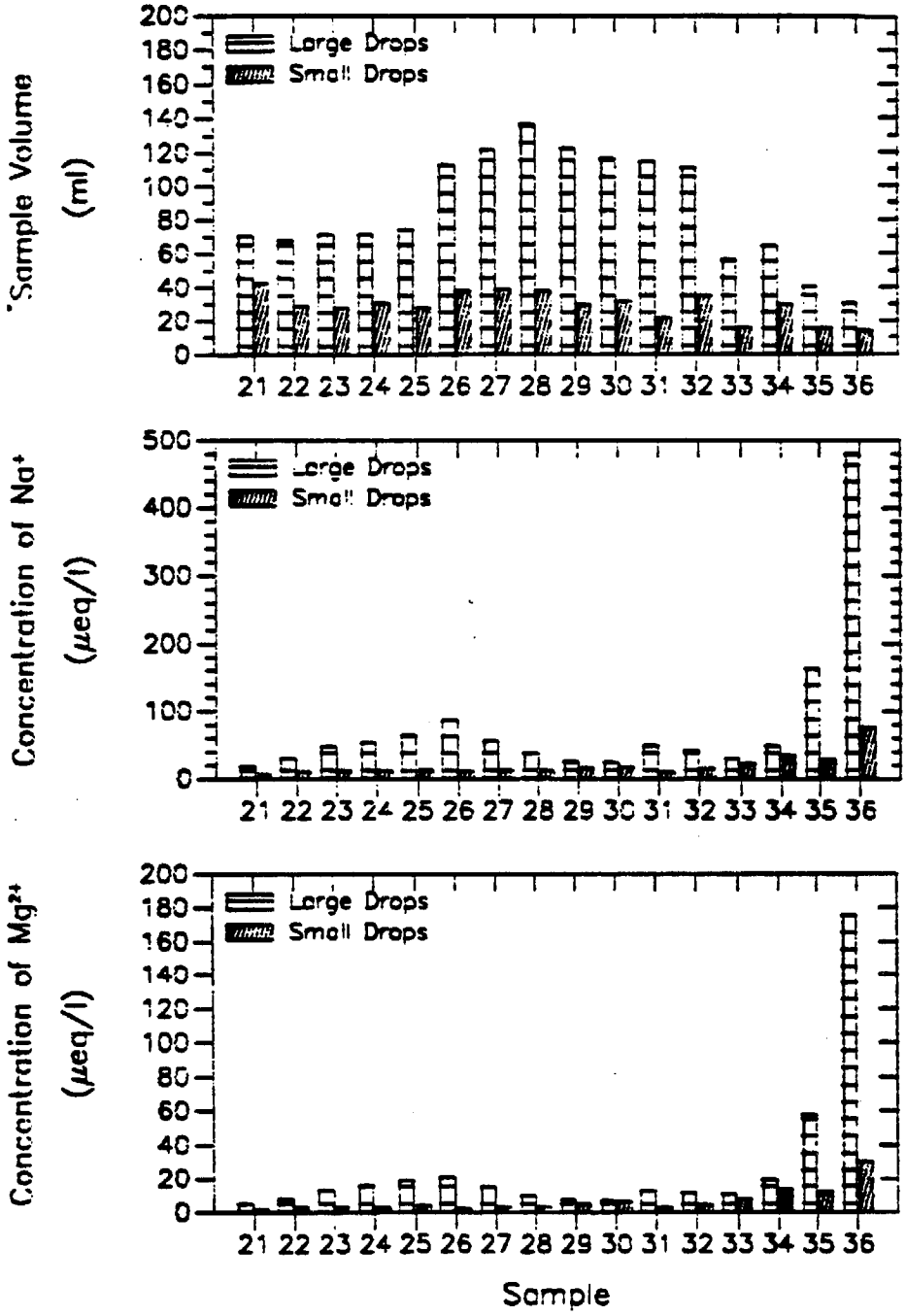

Figure 6. Comparison of sample volumes, Na^+ concentrations, and Mg^{2+} concentrations for the samples collected by the fractionating collector on the morning of July 15, 1987. Samples collected on the large rods in the sampler inlet are labeled "large drops", while those collected by the CASC strands are labeled "small drops."

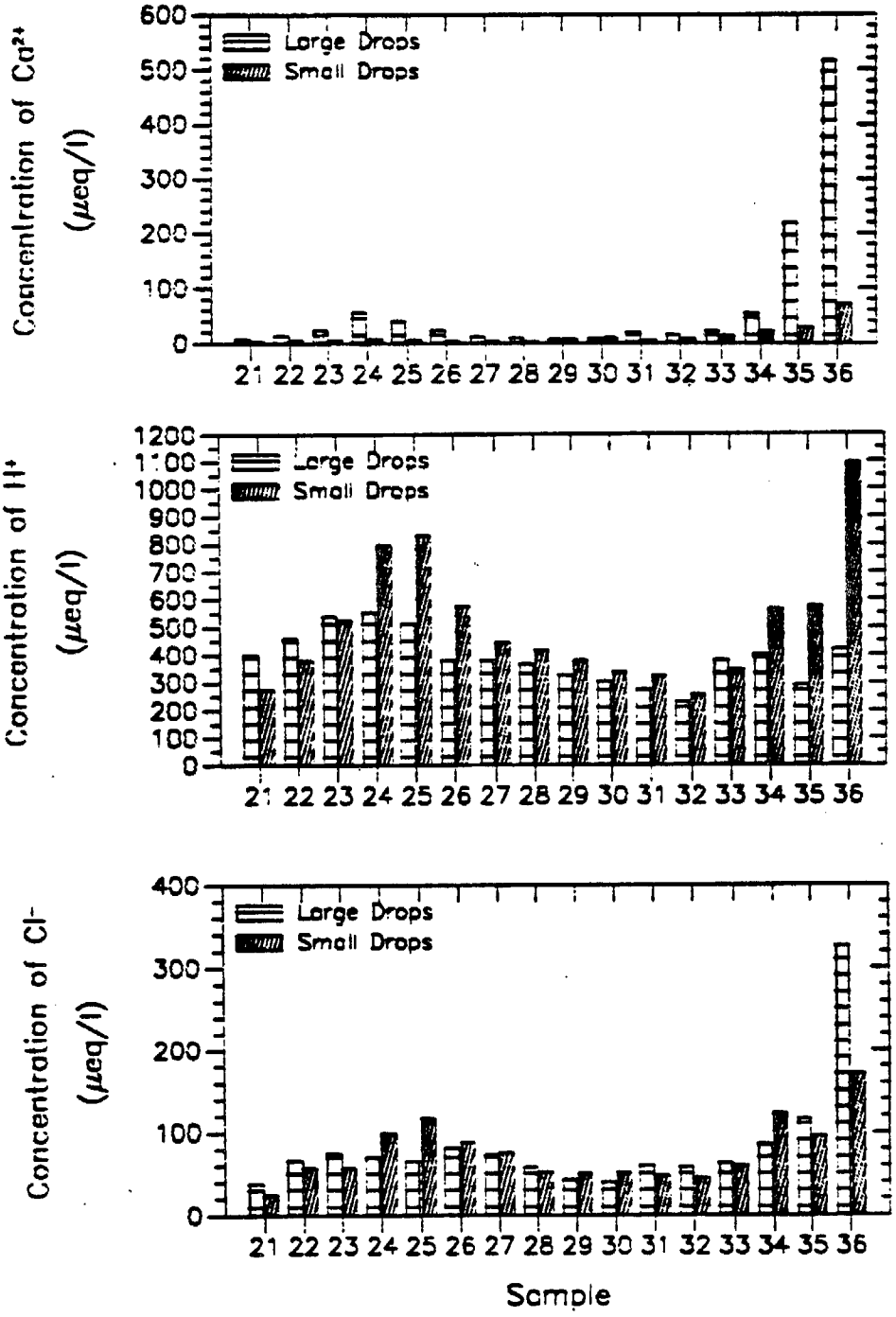

Figure 7. Comparison of Ca^{2+} concentrations, H^{+} concentrations, and Cl^{-} concentrations for the samples collected by the fractionating collector on the morning of July 15, 1987. Samples collected on the large rods in the sampler inlet are labeled "large drops", while those collected by the CASC strands are labeled "small drops."

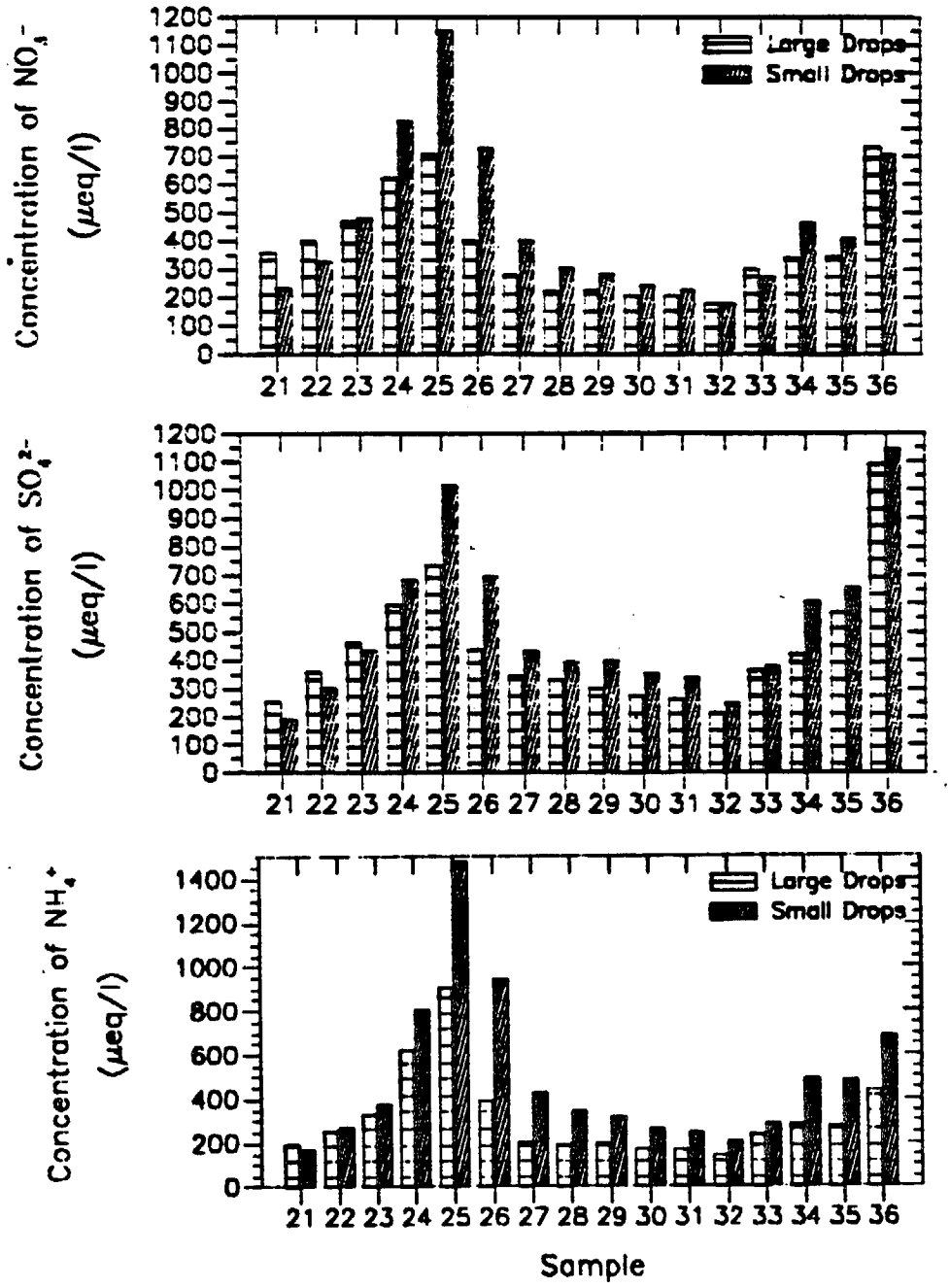

Figure 8. Comparison of NO_3^- concentrations, SO_4^{2-} concentrations, and NH_4^+ concentrations for the samples collected by the fractionating collector on the morning of July 15, 1987. Samples collected on the large rods in the sampler inlet are labeled "large drops", while those collected by the CASC strands are labeled "small drops."

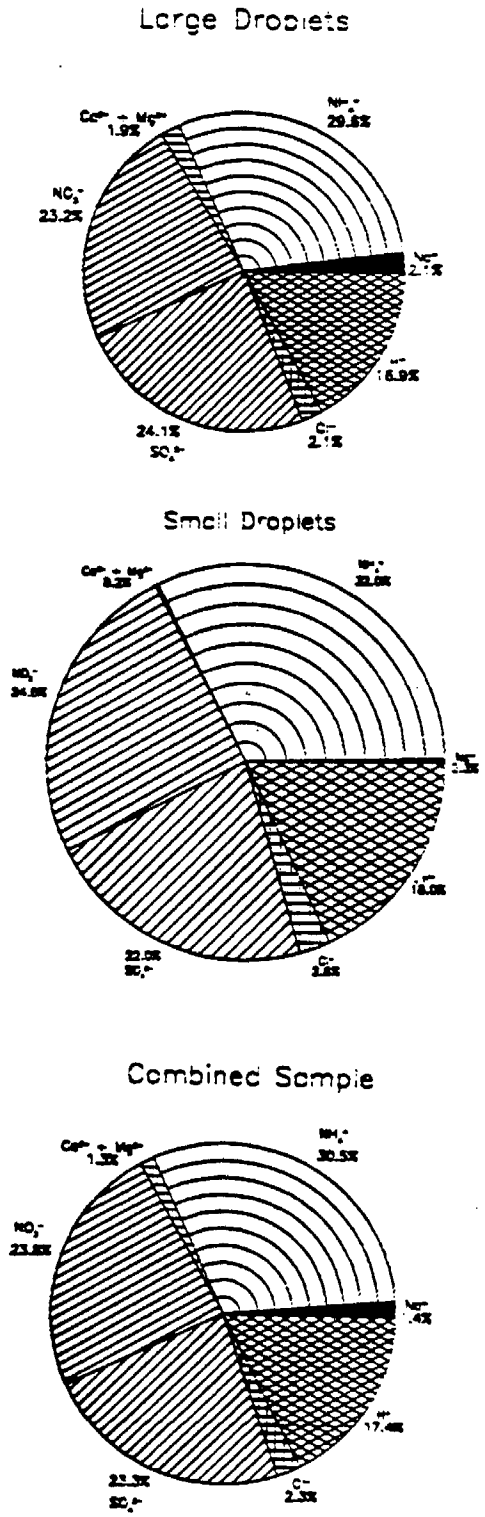

Figure 9. Illustration of the composition of the cloudwater sampled between 0600 and 0630 on July 15, 1987, using the fractionating collector. The fraction labeled "large droplets" was collected on the large rods in the inlet. The fraction labeled "small droplets" was collected on the CASC strands in the main body of the collector. The "combined sample" represents the volume weighted average composition of the two fractions. The area of each diagram is proportional to the total of the measured ionic species concentrations in that fraction of the sample.

CHAPTER 4

CHEMICAL COMPOSITION OF COASTAL STRATUS CLOUDS:

Dependence on Droplet Size and Distance from the Coast

by

J. William Munger†, Jeff Collett, Jr.,

Bruce Daube, Jr., and Michael R. Hoffmann*

Environmental Engineering Science

W. M. Keck Laboratories, 138–78

California Institute of Technology

Pasadena, CA 91125

Submitted to

Atmospheric Environment

9 December 1988

* *To Whom Correspondence Should Be Addressed*

† Present Address: Department of Earth & Planetary Sciences, Harvard University, 29 Oxford St., Cambridge, MA 02138

Abstract

The aerosol at elevated sites in the South Coast air basin is a mixture of sea salt and pollution–derived secondary aerosol. The influence of sea salt declines with increasing distance from the coast. Nitric acid appears to react with the NaCl in sea–salt aerosol to release $HCl_{(g)}$ and form $NaNO_3$ in the aerosol. At inland sites aerosol concentrations differ during onshore and offshore flow. The highest concentrations are observed during the day when the onshore flow transports pollutants to the sites, while lower concentrations were observed at night when drainage flows from nearby mountains influenced the sites. Variations in liquid water content are a major influence on cloudwater concentration.

Comparisons of the ionic concentrations in two size–segregated fractions collected during each sampling interval suggest that there is a large difference between the average composition of the smaller droplets and that of the larger droplets. For each time interval, the concentration of Na^+, Ca^{2+} and Mg^{2+} in the large droplet fraction was observed to be higher than in the small droplet fraction. The concentrations of SO_4^{2-}, NO_3^-, NH_4^+, and H^+ were higher in the small droplet fraction. Chloride concentrations were nearly equal in both fractions. Differences in the composition of size–fractionated cloudwater samples suggest that large droplets are formed from sea salt and soil dust, which are large aerosol, and small droplets are formed on small secondary aerosol composed of primarily ammonium sulfate and ammonium nitrate. The concentrations of several components that exist partly in the gas phase (e.g. Cl^-, HCOOH, and CH_3COOH) appear to be independent of droplet size.

Introduction

Coastal stratus clouds are a major feature of the Los Angeles weather pattern. Cass (1979) noted a correlation between episodes of high SO_4^{2-} concentrations and the presence of cloud or fog. Previous studies by Waldman et al. (1985) and Richards et al. (1983) have indicated that stratus clouds above Los Angeles have high concentrations of NO_3^- and SO_4^{2-}.

The size–dependent composition of aerosol is well known. Soil dust and sea salt generally make up the large aerosol, while nitrate and sulfate, partially neutralized by ammonium, make up much of the sub–micron aerosol. If droplet size is dependent on the size of the condensation nucleus then the composition of droplets could depend on size as well. In Japan, Naruse and Maruyama (1971) observed a correlation between droplet size and nucleus mass. The larger droplets contained large sea–salt nuclei, while the smaller drops contained ammonium sulfate aerosol. Hudson and Rogers (1984) indirectly determined nucleus size by measuring the critical supersaturation of nuclei from different size droplets. They found that the largest drops contained nuclei with low SS_{cr} (i.e. large mass). Noone et al. (1988) have recently provided evidence that solute concentration within cloud droplets can be a function of droplet size in coastal stratus clouds (Cheeka Peak Research Station, Washington). They reported that cloud droplets in the size range of 18 to 23 μm had solute mass 2.7 times that of droplets in the size range of 9 to 18 μm. Their results were consistent with the suggestion by Andreae et al. (1986) that in marine air the larger droplets are nucleated on dust or sea salt, while the smaller droplets form on excess (non–sea–salt) sulfate derived from the photoxidation of dimethyl sulfide. Collett et al. (1988) attributed differences in the composition of cloudwater samples collected by two collectors with different 50% lower droplet size cuts to size–dependent differences in droplet composition. Some of the theoretical aspects of size–dependent variations in droplet composition have been discussed by Perdue and Beck (1988).

In addition to an anticipated dependence of the chemical composition of the coastal stratus on droplet size, we also expected to see significant variations in composition as a function of distance from the coast. In order to acheive these objectives we developed a cloudwater sampler capable of size fractionation and we established cloudwater and aerosol sampling stations at three elevated sites in the Los Angeles air basin during a period of prolonged cloud cover. This effort overlapped in time with the Southern California Air Quality Study (SCAQS) of 1987.

Methods

· ***Site Descriptions***

Three sites, San Pedro Hill, Henninger Flats, and Kellogg Hill (see Fig. 1), were operational during the period of June 13 to July 17, 1987. The San Pedro Hill site (elev. 450 m) was located at a radar and communications facility operated by the U. S. Air Force and the Federal Aviation Administration. San Pedro Hill is the easternmost hill of ridge that forms the Palos Verdes Peninsula. The distance from the site to the ocean was 2.5 km; Los Angeles Harbor was 6 km east. The sampling equipment was placed at the edge of a flat grassy area. A steep hillside sloped away from the site, giving it unobstructed exposure from 70–270°.

Henninger Flats (elev. 780 m) is on a level bench partway up Mount Wilson in the San Gabriel Mountains, 7 km NE of Pasadena, and 45 km NE of the coastline. This site has been used in previous sampling programs (Waldman et al., 1985) and for a cloud/fog collector intercomparison (Hering et al., 1987). The Flats is an experimental forest area that has been planted with pine trees; the sampling equipment was located in a clearing a few hundred meters back from the edge. Because it is partially sheltered by the surrounding trees, cloud interception at the samplers is slightly delayed.

Kellogg Hill is 38 km E of downtown Los Angeles at an elevation of 370 m. It lies 50 km NE of the coastline. The sampling equipment was located in a fenced enclosure adjacent to a small building that housed radio transmission equipment. The building partially obstructed

the sampler when winds were from the south to west, which is the prevailing daytime wind. The site was unobstructed in the direction of the prevailing night–time winds. Construction activity near the site increased aerosol concentrations of soil dust during the daytime.

· ***Sampling Procedure***

Each site was equipped with a Caltech Active Strand Collector (CASC) with an automated fractionating sampler and a cloudwater sensor, shown in Figure 2 (Daube et al., 1987). The CASC collects droplets by inertial impaction on 510 μm Teflon strands. The 50% collection efficiency cutoff, predicted from impaction theory and based on droplet diameter, is 3.5 μm (Friedlander, 1977). A protective rain shield, which had its opening facing downward, was attached to the front of the collector to exclude large (d > 200 μm) sedimenting droplets. The cloudwater sensor, which is a miniature version of the CASC connected to a resistance grid, was used to turn the collector on when fog was present. The cloudwater collected by the CASC was directed to the fractionating sampler. In the fractionating sampler, cloudwater accumulated in a reservoir until a liquid level sensor determined that 60 ml had been collected. The reservoir was then drained to a 60 ml polyethylene sample bottle held in a carousel. The carousel had a capacity of 20 bottles. When all 20 bottles had been filled, the level sensor was deactivated. Any further sample collected was retained in the reservoir. If its capacity was exceeded the sample drained out through an overflow tube. The reservoir and sample bottles were housed in a refrigerator. A printer recorded the times that the sampler came on and off and when the bottles were filled. Also located at each site was an automated filter pack aerosol sampler. Open-faced Teflon filters (Gelman Zefluor, 1μm pore size) were used to collect aerosol for inorganic analysis. $HNO_{3(g)}$ was collected on a nylon filter (Gelman Nylasorb) placed behind one Teflon filter. $NH_{3(g)}$ was collected on two oxalic acid impregnated glass fiber filters behind a second Teflon filter. A rain shield above the filter holders excluded debris and sedimenting droplets.

During the late afternoon or evening prior to an expected cloud event, the samplers were cleaned by rinsing the collection strands, sample tubing, and reservoir with distilled, deionized

water (DDH_2O). After rinsing, the strands were sprayed again with DDH_2O, which was collected in the fraction collector as a system blank. Rinsing and blank collection were repeated the following morning whether cloud was collected or not. Three sets of filters were loaded on the aerosol collector. A timer on the collector controlled the times that each filter set was run.

At San Pedro Hill, a size–fractionating inlet was used on the CASC for the period of 15–16 July, 1987. The rain shield was not used in conjunction with the size–fractionating inlet. Four rows of eight 12.7 mm Teflon rods, which have a 50% lower size cut of 16 μm (diameter) at the sampling velocity of 9 m s^{-1} are arranged at the front of the inlet. Each row covers 46% of the cross–sectional area. Large droplets impact on the rods, while most droplets smaller than 15 μm pass through to be collected on the CASC strands in the main body of the collector. Water from the rods and strands is collected in separate bottles, which were manually emptied at the end of each sampling interval.

· ***Analytical Procedures***

Samples were retrieved in the morning following a cloud event and transported to the lab at Caltech. The samples were weighed to determine their volume and the sample pH was measured with a Radiometer PHM82 pH meter using a combination electrode calibrated against pH 4 and 7 buffers. For selected samples small aliquots were removed and treated to stabilize reactive species. CH_2O was stabilized by addition of SO_3^{2-} (Dong and Dasgupta, 1987). Likewise, in a separate aliquot S(IV) was stabilized with CH_2O. Hydrogen peroxide was reacted with p–hydroxyphenylacetic acid in the presence of peroxidase to form a stable dimer (Lazrus et al., 1985). Carboxylic acids were preserved by addition of chloroform (Keene and Galloway, 1984).

The samples and preserved aliquots were stored in a refrigerator at 4 °C until analysis. Major anions were determined by ion chromatography with a Dionex AS4 or AS4A separator column and a micromembrane suppressor. The eluent was 2.8 mM HCO_3^-/ 2.2 mM CO_3^{2-}. The metallic cations were determined by atomic absorption spectrophotometry. An

air/acetylene flame was used for Na^+ and K^+; N_2O/acetylene was used for Ca^{2+} and Mg^{2+} to minimize interferences. NH_4^+ was determined by flow injection analysis employing the indophenol blue method.

The stabilized CH_2O was determined by a modification of the Nash method for use with an autoanalyzer (Dong and Dasgupta, 1987) Hydrogen peroxide was added to eliminate S(IV), which interferes by forming an adduct with CH_2O. The absorbance of the colored product was measured at 412 nm. S(IV) was analyzed by the pararosaniline method (Dasgupta et al., 1980) adapted for flow injection analysis. Carboxylic acids were determined by ion exclusion chromatography (Dionex ICE–AS1) with dilute HCl as the eluent and by normal ion chromatography using $Na_2B_4O_7$ as the eluent.

The Teflon and oxalic acid–impregnated glass fiber filters were extracted in distilled deionized water (DDH_2O) on a shaker table. A small volume of ethanol was added to the filter prior to extraction to more effectively wet the filter surface. The nylon filters were extracted in HCO_3^-/CO_3^{2-} IC eluent. Composition of the extracts was determined by the same procedures used for the fogwater samples, with the exception of additional buffer in the complexing reagent and oxalic acid in the rinse solution of the ammonia analysis to account for the effect of the oxalic acid. Complete details of the analytical procedures and estimates of their precision and accuracy are presented elsewhere (Munger, 1989).

Results

- ***Aerosol Composition***

The aerosol and gas–phase data for San Pedro Hill, Henninger Flats, and Kellogg Hill are summarized in Table 1. The samples are separated into day and night samples to account for the diurnal variation in wind direction at the sites. Onshore winds prevailed during the day; offshore drainage flows prevailed at night. The major species present were NH_4^+, NO_3^-, and SO_4^{2-}. In many of the daytime samples HNO_3 was equal to or greater than the NO_3^-. In general, the concentrations of N(–III), N(V), and SO_4^{2-} increased with distance from the coast.

Na^+, Cl^- and Mg^{2+} decreased away from the coast. The highest concentrations of NH_3 were observed at Kellogg Hill.

Day and nighttime concentrations at San Pedro Hill were similar. At Henninger Flats and Kellogg Hill there was a tendency towards higher concentrations in the daytime samples. This apparent trend was not statistically significant, however, because of the large degree of variability in the daytime concentrations.

Most of the samples showed a large Cl^- deficit when compared to the sea salt Na^+:Cl^- ratio (see Figure 3A). The averages in Table 1 indicate that the Cl^- deficit is generally greater in the daytime.

Concentrations of the acidic anions, $NO_3^- + SO_4^{2-}$, exceeded those of NH_4^+ in all but one sample from San Pedro Hill (Figure 4A). The overall acid–base balance of the atmosphere is indicated in Figure 4B which plots total acids against total bases (acids = $Cl^- + NO_3^- + SO_4^{2-} + HNO_3$; bases = $NH_4^+ + Na^+ + Ca^{2+} + Mg^{2+} + NH_3$). The difference between the two sums is equivalent to total atmospheric alkalinity, as defined by Jacob et al. (1986). Most of the data plot along the 1:1 line, which indicates neutrality. The samples with excess acids are from Henninger Flats and Kellogg Hill. Kellogg Hill also had the only samples with excess bases.

· ***Cloudwater Composition***

The weather pattern during June and July 1987 was ideal for cloudwater collection. Clouds formed nearly every night. During the sampling period, 242 samples from 18 cloud events were collected at San Pedro Hill. Because the sampling carousel could only hold 20 time–resolved samples, long cloud events with high liquid water content (LWC) were not sampled to the end.

Concentration data for the San Pedro Hill cloudwater samples are summarized in Table 2. Typical LWC values, as estimated from collection rate and the theoretical collection efficiency of the CASC, were $\simeq 0.1$ g m^{-3}. Cloudwater at San Pedro Hill was consistently acidic. The overall range of pH was 2.4 – 5.0; the volume–weighted average pH was 3.15. The major

anions were NO_3^- and SO_4^{2-}; on an equivalent basis NO_3^- was in slight excess. In addition to H^+, the major cations were NH_4^+ and Na^+. Their ranking varied from event to event. Concentrations of CH_2O were typically $20 - 30$ μ**M**, while the concentrations of formate and acetate were found to be in the range of $12 - 43$ μM and $6 - 31$ μM, respectively. Hydrogen peroxide concentrations were found in the range of $4 - 72$ μ**M** while S(IV) was usually absent in samples for which it was determined. In addition to formaldehyde other aldehydes such as acetaldehyde ($1 - 5$ μ**M**), glyoxal ($1 - 10$ μ**M**), and methylglyoxal ($4 - 8$ μ**M**) were identified and quantified in cloudwater collected at San Pedro Hill during this sampling program (Igawa et al., 1988).

Clouds intercepted Henninger Flats less frequently than at San Pedro Hill. Because of the difference in their elevations, clouds did not usually intercept both sites simultaneously. At Henninger Flats, 76 samples from 5 cloud events were obtained during the sampling period. Cloudwater from Henninger Flats was similar in chemical composition to that from San Pedro Hill (see Table 4). The range of pH was comparable at the two sites, but Henninger Flats had a slightly higher pH on the average. Henninger Flats had higher concentrations of NH_4^+ and lower SO_4^{2-} and Na^+. Because of the lower SO_4^{2-}, the ratio of NO_3^- to SO_4^{2-} was greater at Henninger Flats. Stratus clouds did not penetrate far enough inland at low elevation to permit sampling at Kellogg Hill.

In the majority of the samples, Cl^- and Na^+ were present at the sea water ratio (see Figure 3B). A Cl^- deficit (or Na^+ excess) was consistently observed in samples with $Na^+ > 750$ μN. The apparent Cl^- deficit in the average concentrations is due to the influence of the high concentration samples.

· ***Temporal Variations***

Concentration vs. time profiles for 4 representative periods are shown in Figures $5 - 8$. Gaps in the LWC trace indicate non–continuous sampling when the 20 bottles had been filled. Concentrations for the period 0400 –1300 on July 15 at San Pedro Hill are derived from the volume–weighted average of the two size–fractioned samples. Concentrations tended to

decrease as LWC increased, and then increase again at the end of the event as LWC decreased. Some depletion was also apparent during long periods of stable LWC, such as the samples after 0700 on July 15 at San Pedro Hill and the second set of samples from Henninger Flats on July 16.

Most of the samples obtained at the two sites were collected during non-overlapping time periods. Often the stratus clouds would intercept one site on a given day and not the other. At other times, the clouds were observed to intercept the hillside at San Pedro during the period shortly after midnight, while interception at Henninger Flats did not begin until a few hours later. By this time, clouds were no longer intercepting the slopes of San Pedro Hill. The only event with simultaneous collection at both sites was on the night of July 16–17. This event, which was associated with drizzle in the L.A. Basin, was one of the most persistent during the study. Clouds were present at both sites the previous night, though the bottles at San Pedro Hill were full by 0244 on 16 July when continuous cloud interception began at Henninger Flats. The clouds did not completely clear during the day of July 16. Continuous cloud cover returned to both sites around 1740 the evening of July 16 and filled all 20 bottles by approximately 2300 on 16 July. The clouds continued without interruption until 0500 at both sites and was intermittent until mid–morning. This event had the lowest overall concentrations of major ions and the highest pH observed at San Pedro Hill. The pH and ion concentrations at Henninger Flats were close to their average values.

· ***Size–fractionated Samples***

The size–fractionated cloud samples were collected during an extended cloud event at San Pedro Hill. Clouds initially intercepted the site at approximately 1900 on July 14 and remained until approximately 1300 on July 15. Twenty samples were collected between 1900 and 0000. Collection of size–fractionated samples began at 0400 and continued until 1200. A final one–hour unfractionated sample was collected from 1200 to 1300.

The overall concentration in the clouds when the size–fractionated samples were collected

is indicated in Figure 6. The major ions are comparable to those at the beginning of the event and in the subsequent event. The sea salt ions were less than in the preceding and following samples. Figures 9 – 12 illustrate the major ions, sea salts and collection rates in the two fractions. The concentrations of all species increased concurrently around 0600 without appreciable change in collection rate. The sharp increase in the collection rate for large drops subsequent to this corresponded to a period of drizzle. Concentrations gradually decreased over the next several hours until the final samples when they rose again as LWC dropped.

Discussion

· ***Inter–site and Temporal Variations***

The differences in chemical composition at the three sites are consistent with their location. San Pedro Hill, being the closest to the ocean, is the most affected by sea salt. During the day, prevailing winds carry emissions of NO_x and SO_2 and their oxidation products, HNO_3 and SO_4^{2-}, inland where they impact Henninger Flats and Kellogg Hill. Higher N(–III) levels are obtained near the dairy feedlots in Chino (see Figure 1). As noted above, the ratio of SO_4^{2-} to NO_3^- in cloudwater is higher at San Pedro Hill than at Henninger Flats. Local oil refinery emissions, which affect San Pedro Hill at night, when offshore winds prevail, may directly influence this ratio.

Aerosol concentrations at Henninger Flats and Kellogg Hill were generally less at night than during the day. Henninger Flats was frequently above the inversion at night, which could explain the low concentrations there. In addition, downslope flow from the adjacent mountains, which rise to 1800 m, could flush the site with cleaner air at night. Kellogg Hill, which is also near the San Gabriel Mountains, may also be affected by this mechanism. San Pedro Hill, on the other hand, is far from any higher ground and will not be affected by clean–air drainage flows. The offshore winds that influence the site at night may have been influenced by primary emissions and secondary pollutants from the SCAB. A sea breeze during the day would normally be expected to bring relatively clean air to the San Pedro Hill

site. However, as Cass and Shair (1984) have pointed out, pollutants accumulate off the coast of Los Angeles due to the daily sea breeze/land breeze cycle. Thus, the onshore flow of the sea breeze returns pollutants that were carried out to sea by the previous nights offshore flow.

· ***Acid–Base Balance***

The routine observation of pH 3 cloudwater clearly indicates that the airmass in the portion of the SCAB affected by stratus has excess acidity. The acid–base balance at San Pedro Hill and Henninger Flats (Fig. 4B) is generally consistent with this observation. Previous observations by Jacob et al. (1985) noted that coastal areas are generally deficient in acid–neutralizing capacity. Further inland, near the major sources of NH_3 (e.g. cattle feed lots and other agricultural activities), samples with excess alkalinity were collected. In the presence of excess acidity, sea salt aerosol readily loses $HCl_{(g)}$ if the humidity is <99% (Clegg and Brimblecombe, 1985). Apparent loss of Cl^- from aerosol samples has been frequently observed along the California coast (Jacob et al., 1985; Munger et al., 1988). Due to the reaction between $HNO_{3(g)}$ and $NaCl_{(s)}$, NO_3^- replaces Cl^- in the NaCl–dominated aerosol and releases $HCl_{(g)}$. The emitted gas–phase HCl should be included in the acid base balance because it is efficiently scavenged by cloud droplets. Infact, unlike the aerosol samples most of the cloudwater samples did not have a Cl^- deficit.

· ***Size–fractionated Cloudwater Samples***

Figure 14 illustrates the theoretical performance of the size–fractionating inlet. The initial droplet–size spectra are theoretical curves generated from Best's formula (1951). The fraction of the liquid water retained on the rods and the strands is calculated from impaction theory for droplets on a cylinder (Friedlander, 1977). Collection efficiency curves are shown for the strands and rods in Figure 14. The fraction of air sampled by the collector is a function the diameter and spacing of the collector elements as shown in the following relationship:

$$F_s = 1 - [1 - \frac{D_c}{\Delta C}]^n$$

where F_s is the fraction of incoming air that is sampled, D_c is the diameter of an individual collection element, ΔC is the spacing of the elements, and n is the number of rows. The CASC contains 6 rows of 510 μm strands, spaced 1.8 mm apart, which yields an 86% sampling efficiency. The size–fractionating inlet contains 4 rows of 12.7 mm rods, spaced 25.4 mm apart, and samples 91% of the incoming air.

At low liquid water contents, where a higher proportion of the water is present in droplets too small to be collected by the rods, most of the water will be collected on the strands. With increasing LWC the mass median diameter increases and more sample is collected on the rods. Because the rods do not have a sharp lower size cut–off, there is considerable overlap in the portions of the droplet spectrum sampled by the rods and strands. Any differences observed in the composition of the two sample fractions, therefore, should be considered as a lower bound on the actual differences present if the droplets could be separated more cleanly.

Comparisons of the ionic concentrations in the two fractions collected during each interval suggest that there is a large difference between the average composition of the smaller droplets and that of the larger droplets. For every interval sampled, the concentration of Na^+ and Mg^{2+} in the large droplet fraction was observed to be higher than in the small droplet fraction. With the exception of one very low concentration sample, the same was true for Ca^{2+}. Concentrations of SO_4^{2-}, NO_3^-, NH_4^+, and H^+ (Figure 9) were almost always higher in the small droplet fraction. Neither fraction had consistently higher Cl^- concentrations (Figure 10); Cl^- was nearly equal in both fractions. The Cl^-:Na^+ ratio in the two fractions differs, however. In the large–droplet fraction, Na^+ and Cl^- are close to the seawater ratio, while the fine–droplet fraction has an excess of Cl^- relative to seawater. As noted above, Cl^- is removed from the sea salt aerosol by reaction with HNO_3. Gas–phase HCl should be scavenged equally by all droplets.

Comparison of the organic acid concentrations (Fig. 12) in the two fractions indicates that there was little difference; this result would be expected if the clouds were in equilibrium

with the surrounding air and the droplet pH did not vary appreciably with size. The calculated equilibrium partial pressures of each fraction are comparable (i.e. $C_{aq} = K_{h,i}P_i$). Over the observed cloudwater pH range of 3 to 3.6, the majority of the organic acid will be in the gas phase (Munger et al., 1989). The behavior of HCOOH and CH_3COOH is discussed by Munger et al. (1989). In addition, the CH_2O concentrations in the initial fractionated samples are equivalent, which is also consistent with equilibrium considerations. However, beginning at 5:30 there was a spike in $[CH_2O]$, [HCOOH], and $[CH_3CO_2H]$ as well as the major inorganic ions. The organic acids appear to maintain their apparent equilbrium between the gas and aqueous phases, while the CH_2O showed a pronounced increase in the small–droplet fraction. This difference disappears over the subsequent three hours. The sharpness of the pulse suggests the passage of a plume or a major wind shift. The CH_2O data imply that the precursor nuclei for the smaller droplets contain formaldehyde that is not in equilibrium with the gas phase. The presence of α–hydroxymethanesulfonate (HMSA) and other aldehyde–bisulfite adducts could account for this apparent non–equilibrium behavior (Munger et al., 1986). At pH 3.5, the kinetics of aldehyde–bisulfite adduct dissociation is quite slow (Betterton et al., 1988), thus HMSA in the precursor aerosol would be retained in the droplet and measured analytically as CH_2O. The presence of detectable S(IV) during this period is consistent with this argument. Of special interest in this regard, S(IV) and H_2O_2 were not found to be present simultaneously in either size fraction.

The differences in concentration between the size fractions are consistent with the suggestion that large nuclei produce large droplets and small nuclei produce small droplets (Best, 1951; Mason and Chien; 1962; Hudson, 1984; Jensen and Charlson, 1984; Noone et al., 1988). For the size–dependent aerosol composition to be preserved in the droplets requires nucleation scavenging to be the dominant scavenging process. Because Na^+, Ca^{2+} and Mg^{2+} are associated with sea salt and soil dust (Seinfeld, 1986) they are found predominantly in the large droplets; while NH_4^+, SO_4^{2-}, and to some extent NO_3^-, which are mostly found in secondary aerosol, would be in the small droplets (Seinfeld, 1986). However, NO_3^-, which can exist in the

gas phase or on large aerosol by exchange with Cl^-, would also be found to a substantial extent in large droplets. However, the cloudwater concentrations of these ions may be altered by absorption of precursor gas phase species followed by chemical reaction. For example, $NH_{3(g)}$ can be absorbed by the droplets and protonated to form NH_4^+; $HNO_{3(g)}$ can be absorbed, followed by deprotonation to yield NO_3^-; $SO_{2(g)}$ can be absorbed and oxidized to SO_4^{2-}. The first two processes are extremely rapid, while the oxidation of S(IV) to S(VI) in cloudwater is also rapid in the presence H_2O_2 or a metal catalyst (Hoffmann and Jacob, 1984). Since S(IV) and H_2O_2 were not found concurrently in the time– and size–resolved samples, the rapid oxidation of S(IV) to S(VI) by H_2O_2 was likely to have taken place (McArdle and Hoffmann, 1983).

Summary

Aerosol composition at elevated sites in the South Coast air basin was a mixture of sea salt and pollution–derived secondary aerosol. The influence of sea salt declined with increasing distance from the coast. Abundant HNO_3 reacted with the NaCl in sea–salt aerosol to give $HCl_{(g)}$ and $NaNO_3$ in the aerosol. At inland sites aerosol concentrations differ during onshore and offshore flow. The highest concentrations were observed during the day when the onshore flow transports pollutants to the sites, while lower concentrations were observed at night when drainage flows from nearby mountains influenced the sites. Variations in liquid water content are a major influence on cloudwater concentration. Steady declines in concentration were also observed during periods of steady LWC. These may be due to removal by drizzle, dilution by advection, or entrainment of cleaner air from aloft.

Differences in the composition of size–fractionated cloudwater samples suggest that large droplets are formed from sea salt and soil dust, which are large aerosol, and small droplets are formed on small secondary aerosol composed of ammonium sulfate and nitrate. Components that exist partly in the gas phase (e.g. Cl^-, HCOOH, and CH_3COOH) did not appear to be size segregated. The exchange of HNO_3 for HCl on sea salt provides a means for Cl^- to associate

with small droplets. Because Cl^- is removed from the sea salt aerosol during the day, the large droplets that form from them are deficient in Cl^-. Chloride is retained in the air mass and some ends up in the small droplets that formed on secondary aerosol.

Acknowledgements

This research was supported by the California Air Resources Board (Contract #A4–142–32). We thank the Federal Aviation Administration, Los Angeles County Fire Department and Pomona Dispatch for their cooperation in allowing us access to sampling sites. We thank Aram Kaloustian and Walter Chong for their assistance in the field and laboratory.

References

Andreae, M. O., Charlson, R. J., Bruynseels, F., Storms, H., Van Grieken, R. and Maenhaut, W. (1986) Internal mixture of sea salt, silicates, and excess sulfate in marine aerosols. *Science*, **295**, 683–685.

Best, A. C. (1951a) Drop–size distribution in cloud and fog. *Q. J. R. Met. Soc.* **77**, 418–426.

Best, A. C. (1951b) The size of cloud droplets in layer–type cloud. *Q. J. R. Met. Soc.* **77**, 241–248.

Betterton, E., Erel, Y., and Hoffmann, M. R. (1988) Aldehyde–bisulfite adducts. Prediction of some of their thermodynamic and kinetic properties. *Environ. Sci. Technol.* **22**, 92–98.

Cass, G. R., and Shair, F. H. 1984. Sulfate accumulation in a sea breeze/land breeze circulation system. *J. Geophys. Res.* **89**, 1429–1438.

Clegg, S. L. and Brimblecombe, P. (1985) Potential degassing of hydrogen chloride from acidified sodium chloride droplets. *Atmos. Environ.* **19**, 465–470.

Collett, J. L., Jr., Munger, J. W., Daube, B. D., Jr., and Hoffmann, M. R. (1988) A comparison of two cloudwater/fogwater collectors: the rotating arm collector and the Caltech active strand collector. submitted to *Atmos. Environ.*

Dasgupta, P. K., DeCesare, K. and Ullrey, J. C. (1980) Determination of atmospheric sulfur dioxide without tetrachloromercurate (II) and the mechanism of the Schiff reaction, *Anal. Chem.* **52**, 1912–1922.

Daube, B. C., Jr., Flagan, R. C., and Hoffmann, M. R. (1987) *Active Cloudwater Collector* United States Patent # 4,697,462, Oct. 6, 1987.

Dong, S. and Dasgupta, P. K (1987) Fast flourimetric flow injection analysis of formaldehye in atmospheric water, *Environ. Sci. Technol.* **21**. 581.

Friedlander, S. K. (1977) *Smoke, Dust and Haze, Fundamentals of Aerosol Behavior.* John Wiley and Sons, New York.

Hering, S. V., Blumenthal, D. L., Brewer, R. L., Gertler, A., Hoffmann, M., Kadlecek, J. A., and Pettus, K. (1987) Field intercomparison of five types of fogwater collectors. *Environ. Sci. Technol.* **21**, 654–663.

Hoffmann, M. R. and Jacob, D. J. (1984) Kinetics and mechanisms of the catalytic oxidation of dissolved sulfur dioxide in aqueous solution: an application to nighttime fogwater chemistry, in ***Acid Precipitation: SO_2, NO, and NO_x Oxidation Mechanisms: Atmospheric Considerations***, J. G. Calvert, ed., Butterworth Publishers, Boston, 101–172.

Hudson, J. G. and Rogers, C. F. (1984) Interstitial CCN measurements related to mixing in clouds. *Proc. 9th Int. Cloud. Physics. Conf.* August 21–28, TalinnUSSR.

Hudson, J. G. (1984) Ambient CCN and FCN measurements, in ***Hygroscopic Aerosols***, L. H. Ruhnke and A. Deepak, eds., A. Deepak Publishing, Hampton, VA.

Igawa, M., Munger, J. W. and Hoffmann, M. R. (1989) Analysis of aldehydes in cloud and fogwater samples by HPLC with a postcolumn reaction detector. *Environ. Sci. Technol.* in press.

Jacob, D. J., Waldman, J. M., Munger, J. W., and Hoffmann, M. R. (1985) Chemical composition of fogwater collected along the California coast. *Environ. Sci.* Technol. **19**, 730–736.

Jacob, D. J., Munger, J. W., Waldman, J. M., and Hoffmann, M. R. (1986) The H_2SO_4–$HNO_3^-NH_3$ system at high humidities and in fogs: I. Spatial and temporal patterns in the San Joaquin Valley of California. *J. Geophys. Res.* **91**, 1073–1088.

Jensen, J. B. and Charlson, R. J. (1984) On the efficiency of nucleation scavenging.

Tellus, **36B**, 367–375.

Keene, W. C. and Galloway, J. N. (1984) Organic acidity in precipitation of North America, *Atmos. Environ.* **18**, 2491–2497.

McArdle, J. V. and Hoffmann, M. R. (1983) Kinetics and mechanism of the oxidation of aquated sulfur dioxide by hydrogen peroxide at low pH. *J. Phys. Chem.*, **87**, 5425–5429.

Mason, B. J. (1971) ***The Physics of Clouds***, 2nd Ed., Oxford University Press, London.

Mason, B. J. and Chien, C. W. (1962) Cloud–droplet growth by condensation in cumulus. Q. *J. R. Met. Soc.* **88**, 133–138.

Munger, J. W., Tiller, C. T., and Hoffmann, M. R. (1986) Determination of hydroxymethanesulfonate in fog water. *Science*, **231**, 247–249.

Munger, J. W., Collett, J., Jr., Daube, B. C., Jr., and Hoffmann, M. R. (1989) Carboxylic acids and carbonyl compounds in Southern California fogs. *Tellus*, in press.

Munger, J. W., Collett, J., Jr., Daube, B. C., Jr., and Hoffmann, M. R. (1988) Chemical composition of intercepted stratus cloud along the Santa Barbara Channel coast. (submitted to *Environ. Sci. Technol.*)

Naruse, H. and Maruyama, H. (1971) On the hygroscopic nuclei in cloud droplets, *Papers in Meteor. and Geophys.* **22**, 1–21.

Noone, K. J., Charlson, R. J., Covert, D. S., Ogren, J. A., and Heintzenberg, J. (1988) Cloud droplets: solute concentration is size dependent. *J. Geophys. Res.* **93**, 9477–9482.

Perdue, E. M. and Beck, K. C. (1988) Chemical consequences of mixing atmospheric droplets of varied pH. *J. Geophys. Res.* **93**, 691–698.

Richards, L. W., Anderson, J. A., Blumenthal, D. L., McDonald, J. A., Kok, G. L., and Lazrus, A. L. (1983) Hydrogen peroxide and sulfur (IV) in Los Angeles cloud water, *Atmos. Environ.* **17**, 911–914.

Seinfeld, J. H. (1986) ***Atmospheric Chemistry and Physics of Air Pollution***, Wiley Interscience, New York.

Shair, F. H., Sasaki, E. J., Carlan, D. E., Cass, G. R., Goodin, W. R., Edinger, J. G. and Schacher, G. E. (1982) Transport and dispersion of airborne pollutants associated with the land breeze–sea breeze system. *Atmos. Environ.* **16**, 2043–2053.

Waldman, J. M., Munger, J. W., Jacob, D. J., and Hoffmann, M. R. (1985) Chemical characterization of stratus cloudwater and its role as a vector for pollutant deposition in a Los Angeles pine forest. *Tellus* **37**, 91–108.

Table 1. Summary Statistics for Aerosol Samples Collected at Three Elevated in the Los Angeles Basin (6–13 to 7–17–88)

San Pedro Hill

	Na^+	NH_4^+	Ca^{2+}	Mg^{2+}	Cl^-	NO_3^-	SO_4^{2-}	NH_3	HNO_3	N(–3)	N(V)
	‖⟵ neq m^{-3} ⟶‖							‖⟵ nmole m^{-3} ⟶‖			
Day											
N	18	13	18	18	16	18	18	18	14	13	14
Min	0	17	0	0	0	7	22	0	0	36	7
Max	188	430	47	49	105	147	448	105	166	479	279
Avg	81	186	22	19	25	69	179	19	91	206	164
σ	65	122	10	16	33	37	106	28	57	131	74
Night											
N	19	12	19	19	16	18	19	19	17	10	17
Min	0	0	0	0	0	6	32	0	0	71	12
Max	170	624	56	44	90	435	475	29	124	635	448
Avg	52	169	22	15	34	127	162	5	28	212	155
σ	46	183	12	13	31	118	121	9	31	180	129

Henninger Flats

	Na^+	NH_4^+	Ca^{2+}	Mg^{2+}	Cl^-	NO_3^-	SO_4^{2-}	NH_3	HNO_3	N(–3)	N(V)
	‖⟵ neq m^{-3} ⟶‖							‖⟵ nmole m^{-3} ⟶‖			
Day											
N	9	9	9	9	9	9	9	9	8	9	8
Min	0	4	0	0	0	7	5	0	11	4	19
Max	134	838	93	54	29	442	533	99	897	916	1255
Avg	59	367	39	19	6	173	255	40	363	407	526
σ	46	284	31	15	11	136	195	40	317	310	450
Night											
N	12	12	12	12	12	12	12	12	10	12	10
Min	4	3	0	0	0	9	5	0	13	3	22
Max	59	284	35	15	21	123	234	31	113	302	186
Avg	33	141	23	10	3	59	119	12	57	153	118
σ	18	87	12	5	6	35	70	11	29	93	56

Table 1. (continued)

Kellogg Hill

	Na^+	NH_4^+	Ca^{2+}	Mg^{2+}	Cl^-	NO_3^-	SO_4^{2-}	NH_3	HNO_3	N(–3)	N(V)
	‖⟵ neq m^{-3} ⟶‖							‖⟵ nmole m^{-3} ⟶‖			
	Day										
N	7	7	7	7	7	7	7	7	7	7	7
Min	8	9	62	12	0	10	7	0	6	8	16
Max	149	875	270	62	16	629	451	339	624	1063	1191
Avg	92	575	162	44	5	413	296	140	277	714	690
σ	48	302	60	16	6	204	156	120	185	353	358
	Night										
N	11	11	11	11	11	11	11	11	11	11	11
Min	44	139	40	11	0	91	94	0	9	279	133
Max	183	594	109	61	72	452	372	283	63	620	512
Avg	112	343	75	33	20	266	201	89	40	432	306
σ	43	167	21	16	24	118	80	82	19	128	128

Table 2. Concentrations in Cloudwater Samples Collected at San Pedro Hill (6–13 to 7–17–87).

	V(mL)	pH	Na^+	NH_4^+	Ca^{2+}	Mg^{2+}	Cl^-	NO_3^-	SO_4^{2-}	CH_2O	−/+	LWC
			‖⟵			⟶ μN ⟵			⟶‖	μM		g m^{-3}
14 June 1987												
N	15	15	15	15	15	15	15	15	15	0	15	15
Min	18	2.80	149	323	15	47	247	702	574	—	1.09	0.02
Max	68	3.28	734	744	88	214	787	1608	1407	—	1.19	0.11
Avg	48	3.02	506	501	58	149	538	1062	939	—	1.14	0.07
Vol Wt. Avg		3.02	468	466	54	139	502	991	880	—	—	0.06
19 June 1987												
N	3	3	3	3	3	3	3	3	3	3	3	3
Min	26	3.18	3258	665	281	593	1654	1281	978	25	0.73	0.02
Max	36	3.33	3796	1237	460	731	1701	2137	1131	31	0.75	0.06
Avg	33	3.25	3486	909	353	652	1676	1674	1078	27	0.74	0.04
Vol Wt. Avg		3.25	3553	980	375	670	1682	1784	1102	—	—	0.04
20 June 1987												
N	6	6	5	6	4	6	6	6	6	4	6	6
Min	9	3.11	1722	347	173	388	1379	498	749	21	0.73	0.03
Max	65	3.35	2574	605	272	715	1756	1402	1290	31	1.84	0.10
Avg	48	3.24	2024	478	225	476	1468	850	1032	24	1.06	0.06
Vol Wt. Avg		3.24	1812	470	127	444	1434	815	964	—	—	0.06
21 June 1987												
N	3	3	3	3	3	3	3	3	3	2	3	3
Min	12	3.48	706	169	79	192	735	377	312	12	1.00	0.03
Max	66	3.55	995	295	142	253	837	915	447	14	1.07	0.17
Avg	47	3.52	841	228	108	215	793	590	373	13	1.04	0.09
Vol Wt. Avg		3.51	866	238	113	216	787	606	382	—	—	0.09
22 June 1987												
N	9	9	9	9	9	9	9	9	9	7	9	9
Min	13	2.84	206	311	27	53	267	436	354	11	0.94	0.04
Max	62	3.43	1257	1126	243	311	978	1632	1478	27	1.09	0.12
Avg	56	3.21	462	552	79	120	485	827	641	16	1.01	0.08
Vol Wt. Avg		3.23	424	467	70	110	447	704	540	—	—	0.07

Table 2. (continued)

	V(mL)	pH	Na^+	NH_4^+	Ca^{2+}	Mg^{2+}	Cl^-	NO_3^-	SO_4^{2-}	CH_2O	−/+	LWC
			‖⟵			μN		⟶‖		μM		g m^{-3}
23 June 1987												
N	20	20	20	20	20	20	20	20	20	0	20	20
Min	61	3.15	123	223	17	33	173	277	224	—	0.95	0.02
Max	66	3.62	452	528	95	131	505	1024	608	—	1.27	0.16
Avg	62	3.47	200	293	38	55	257	407	342	—	1.08	0.12
Vol Wt. Avg		3.49	185	277	34	50	241	371	324	—	—	0.10
24 June 1987												
N	24	24	24	24	20	24	24	24	24	22	24	22
Min	17	2.53	189	462	30	56	309	1291	1119	18	1.09	0.02
Max	66	2.94	3148	2859	560	601	1613	5623	3246	51	1.51	0.25
Avg	56	2.76	794	1495	134	179	666	2627	1871	34	1.18	0.11
Vol Wt. Avg		2.78	553	1340	99	133	552	2226	1669	—	—	0.09
25 June 1987												
N	23	23	23	23	23	23	23	23	23	15	23	21
Min	10	2.63	142	410	30	37	132	832	660	16	0.89	0.00
Max	68	3.11	1618	9383	1143	1151	2096	8191	5796	37	1.42	0.34
Avg	42	2.78	468	1702	138	135	402	2708	1874	26	1.18	0.18
Vol Wt. Avg		2.81	323	1072	73	73	254	2062	1365	—	—	0.11
26 June 1987												
N	21	21	21	21	21	21	21	21	21	0	21	19
Min	32	2.99	28	423	8	10	43	454	387	—	0.79	0.08
Max	69	3.51	315	1979	164	86	223	2462	1971	—	1.36	0.29
Avg	55	3.31	89	1058	27	25	90	1044	794	—	1.11	0.21
Vol Wt. Avg		3.34	67	931	20	19	71	915	660	—	—	0.21
01 July 1987												
N	6	6	7	7	7	7	7	7	7	0	6	6
Min	8	3.15	336	242	57	90	339	401	435	—	0.95	0.02
Max	29	3.23	912	638	215	248	745	1138	836	—	1.02	0.15
Avg	15	3.18	480	517	111	129	454	741	652	—	0.98	0.10
Vol Wt. Avg		3.18	440	555	108	120	415	754	671	—	—	0.04

Table 2. (continued)

	V(mL)	pH	Na^+	NH_4^+	Ca^{2+}	Mg^{2+}	Cl^-	NO_3^-	SO_4^{2-}	CH_2O	−/+	LWC
			‖⟵			μN		⟶‖		μM		g m^{-3}
03 July 1987												
N	14	14	14	14	14	14	14	14	14	0	14	14
Min	20	2.42	308	394	71	83	327	535	492	—	0.98	0.02
Max	62	3.30	683	2770	286	202	656	4656	3028	—	1.26	0.11
Avg	55	2.72	443	1652	128	124	466	2987	1900	—	1.16	0.07
Vol Wt. Avg		2.66	415	1675	119	116	445	2994	1892	—	—	0.06
07 July 1987												
N	7	7	7	7	7	7	7	7	7	7	7	7
Min	23	3.14	235	266	28	53	284	332	384	12	1.07	0.03
Max	66	3.51	719	1108	127	156	821	1301	810	22	1.19	0.21
Avg	55	3.33	489	473	57	107	537	706	562	16	1.13	0.12
Vol Wt. Avg		3.31	412	470	52	91	453	713	555	—	—	0.10
08 July 1987												
N	9	9	9	9	9	9	9	9	9	0	9	9
Min	4	2.81	59	88	20	15	71	172	143	—	1.07	0.00
Max	65	3.91	1365	2458	508	335	1055	3419	2647	—	1.27	0.25
Avg	53	3.09	485	866	130	117	415	1435	1044	—	1.15	0.13
Vol Wt. Avg		2.99	481	855	119	116	409	1435	1052	—	—	0.11
13 July 1987												
N	2	2	2	2	2	2	2	2	2	0	2	2
Min	9	3.79	204	210	45	57	242	174	230	10	0.93	0.01
Max	36	3.83	223	240	52	57	264	217	230	—	1.10	0.05
14 July 1987												
N	21	21	21	21	21	21	21	21	21	11	21	19
Min	29	3.13	64	129	13	19	95	112	182	5	0.94	0.12
Max	65	3.91	207	977	55	59	240	600	820	38	1.17	0.31
Avg	40	3.61	106	351	26	29	146	285	382	15	1.02	0.22
Vol Wt. Avg		3.63	97	295	22	26	138	235	319	—	—	0.21
14 July 1987												
N	19	21	21	21	21	21	21	21	21	8	21	19
Min	37	3.23	40	131	10	13	57	167	212	6	0.95	0.05
Max	42	3.73	267	391	77	65	272	602	550	15	1.08	0.23
Avg	39	3.50	160	227	30	38	162	307	327	10	1.01	0.17
Vol Wt. Avg		3.52	175	210	29	40	173	277	311	—	—	0.14

Table 2. (continued)

	V(mL)	pH	Na^+	NH_4^+	Ca^{2+}	Mg^{2+}	Cl^-	NO_3^-	SO_4^{2-}	CH_2O	−/+	LWC
			‖⟶			μN		⟵‖		μM		g m^{-3}
16 July 1987												
N	16	16	16	16	16	16	16	16	16	0	16	15
Min	12	2.64	22	328	14	8	40	190	219	—	0.93	0.02
Max	68	3.93	271	2161	236	100	357	2797	2438	—	1.12	0.24
Avg	51	3.12	119	727	110	43	155	854	992	—	1.06	0.14
Vol Wt. Avg		3.06	93	639	87	35	131	819	888	—	—	0.11
17 July 1987												
N	20	20	20	20	9	9	20	20	20	0	20	18
Min	25	3.50	6	44	3	1	11	28	39	—	0.92	0.05
Max	56	4.98	92	504	47	28	98	300	376	—	1.23	0.26
Avg	49	4.09	35	136	14	10	43	125	161	—	1.09	0.16
Vol Wt. Avg		3.94	28	101	6	4	35	100	138	—	—	0.14
All Samples 6–14 to 7–17–88												
N	240	242	241	242	225	231	242	242	242	80	241	227
Min	1	2.42	6	44	3	1	11	28	39	5	0.73	0.00
Max	69	4.98	3796	9383	1143	1151	2096	8191	5796	51	1.84	0.34
Avg	49	3.25	404	775	82	107	369	1185	917	23	1.09	0.14
Vol Wt. Avg		3.15	263	632	51	65	256	941	736	—	—	0.103

Table 3. Concentrations of Organic Acids, S(IV), HCHO, and H_2O_2 Cloudwater Samples Collected at San Pedro Hill

V(mL)	pH	Time (hrs)	S(IV)	CH_2O	H_2O_2	HCO_2H*	CH_3COOH*	+/−
			‖⟵		μM		⟶‖	
7–15–88 Size–fractionated Sample from the Front Rods of the CASC								
68	3.34	4:33–5:00	0	10	10	19	11	1.08
71	3.27	5:00–5:30	0	16	0	21	13	1.06
71	3.26	5:30–6:00	0	27	0	40	19	1.00
74	3.29	6:00–6:30	6	29	0	37	18	0.98
112	3.42	6:30–7:00	6	16	0	26	11	1.02
121	3.42	7:00–7:30	6	13	0	17	9	1.04
136	3.44	7:30–8:00	0	13	4	19	9	0.99
122	3.49	8:00–8:30	0	13	10	18	10	1.02
116	3.52	8:30–9:00	0	13	16	20	9	1.02
64	3.40	10:30–11:00	0	18	49	33	13	1.06
7–15–88 Size–fractionated Sample from the Back Strings of the CASC								
29	3.42	4:33–5:00	0	11	9	16	10	1.03
28	3.28	5:00–5:30	0	13	0	18	11	1.05
31	3.10	5:30–6:00	6	26	0	34	17	0.99
28	3.08	6:00–6:30	10	55	0	38	22	0.98
38	3.24	6:30–7:00	5	25	0	32	20	0.98
39	3.35	7:00–7:30	0	17	0	18	9	1.02
38	3.38	7:30–8:00	0	16	3	19	9	0.96
30	3.42	8:00–8:30	0	17	6	19	10	1.01
32	3.47	8:30–9:00	0	14	11	23	10	1.02
30	3.25	10:30–11:00	0	21	39	40	17	1.06
Samples Collected from 7–7–87 to 7–14–87								
Parameter	V(mL)	pH	S(IV)	CH_2O	H_2O_2	HCOOH*	CH_3COOH*	
			‖⟵		μM		⟶‖	
N	21	21	—	20	16	21	21	
Min	9	3.14	—	5	4	12	6	
Max	59	3.83	—	38	72	43	31	
Avg.	38	3.58	—	13	42	20	10	

* This represents the total RCOOH (i.e. [RCOOH] + [RCO_2^-]) unless otherwise noted.

Table 4. Concentrations in Cloudwater Samples Collected at Henninger Flats during the Period of 6–20 to 7–17–87.

	V(mL)	pH	Na^+	NH_4^+	Ca^{2+}	Mg^{2+}	Cl^-	NO_3^-	SO_4^{2-}	CH_2O	−/+	LWC
			‖←———			μN		———→‖		μM		g m^{-3}
20 June 1987												
N	6	6	6	6	6	6	6	6	6	6	6	6
Min	24	2.75	180	805	39	48	169	877	447	66	0.90	0.03
Max	65	3.59	1652	3509	454	435	975	4034	2028	91	1.04	0.09
Avg	48	3.15	542	1575	136	144	377	1879	885	76	0.99	0.05
Vol Wt. Avg		3.09	442	1418	106	118	327	1715	796	78	—	0.05
21 June 1987												
N	12	12	12	12	12	12	12	12	12	11	12	12
Min	7	2.62	183	603	42	49	161	787	36	53	0.76	0.01
Max	45	3.75	1553	3172	520	400	666	5472	2606	109	1.09	0.18
Avg	39	3.01	485	1583	138	129	308	2116	1084	68	0.98	0.08
Vol Wt. Avg		2.96	340	1368	89	90	259	1773	963	62	—	0.05
10 July 1987												
N	20	20	20	20	20	20	20	20	20	0	20	19
Min	29	2.88	48	671	47	20	91	735	368	—	0.81	0.01
Max	63	3.88	195	1760	167	99	214	2065	1094	—	1.08	0.17
avg	37	3.24	82	1022	91	36	128	1076	589	—	0.96	0.10
Vol Wt. Avg		3.22	68	864	76	29	111	949	526	—	—	0.05
16 July 1987												
N	20	20	20	20	20	20	20	20	20	0	20	18
Min	9	2.68	5	324	7	2	18	284	137	—	0.46	0.01
Max	65	4.78	149	4085	397	77	115	1908	1474	—	1.33	0.40
Avg	58	3.36	43	1392	80	23	48	804	549	—	0.78	0.24
Vol Wt. Avg		3.48	27	740	27	10	35	525	346	—	—	0.14
17 June 1987												
N	18	18	18	18	18	18	18	18	18	0	18	17
Min	40	3.03	3	273	15	7	22	231	159	—	0.95	0.07
Max	65	3.94	273	2435	985	171	301	3319	2028	—	1.18	0.23
Avg	62	3.35	55	817	171	40	73	967	628	—	1.05	0.17
Vol Wt. Avg		3.31	46	752	136	34	63	897	572	—	—	0.15

Table 4. (continued)

	V(mL)	pH	Na^+	NH_4^+	Ca^{2+}	Mg^{2+}	Cl^-	NO_3^-	SO_4^{2-}	CH_2O	−/+	LWC
			‖⟵			μN			⟶‖	μM		$g\ m^{-3}$
All Samples 6–20 to 7–17–88												
N	76	76	76	76	76	76	76	76	76	17	76	72
Min	7	2.62	3	273	7	2	18	231	36	53	0.46	0.01
Max	65	4.78	1652	4085	985	435	975	5472	2606	109	1.33	0.40
Avg	50	3.25	166	1203	118	57	142	1206	689	71	0.94	0.14
Vol Wt. Avg		3.29	82	845	74	31	86	855	511	—	—	0.09

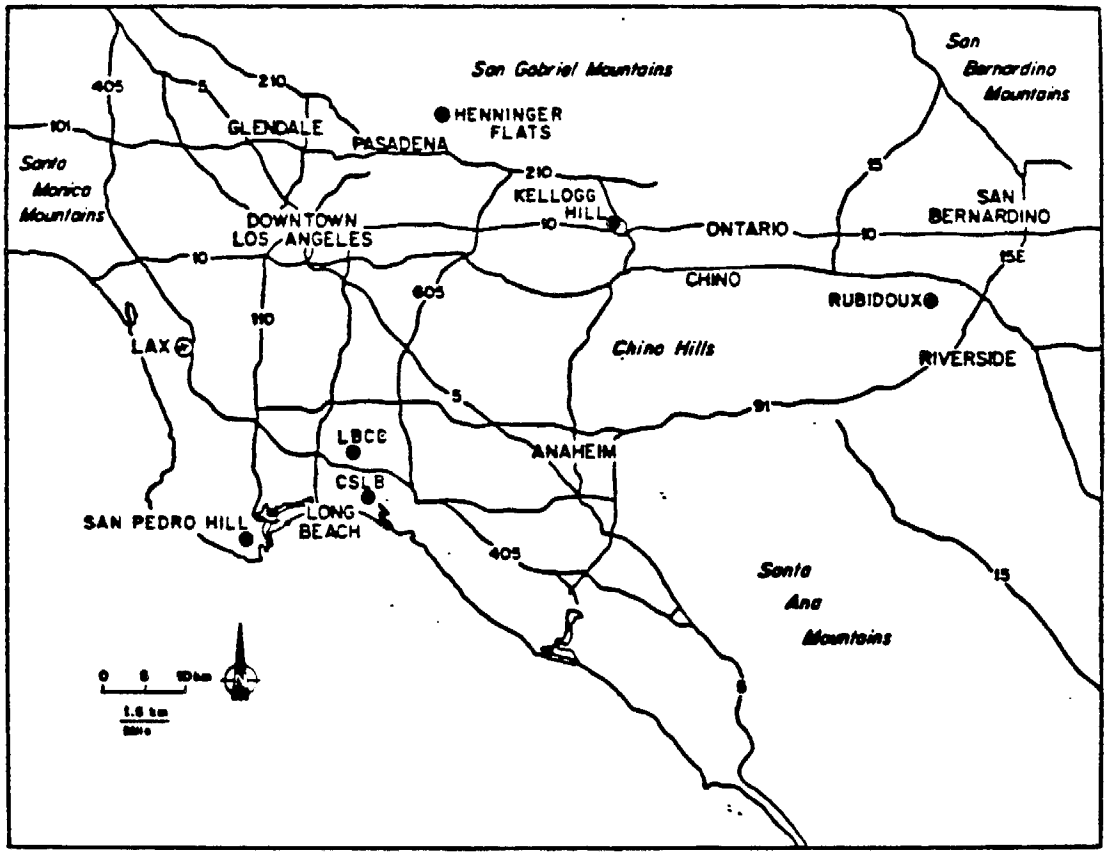

Figure 1

Map of the South Coast Air Basin. Major freeways and selected cities are shown. Sampling sites are indicated by •.

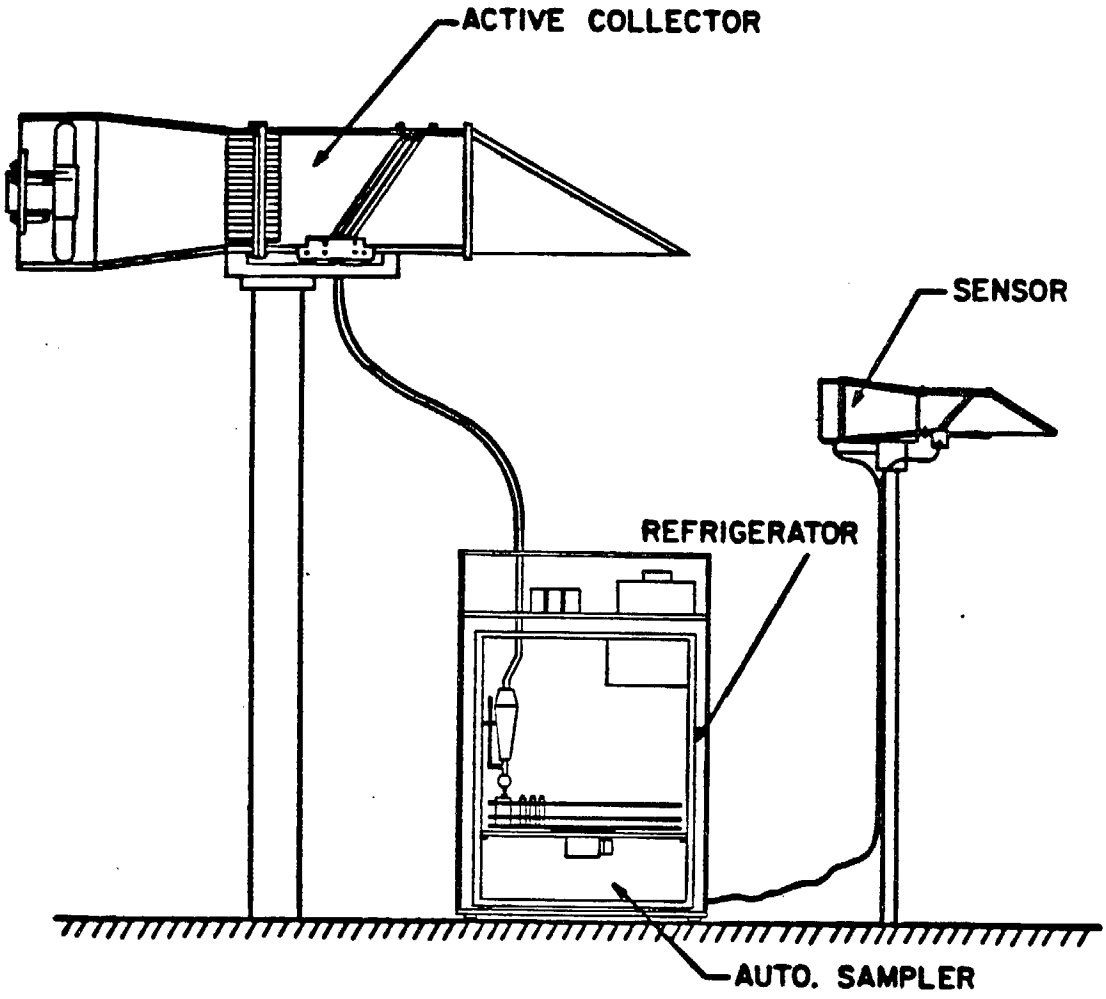

Figure 2

Diagram of the automated cloudwater collector system. Depicted in the figure are the CASC, a cloudwater sensor, and the fractionating collector, housed in a refrigerator.

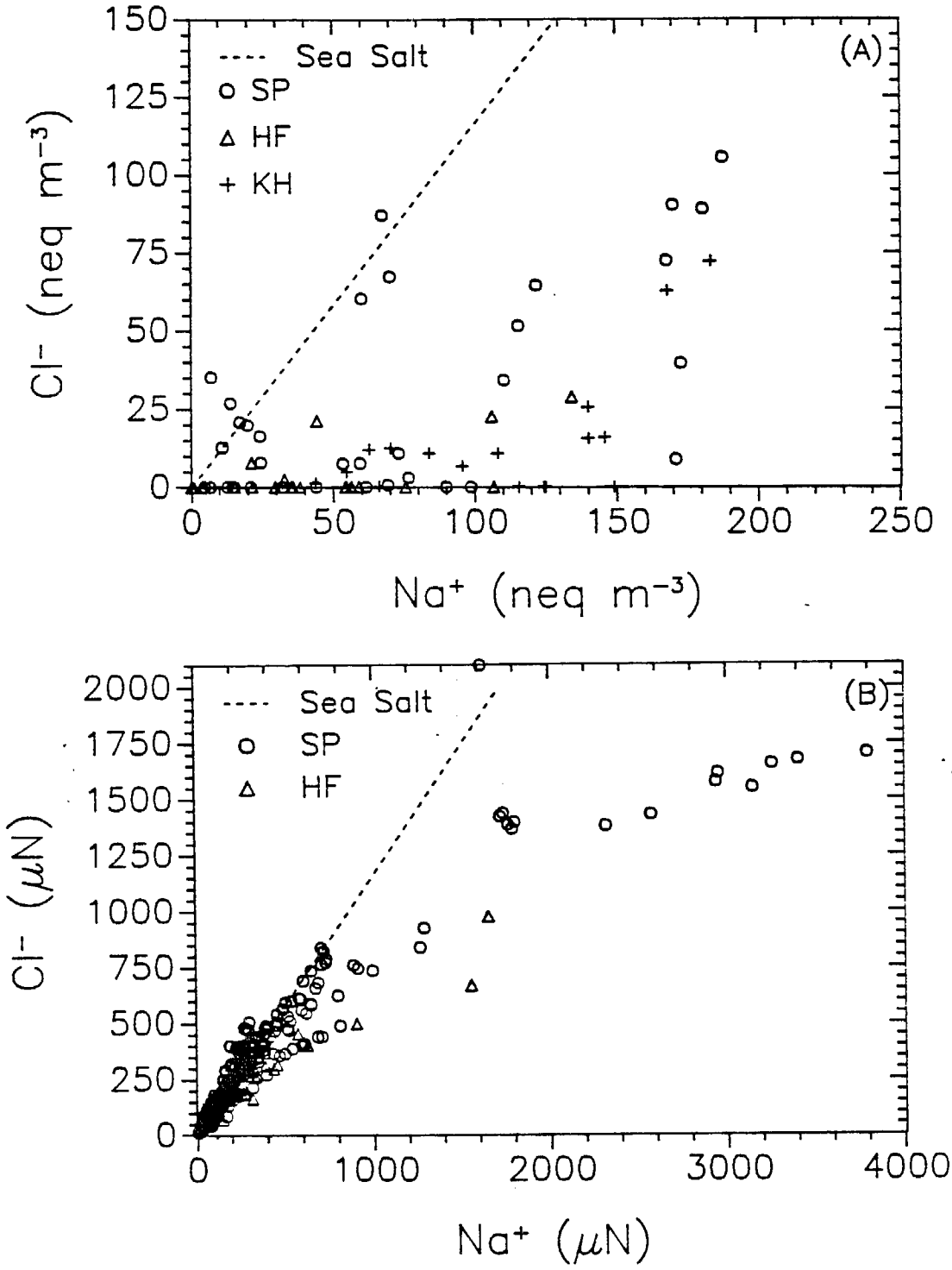

Figure 3

A) Cl- concentrations in aerosol samples, plotted against Na^+. --- indicates the sea-salt ratio. B) Same as A, but for cloudwater.

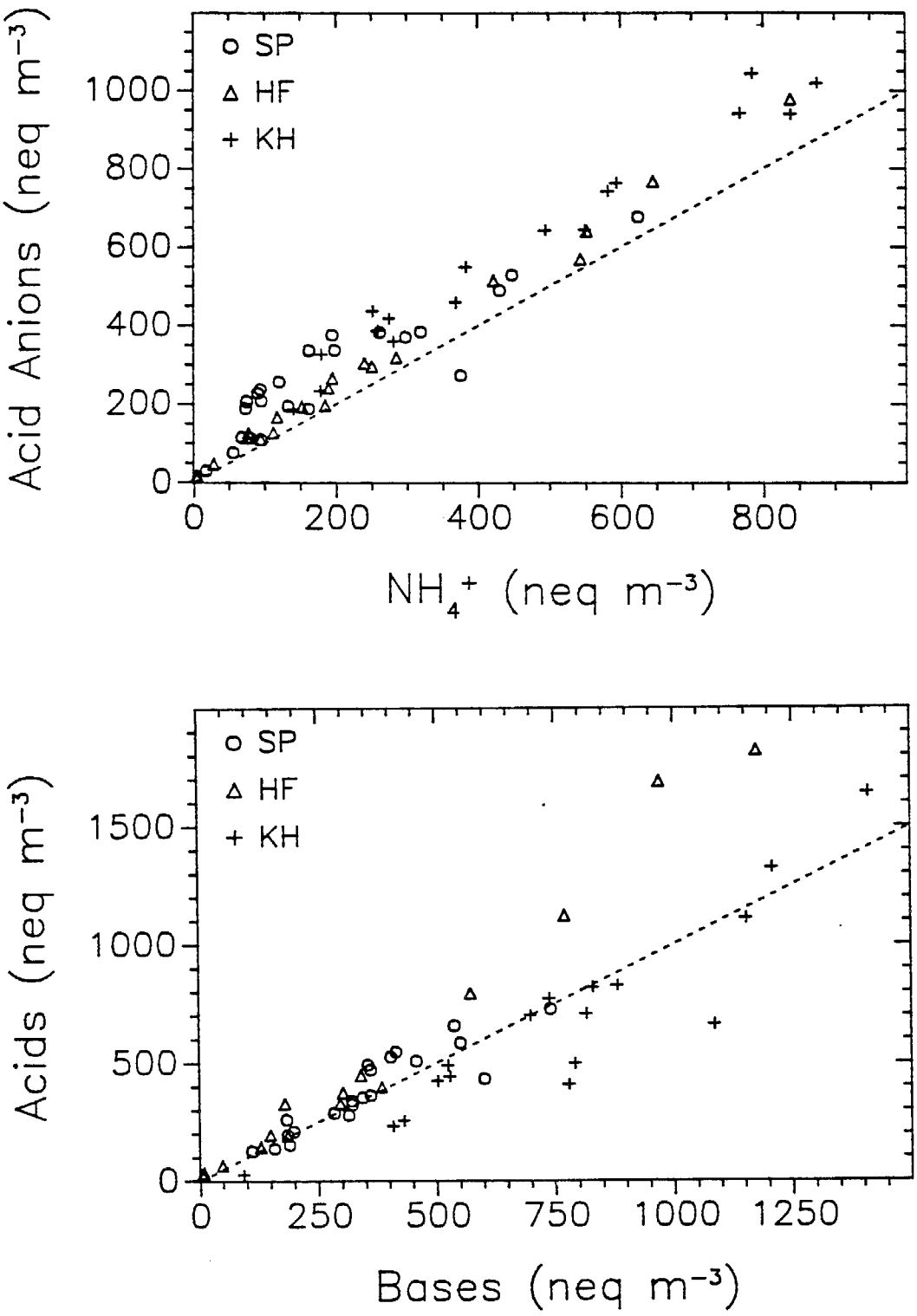

Figure 4

A) The sum, $NO_3^- + SO_4^{2-}$, plotted vs NH_4^+ in aerosol samples.

B) Total anions ($Cl^- + NO_3^- + SO_4^{2-} + HNO_3$) plotted vs total cations ($Na^+ + Ca^{2+} + Mg^{2+} + NH_4^+ + NH_3$) in aerosol samples

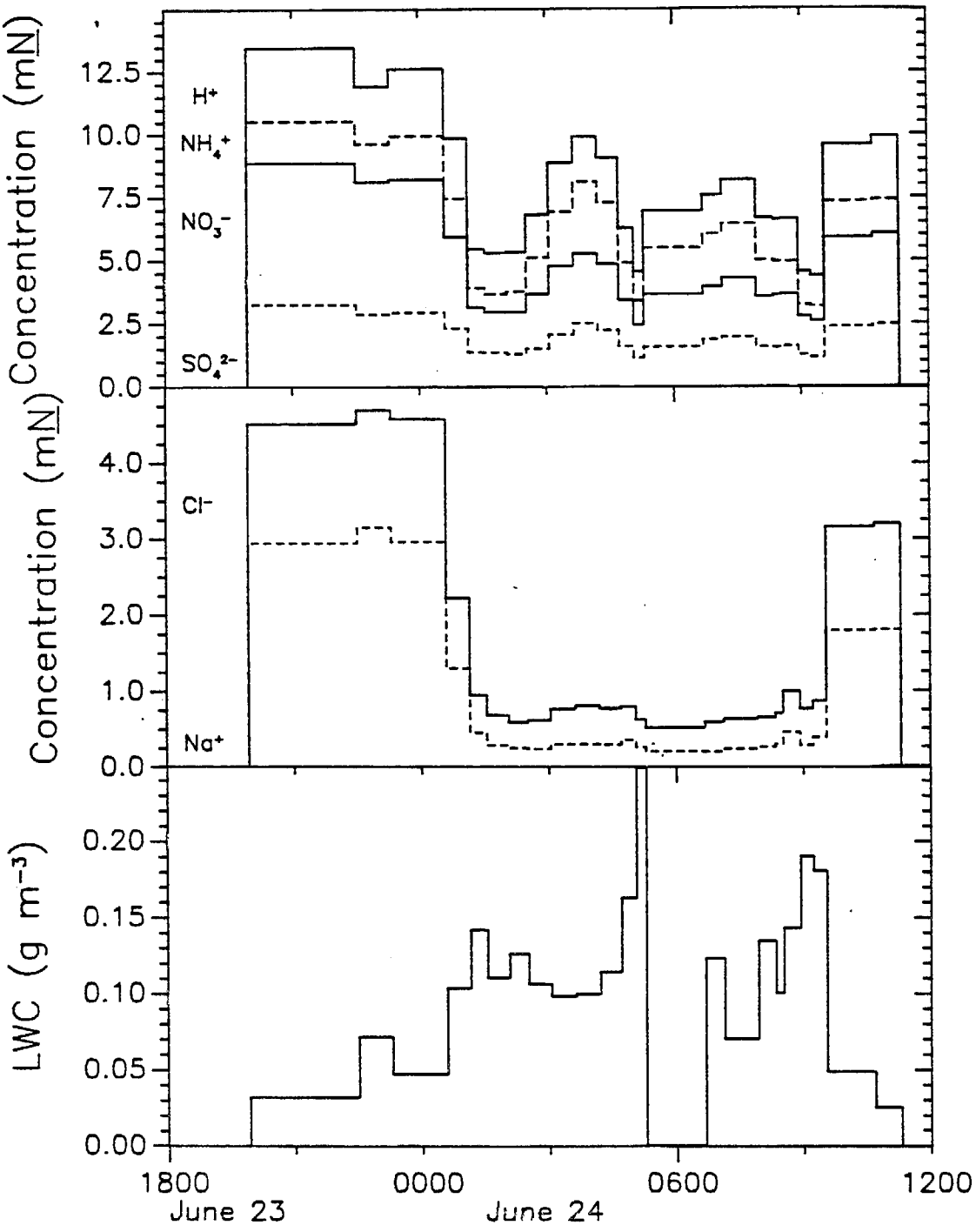

Figure 5

Concentrations of major ions and sea salts and LWC in cloudwater samples collected at San Pedro Hill on June 23 and 24, 1987. LWC is estimated from the sample collection rate and its theoretical efficiency.

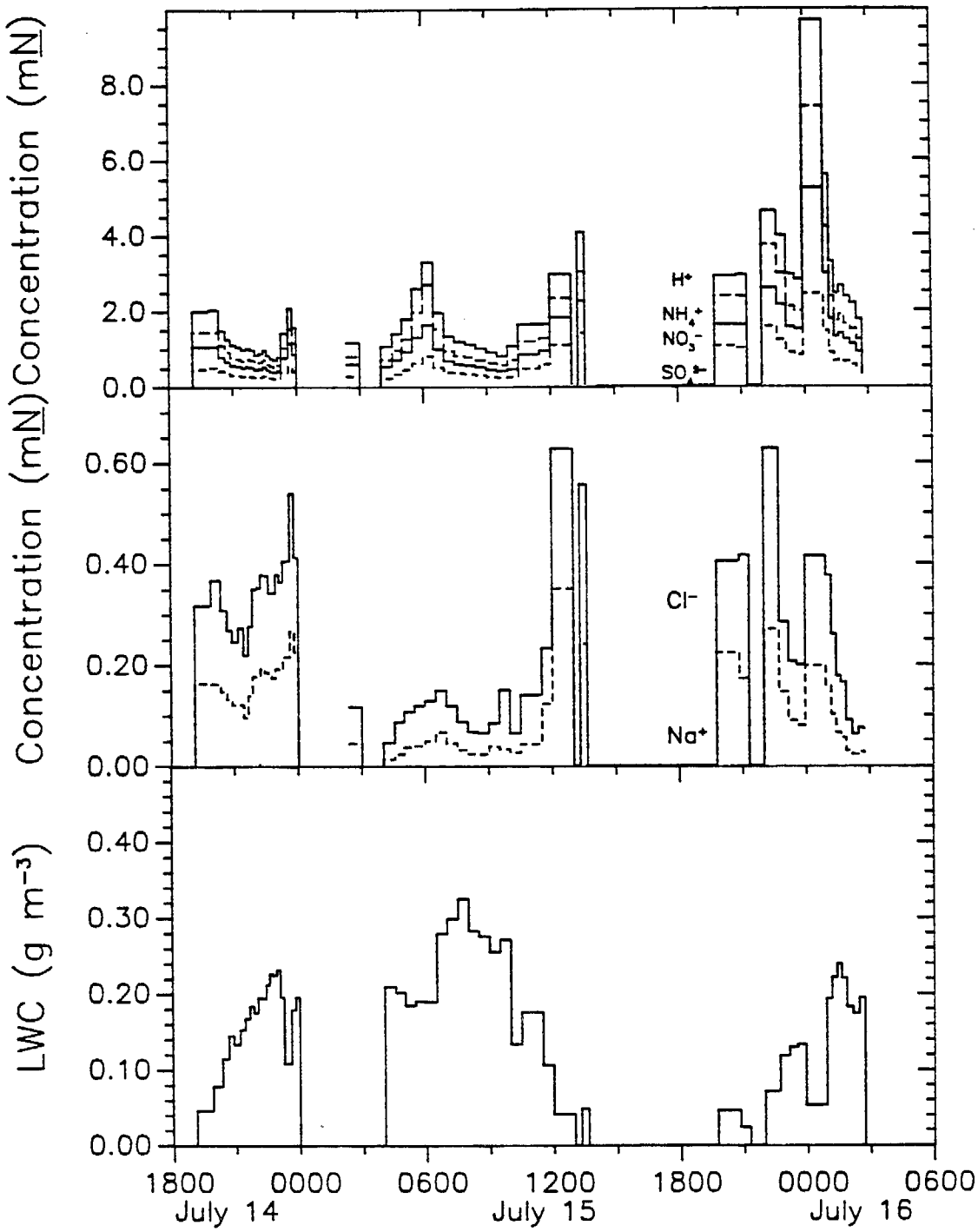

Figure 6

Concentrations of major ions and sea salts and LWC in cloudwater samples collected at San Pedro Hill over the period July 14 – July 16, 1987. LWC is estimated from the sample collection rate and its theoretical efficiency.

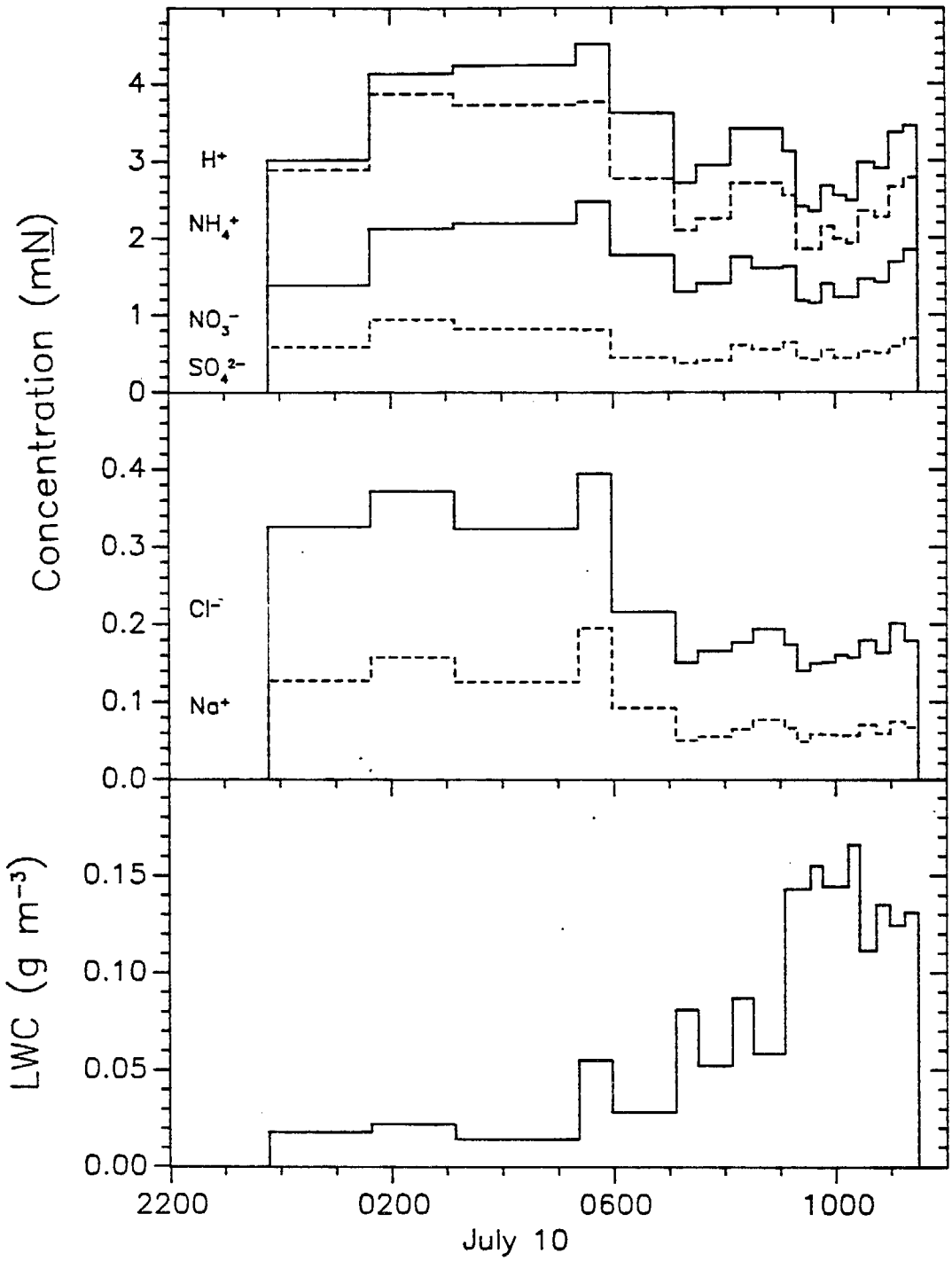

Figure 7

Concentrations of major ions and sea salts and LWC in cloudwater samples collected at Henninger Flats on July 10, 1987. LWC is estimated from the sample collection rate and its theoretical efficiency.

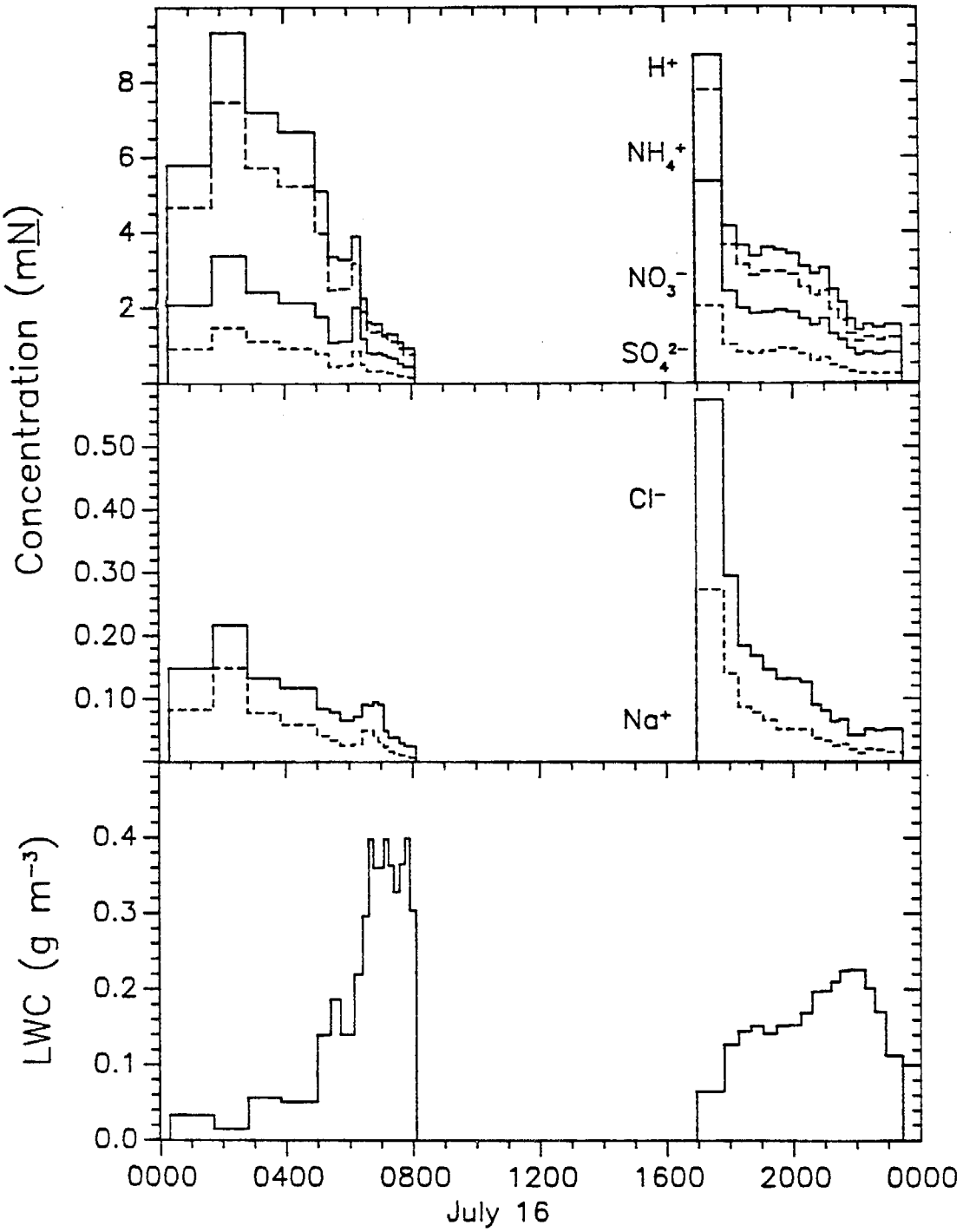

Figure 8

Concentrations of major ions and sea salts and LWC in cloudwater samples collected at Henninger Flats on July 16, 1987. LWC is estimated from the sample collection rate and its theoretical efficiency.

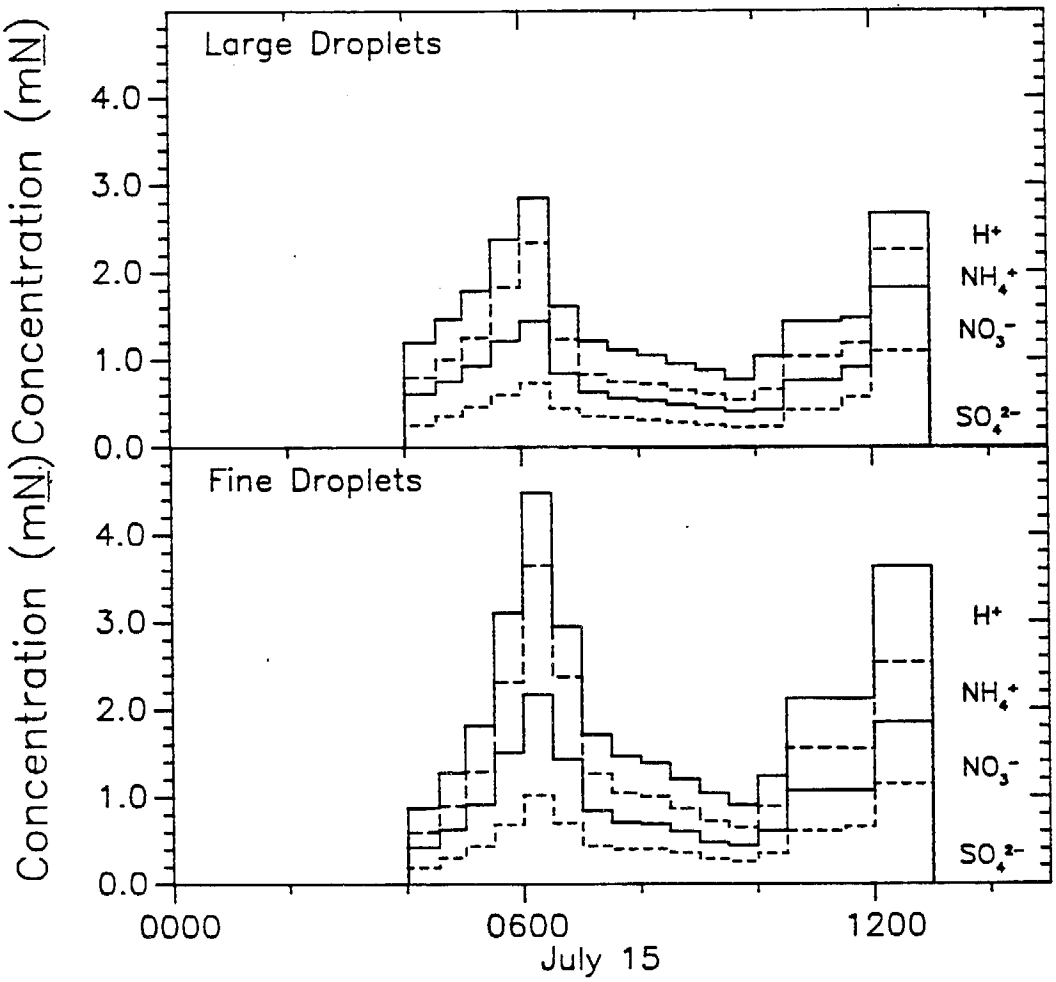

Figure 9

Concentrations of major ions in size–fractionated cloudwater samples collected at San Pedro Hill on the morning of July 15, 1987.

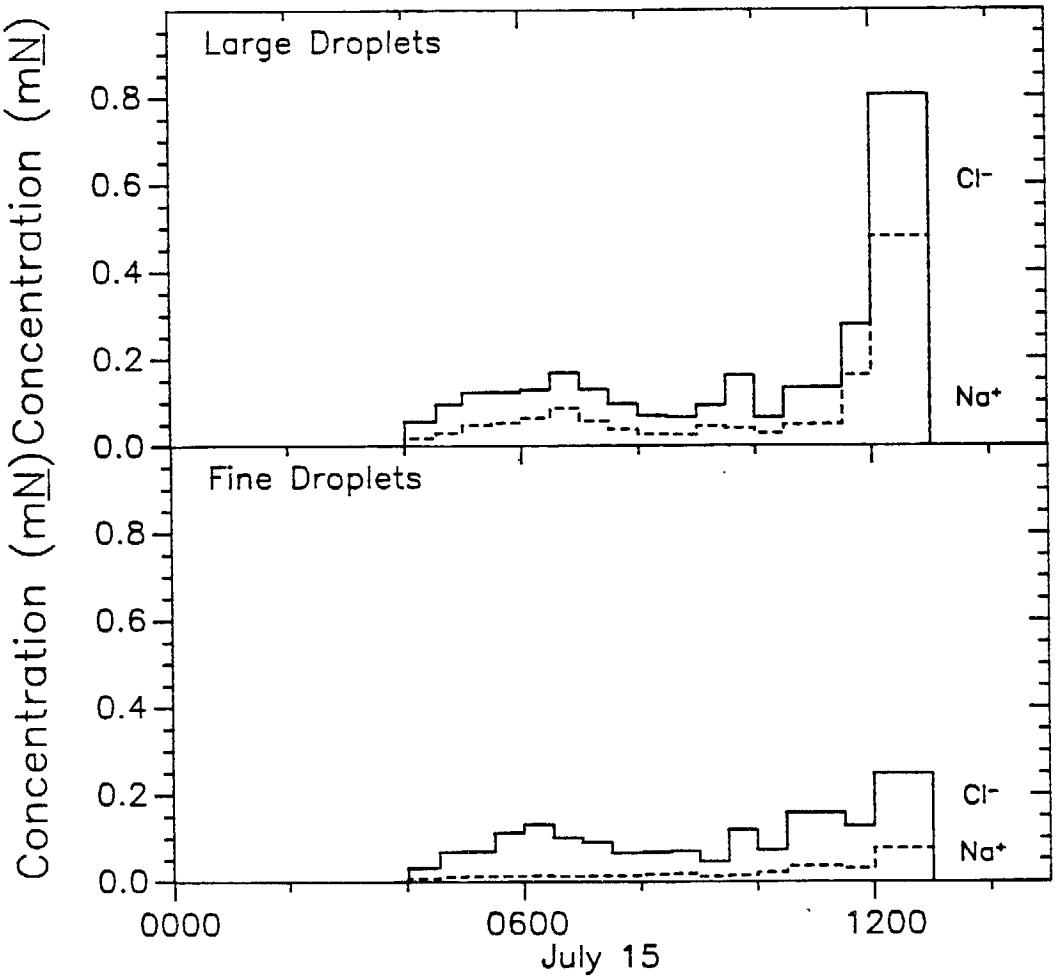

Figure 10

Concentrations of sea salts in size-fractionated cloudwater samples collected at San Pedro Hill on the morning of July 15, 1987.

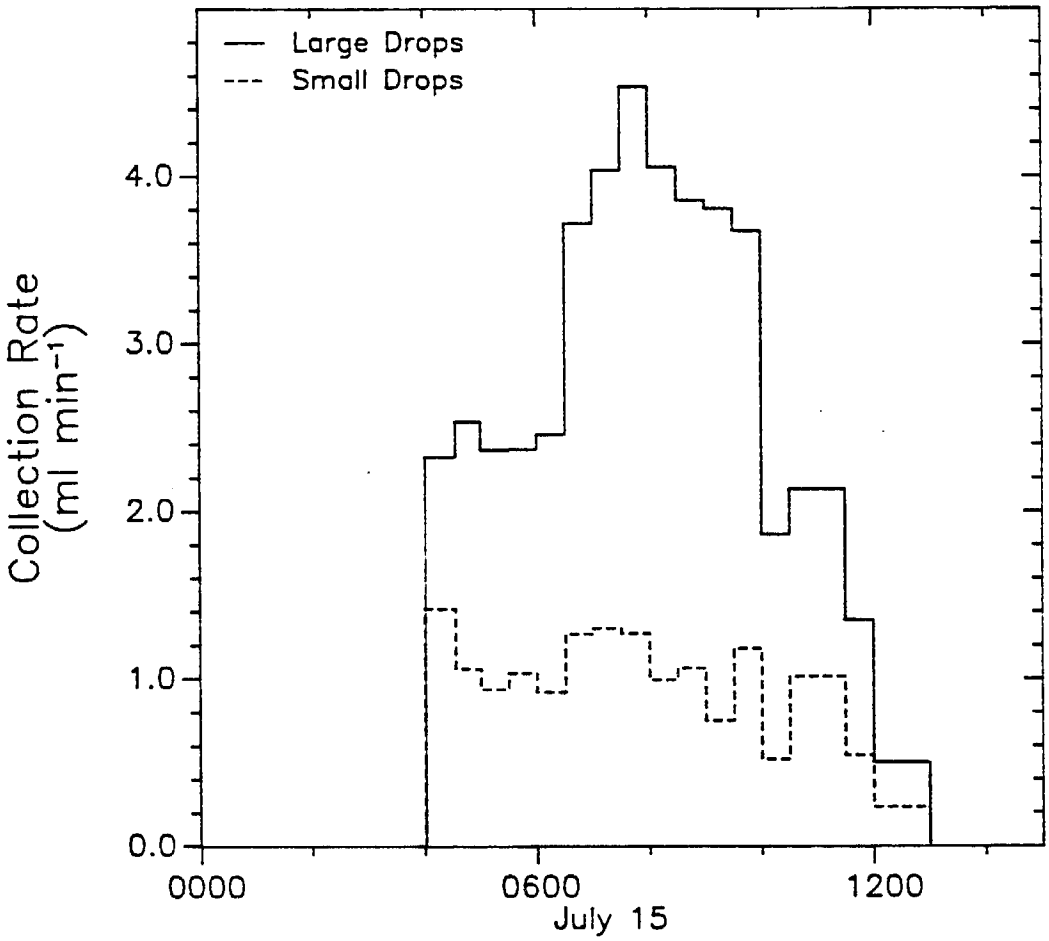

Figure 11

Collection rate for size-fractionated cloudwater samples collected at San Pedro Hill on the morning of July 15, 1987.

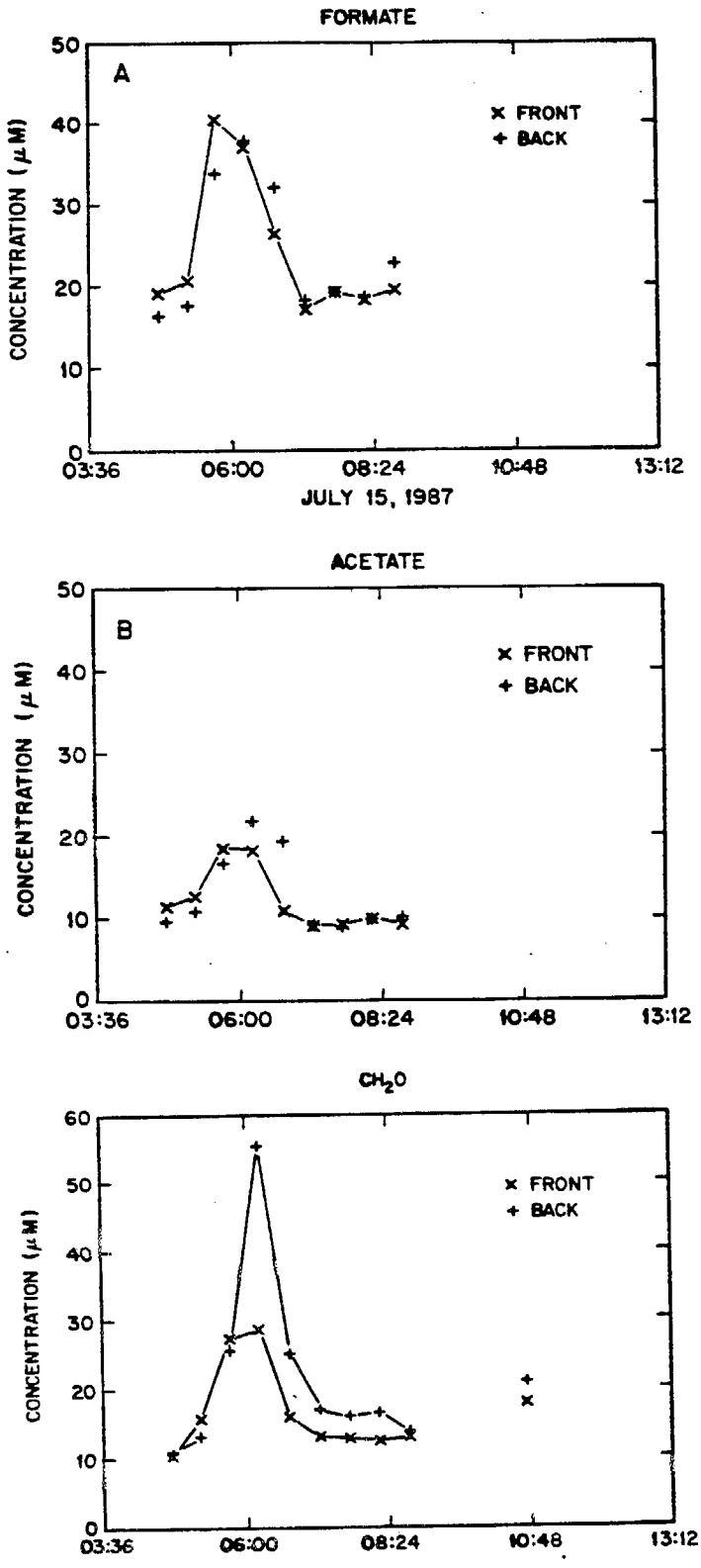

Figure 12

Formate (A), acetate (B), and formaldehyde (C) in size-fractionated cloudwater samples from San Pedro Hill. Large droplets are collected in the front fraction;are collected in the back fraction.

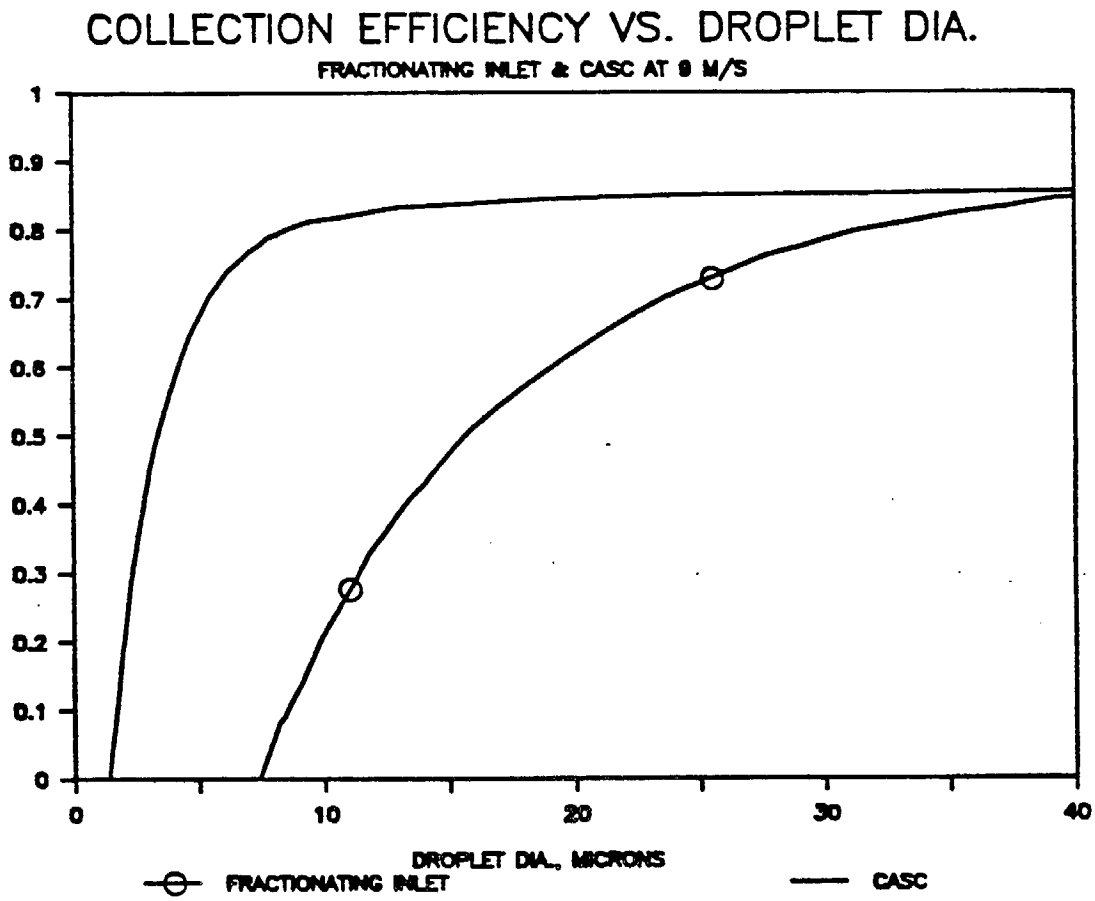

Figure 13

Theoretical collection efficiency vs droplet diameter for collection on the rods of the fractionating inlet and the strands of the CASC.

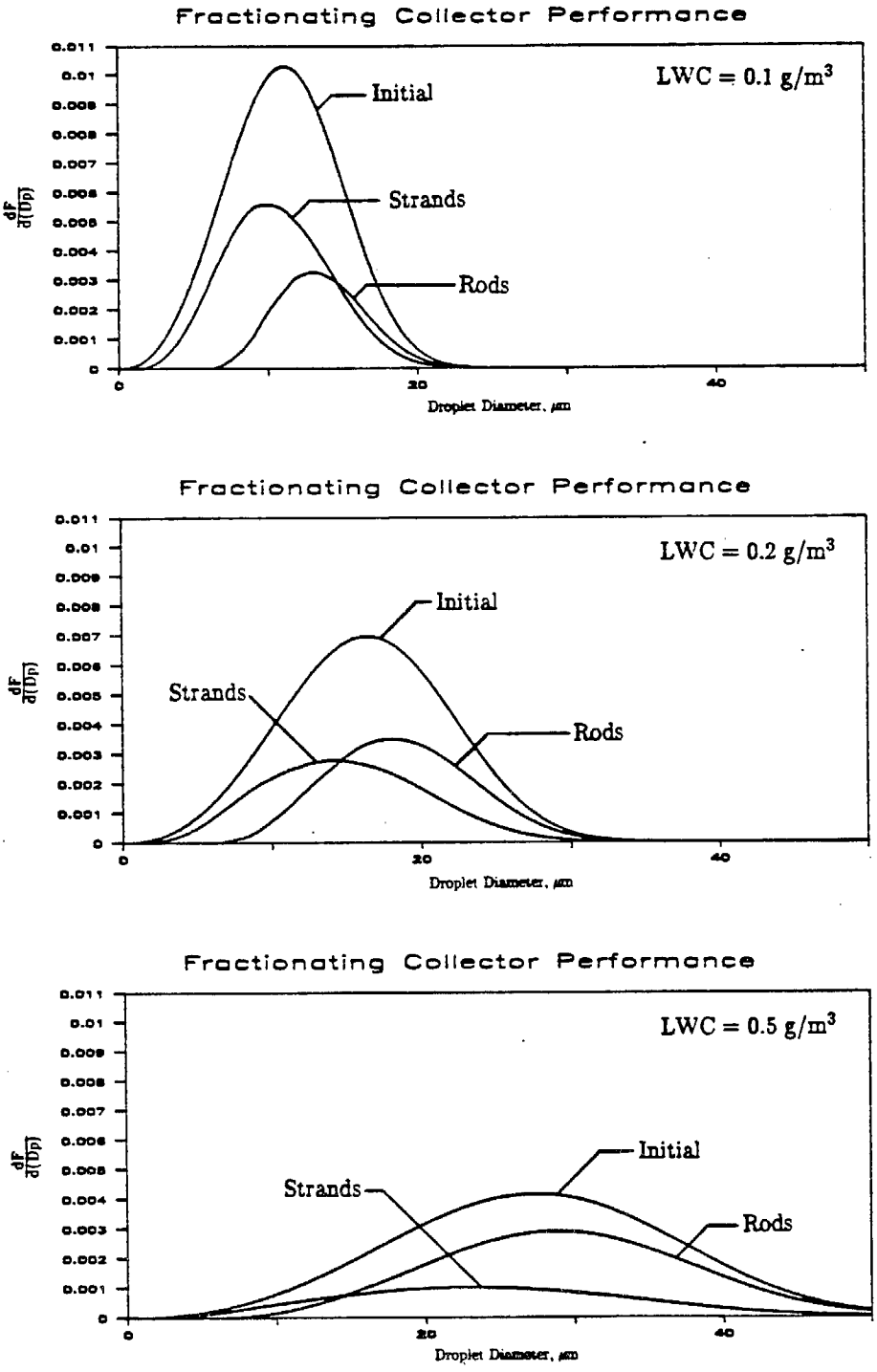

Figure 14

Collection of water on the fractionating inlet rods and CASC strands under three LWC conditions. Initial droplet-size distributions are given by Best's parameterized curves.